

---

# Identifying Incompatible Combinations of Concrete Materials: Volume I—Final Report

---

PUBLICATION NO. FHWA-HRT-06-079

AUGUST 2006



U.S. Department of Transportation  
**Federal Highway Administration**

Research, Development, and Technology  
Turner-Fairbank Highway Research Center  
6300 Georgetown Pike  
McLean, VA 22101-2296

## **FOREWORD**

Unexpected interactions between otherwise acceptable ingredients in portland cement concrete are becoming increasingly common as cementitious systems become more and more complex and demands on the systems are more rigorous. Such incompatibilities are exhibited as early stiffening or excessive retardation, potential for uncontrolled early-age cracking, and unstable or unacceptable air void systems.

Based on the experimental work described in this volume, a protocol has been developed to allow product manufacturers, concrete producers, contractors and owners to monitor their materials and concrete systems. The protocol is phased to allow relatively simple field tests to provide early warnings of potential problems, and central laboratory tests to support and confirm the field work. Tests conducted before beginning construction allows users to plan for changes in materials and environment. By monitoring materials with relatively simple field tests during construction, the users can detect when significant changes have occurred, indicating potential construction problems.

Gary Henderson  
Director, Office of Infrastructure  
Research and Development

### **Notice**

This document is disseminated under the sponsorship of the U.S. Department of Transportation in the interest of information exchange. The U.S. Government assumes no liability for the use of the information contained in this document. This report does not constitute a standard, specification, or regulation.

The U.S. Government does not endorse products or manufacturers. Trademarks or manufacturers' names appear in this report only because they are considered essential to the objective of the document.

### **Quality Assurance Statement**

The Federal Highway Administration (FHWA) provides high-quality information to serve Government, industry, and the public in a manner that promotes public understanding. Standards and policies are used to ensure and maximize the quality, objectivity, utility, and integrity of its information. FHWA periodically reviews quality issues and adjusts its programs and processes to ensure continuous quality improvement.

## Technical Report Documentation Page

1. Report No. FHWA-HRT-06-079		2. Government Accession No.		3. Recipient's Catalog No.	
4. Title and Subtitle Identifying Incompatible Combinations of Concrete Materials: Volume I—Final Report				5. Report Date August 2006	
				6. Performing Organization Code:	
7. Author(s) Peter C. Taylor Luis A. Graf Jerzy Z. Zemajtis				8. Performing Organization Report No.	
9. Performing Organization Name and Address CTLGroup 5400 Old Orchard Road Skokie, IL 60077				10. Work Unit No.	
				11. Contract or Grant No. DTFH61-03-X-00102	
12. Sponsoring Agency Name and Address FHWA and Portland Cement Association (24 percent) 5420 Old Orchard Road Skokie, IL 60077				13. Type of Report and Period Covered	
				14. Sponsoring Agency Code	
15. Supplementary Notes Chiara F. Ferraris of NIST worked under separate contract to FHWA. The Contract Officer's Technical Representative was Peter Kopac, HRDI-12.					
16. Abstract Unexpected interactions between otherwise acceptable ingredients in portland cement concrete are becoming increasingly common as cementitious systems become more and more complex and demands on the systems are more rigorous. Such incompatibilities are exhibited as early stiffening or excessive retardation, potential for uncontrolled early-age cracking, and unstable or unacceptable air void systems.  A number of test methods have been reviewed to assess their usefulness in detecting incompatibility early to help prevent problems with pavements in the field. A protocol has been developed to allow product manufacturers, concrete producers, contractors, and owners to monitor their materials and concrete systems. The protocol is phased to allow relatively simple field tests to provide early warnings of potential problems and then central laboratory tests to support and confirm the field work.  This is the first of two volumes. The other volume in this series is: FHWA HRT-06-080, <i>Identifying Incompatible Combinations of Concrete Materials: Volume II—Test Protocol</i> .					
17. Key Words Cement, fly ash, slag, incompatibility, admixture, early stiffening, cracking, air void system				18. Distribution Statement	
19. Security Classif. (of this report) Unclassified		20. Security Classif. (of this page) Unclassified		21. No. of Pages 159	22. Price

# SI\* (MODERN METRIC) CONVERSION FACTORS

## APPROXIMATE CONVERSIONS TO SI UNITS

Symbol	When You Know	Multiply By	To Find	Symbol
<b>LENGTH</b>				
in	inches	25.4	millimeters	mm
ft	feet	0.305	meters	m
yd	yards	0.914	meters	m
mi	miles	1.61	kilometers	km
<b>AREA</b>				
in <sup>2</sup>	square inches	645.2	square millimeters	mm <sup>2</sup>
ft <sup>2</sup>	square feet	0.093	square meters	m <sup>2</sup>
yd <sup>2</sup>	square yard	0.836	square meters	m <sup>2</sup>
ac	acres	0.405	hectares	ha
mi <sup>2</sup>	square miles	2.59	square kilometers	km <sup>2</sup>
<b>VOLUME</b>				
fl oz	fluid ounces	29.57	milliliters	mL
gal	gallons	3.785	liters	L
ft <sup>3</sup>	cubic feet	0.028	cubic meters	m <sup>3</sup>
yd <sup>3</sup>	cubic yards	0.765	cubic meters	m <sup>3</sup>
NOTE: volumes greater than 1000 L shall be shown in m <sup>3</sup>				
<b>MASS</b>				
oz	ounces	28.35	grams	g
lb	pounds	0.454	kilograms	kg
T	short tons (2000 lb)	0.907	megagrams (or "metric ton")	Mg (or "t")
<b>TEMPERATURE (exact degrees)</b>				
°F	Fahrenheit	5 (F-32)/9 or (F-32)/1.8	Celsius	°C
<b>ILLUMINATION</b>				
fc	foot-candles	10.76	lux	lx
fl	foot-Lamberts	3.426	candela/m <sup>2</sup>	cd/m <sup>2</sup>
<b>FORCE and PRESSURE or STRESS</b>				
lbf	poundforce	4.45	newtons	N
lbf/in <sup>2</sup>	poundforce per square inch	6.89	kilopascals	kPa

## APPROXIMATE CONVERSIONS FROM SI UNITS

Symbol	When You Know	Multiply By	To Find	Symbol
<b>LENGTH</b>				
mm	millimeters	0.039	inches	in
m	meters	3.28	feet	ft
m	meters	1.09	yards	yd
km	kilometers	0.621	miles	mi
<b>AREA</b>				
mm <sup>2</sup>	square millimeters	0.0016	square inches	in <sup>2</sup>
m <sup>2</sup>	square meters	10.764	square feet	ft <sup>2</sup>
m <sup>2</sup>	square meters	1.195	square yards	yd <sup>2</sup>
ha	hectares	2.47	acres	ac
km <sup>2</sup>	square kilometers	0.386	square miles	mi <sup>2</sup>
<b>VOLUME</b>				
mL	milliliters	0.034	fluid ounces	fl oz
L	liters	0.264	gallons	gal
m <sup>3</sup>	cubic meters	35.314	cubic feet	ft <sup>3</sup>
m <sup>3</sup>	cubic meters	1.307	cubic yards	yd <sup>3</sup>
<b>MASS</b>				
g	grams	0.035	ounces	oz
kg	kilograms	2.202	pounds	lb
Mg (or "t")	megagrams (or "metric ton")	1.103	short tons (2000 lb)	T
<b>TEMPERATURE (exact degrees)</b>				
°C	Celsius	1.8C+32	Fahrenheit	°F
<b>ILLUMINATION</b>				
lx	lux	0.0929	foot-candles	fc
cd/m <sup>2</sup>	candela/m <sup>2</sup>	0.2919	foot-Lamberts	fl
<b>FORCE and PRESSURE or STRESS</b>				
N	newtons	0.225	poundforce	lbf
kPa	kilopascals	0.145	poundforce per square inch	lbf/in <sup>2</sup>

\*SI is the symbol for the International System of Units. Appropriate rounding should be made to comply with Section 4 of ASTM E380.  
(Revised March 2003)

## TABLE OF CONTENTS

<b>CHAPTER 1. INTRODUCTION.....</b>	<b>1</b>
Overview .....	1
Background .....	1
Study Goals, Objectives, and Scope.....	3
<b>CHAPTER 2. LITERATURE REVIEW .....</b>	<b>5</b>
General .....	5
Need for Information Request Responses .....	5
Construction Materials and Practices .....	6
Findings on Rheology, Cracking, and Air void System.....	9
Summary .....	33
<b>CHAPTER 3. PROJECT TASKS .....</b>	<b>35</b>
TASK 2.1.1—EARLY SETTING OR EXCESSIVE RETARDATION .....	35
Test Matrix for Paste and Mortar Systems .....	40
Testing Concrete .....	51
Test Methods Discussion .....	57
Observations.....	64
Summary .....	85
TASK 2.1.2—CRACKING.....	91
Mix designs .....	95
TASK 2.1.3—AIR VOID SYSTEM.....	115
<b>CHAPTER 4. SUMMARY.....</b>	<b>135</b>
Introduction .....	135
Early Setting and Excessive Retardation .....	135
Protocol .....	140
Implementation Plan .....	141
<b>ACKNOWLEDGEMENTS .....</b>	<b>143</b>
<b>REFERENCES.....</b>	<b>145</b>

## LIST OF FIGURES

Figure 1. Example plot with a strong relationship between data sets. ....	58
Figure 2. Example plot of data sets with little or no relationship. ....	58
Figure 3. A plot comparing sets of initial setting time measurements determined by different methods. ....	59
Figure 4. Correlation between initial and final set for concrete tests. ....	60
Figure 5. Correlation between initial and final set for paste tests. ....	60
Figure 6. Device used at NIST to lift the mold for the minislump test. ....	67
Figure 7. A plot of minislump data for mixtures tested in round 1. ....	68
Figure 8. A plot of minislump data for mixtures tested in round 2. ....	71
Figure 9. A plot of minislump data for mixtures tested in round 3. ....	72
Figure 10. A plot of minislump data for mixtures tested in round 4. ....	73
Figure 11. A plot of minislump data for mixtures tested in round 5. ....	74
Figure 12. A plot of minislump data for mixtures tested in round 6. ....	75
Figure 13. Stress growth measurement. ....	81
Figure 14. Typical plots of yield stress versus time for accelerated, untreated, and retarded cementitious systems. ....	81
Figure 15. A photograph of the rheometer used at NIST. ....	82
Figure 16. Die set for squeezing pore solution from hardened cement paste specimens. ....	85
Figure 17. Pore fluid being collected from die set. ....	85
Figure 18. Equation. Solubility product of gypsum. ....	86
Figure 19. Equation. Ion activity product of gypsum. ....	86
Figure 20. Equation. Pulse velocity. ....	90
Figure 21. Compressive strength development. ....	102
Figure 22. Modulus of elasticity development. ....	103
Figure 23. Splitting tensile strength development. ....	103
Figure 24. Early age properties for mix WRA1. ....	105
Figure 25. Early age properties for mix WRA2. ....	105
Figure 26. Long-term properties for mix WRA1. ....	106
Figure 27. Long-term properties for mix WRA2. ....	106
Figure 28. Early age properties for mix FA1. ....	107
Figure 29. Early age properties for mix FA2. ....	107
Figure 30. Long-term properties for mix FA1. ....	108
Figure 31. Long-term properties for mix FA2. ....	108
Figure 32. Early age properties for mix 25FA90. ....	109
Figure 33. Early age properties for mix 4FA90. ....	110
Figure 34. Long-term properties for mix 25FA90. ....	110
Figure 35. Long-term properties for mix 4FA90. ....	111

Figure 36. Conduction calorimetry plot of paste system for mixture 25FA90 conducted at 32 °C (90 °F). .....	112
Figure 37. Early age properties for mix 25FA70.....	113
Figure 38. Early age properties for mix 4FA70.....	113
Figure 39. Long-term properties for mix 25FA70.....	114
Figure 40. Long-term properties for mix 4FA70.....	114
Figure 41. Foam drainage procedure. ....	119
Figure 42. Equation. Foam drainage.....	119
Figure 43. Equation. Percent drained.....	119
Figure 44. Rating 0–No clustering present. Visual rating guide for analysis of air void clustering severity (PCA R&D Serial No. 2789).....	124
Figure 45. Rating 1, Minor clustering Visual rating guide for analysis of air void clustering severity (PCA R&D Serial No. 2789).....	124
Figure 46. Rating 2, Moderate clustering. Visual rating guide for analysis of air void clustering severity (PCA R&D Serial No. 2789).....	125
Figure 47. Rating 3, severe clustering. Visual rating guide for analysis of air void clustering severity (PCA R&D Serial No. 2789).....	125
Figure 48. Example of clustering rating for a cylinder. ....	126
Figure 49. Correlation between pressure meter and AVA-generated fresh air contents. ....	128
Figure 50. Correlation of total air contents between pressure meter and ASTM C 457.....	131
Figure 51. Correlation of total air contents between AVA and ASTM C 457. ....	131
Figure 52. Correlation between AVA and ASTM C 457 generated spacing factors.....	132
Figure 53. Spacing factor versus air content relationship for ASTM C 457 and AVA.....	132
Figure 54. Reactions in hydrating cement. ....	138

## LIST OF TABLES

Table 1. Commercial portland cement characteristics used in Task 2.1.1.....	36
Table 2. Oxide analyses of cements.....	37
Table 3. Oxide analyses of supplementary cementing materials.....	38
Table 4. Particle size distributions of cementitious materials.....	38
Table 5. Tests conducted on paste systems in all rounds.....	41
Table 6. Summary of paste and mortar data from round 1. ....	43
Table 7. Summary of data from round 2.....	45
Table 8. Summary of data from rounds 3 and 4. ....	47
Table 9. Summary of all paste and mortar data. ....	48
Table 10. Test plan for early stiffening and normal concrete systems. ....	51
Table 11. Test plan for retarding and normal concrete systems. ....	51
Table 12. Physical properties of aggregates. ....	52
Table 13. Nominal concrete mix proportions (SSD). ....	52
Table 14. Temperature, air content, unit weight, slump, and impedance results.....	54
Table 15. Slump loss and mortar flow loss.....	55
Table 16. Setting time, NDT, and semi-adiabatic cell results. ....	56
Table 17. Minislump test data for round 1.....	68
Table 18. Minislump test data for round 2.....	70
Table 19. Minislump test data for round 3 and 4.....	76
Table 20. Minislump test data for investigating effect of w/cm. ....	77
Table 21. NIST test data for round 1. ....	78
Table 22. NIST test data for round 2. ....	79
Table 23. NIST Test Data For Round 3 and 4.....	80
Table 24. Oxide analyses of cements.....	93
Table 25. Oxide analyses of supplementary cementing materials.....	94
Table 26. Physical properties of aggregates. ....	94
Table 27. Concrete mixtures. ....	95
Table 28. Concrete mix proportions. ....	96
Table 29. Fresh concrete properties.....	97
Table 30. Setting time data. ....	97
Table 31. Results of ASTM ring tests.....	98
Table 32. Hardened concrete properties for mix WRA1. ....	99
Table 33. Hardened concrete properties for mix WRA2.....	99
Table 34. Hardened concrete properties for mix FA1. ....	100
Table 35. Hardened concrete properties for mix FA2. ....	100
Table 36. Hardened concrete properties for mix 25FA90. ....	101
Table 37. Hardened concrete properties for mix 4FA90. ....	101



Table 38. Hardened concrete properties for mix 25FA70. ....	101
Table 39. Hardened concrete properties for mix 4FA70. ....	102
Table 40. Results of minislump tests conducted on 25FA90 pastes.....	112
Table 41. Air entraining admixtures and related properties. ....	116
Table 42. Cementitious materials composition and fineness.....	116
Table 43. Coarse aggregate grading.....	117
Table 44. Fine Aggregate Grading.....	117
Table 45. Concrete test matrix used in stages 2 and 3 of subtask 2.1.3.....	122
Table 46. Base concrete mixture.....	123
Table 47. Corresponding calculations for average clustering rate.....	126
Table 48. Foam drainage results. ....	127
Table 49. Fresh concrete properties.....	129
Table 50. Hardened concrete properties. ....	130
Table 51. Compounds of calcium sulfate in cement.....	136



## CHAPTER 1. INTRODUCTION

### OVERVIEW

The objectives of this project were to develop practical test protocols and procedures with criteria in the following three areas to assess the effects of combinations of materials for concrete pavements:

- Early stiffening and excessive retardation that can affect workability, placeability, consolidation, and finishing.
- Potential for early-age cracking including plastic shrinkage; and possibly the ability to attribute the cause of cracking to chemical, physical, and environmental phenomena.
- Characteristics of the air void system including nonuniformity, insufficient air, coalescence of air voids around aggregate, and excessive large voids, all of which influence strength or durability, or both.

This study considered the following materials:

- Portland cement and blended cements.
- Fly ash, slag, silica fume, and other pozzolans.
- Chemical admixtures.
- Aggregates.

The research also considered the following effects of production and placement methods:

- Factors influencing segregation.
- Bleeding and cohesiveness relative to finishability.
- Influence of environmental conditions such as temperature and humidity.

The developed procedures have been incorporated into guidelines for evaluating and qualifying combinations of materials for use in pavements. An implementation plan with recommendations and materials for dissemination of the information (e.g., technical summaries, presentations) appears in this volume in Chapter 4, Summary, and in Volume II.

The protocol is phased to allow combinations of materials to be filtered through a set of relatively accessible tests. Potentially problematic combinations then can be subjected to more rigorous investigation.

### BACKGROUND

Premature pavement distress can result from causes such as alkali-silica reactivity, D-cracking, and materials contamination, all problems that have been researched extensively and solutions are known. Other incidents of premature pavement distress have led to questions about the

ability of concrete pavement to achieve a desired service life.<sup>(1)</sup> Examples of these types of distress are early stiffening, poor consolidation, early-age cracking, and lack of proper air entrainment. Little is known about these early pavement distresses, mainly because of a lack of tests to determine the susceptibility of materials combinations to these distresses.

Lack of compatibility among various cementitious materials and admixtures can lead to early stiffening, which could account for many other problems. The tendency to early stiffening may be attributed not only to the individual cementitious materials, but also to interactions among the various cementitious materials and the chemical admixtures. Early stiffening may be caused by excessive calcium sulfate in the form of hemihydrate (plaster) in the cement (false set) or the uncontrolled early hydration reactions of the tricalcium aluminate ( $C_3A$ ) (flash set). False set may be overcome by continued mixing of the concrete. Early stiffening is not reversible and leads to loss of workability. When concrete is hard to place, it is likely water will be added, which reduces both strength and durability and increases the potential for shrinkage and cracking. The addition of some admixtures improves workability without these negative effects, but the admixtures also add considerably to the cost of the concrete, and they may retard setting.

Early stiffening depends on several factors, including  $C_3A$  content and reactivity; alkali content; and the form, content, and distribution of sulfates in the cement.  $C_3A$  hydrating in the presence of sulfate ions forms ettringite on its surface. The ettringite acts as a barrier, further limiting reactivity. If supplementary cementing materials, particularly Class C fly ash, contain aluminate phases, and the sulfate is not well distributed in the cement paste, the concrete may experience early stiffening. A balance among the ions in plastic concrete is necessary to prevent early stiffening. Some chemical admixtures, particularly Type A water reducers, may disturb this balance.

Early stiffening can be deleterious to pavement performance. If the concrete cannot be thoroughly consolidated, loss of strength and durability can result, as well as early development of cracking and pavement failures.<sup>(2)</sup> If extraordinary consolidation efforts are used to achieve the required concrete density, the entrained air-void system may be altered, leading to decreased freeze-thaw durability.<sup>(3,4)</sup>

Cracking in concrete can also be caused by a host of factors. Shrinkage can occur in fresh or hardened concrete. The major cause of plastic shrinkage cracking is thought to be the tensile stress developed as water evaporates from the surface of the concrete, leaving the capillaries partially filled and creating a disjoining pressure caused by surface tension effects. The risk of cracking may be higher in concretes that exhibit early stiffening because the mix does not remain fluid long enough to allow a layer of bleed water to remain on the surface. While bleeding is generally thought of as detrimental to concrete, bleeding may also have some benefit with relation to the potential for plastic cracking: drying of the surface cannot occur if it is covered with bleed water. Precautions to prevent plastic shrinkage cracking include (1) strict adherence to specifications regarding evaporation rates and cessation of concrete placement if relative humidity is low and temperatures and wind speeds are high, (2) use of fog sprays, and (3) use of evaporation retarding admixtures during and immediately after finishing.

Cracking can also occur because of autogenous shrinkage, drying shrinkage, thermal effects, and external loads. Cracking occurs when and where the maximum principal tensile stress exceeds the tensile strength of the concrete.

A number of paving projects have experienced problems related to use of synthetic air-entraining agents resulting in accumulations (coalescence) of air voids around the aggregate particles. In addition to this problem, the quality of the air void system in the hardened concrete continues to be a matter of concern. The spacing factor and specific surface are the main parameters of the concrete air void system that indicate the ability of the concrete to resist the damaging effects of frost. In recent years, it has been observed that marginal air void systems may result from incompatibility between certain water reducers and air-entraining agents.

## **STUDY GOALS, OBJECTIVES, AND SCOPE**

The primary goal of the study was to develop reliable tests or standards to predict potential incompatibility of concrete materials that adversely affect the properties of concrete at early ages. The availability of such tests and standards will allow material suppliers, concrete producers, and users to identify undesirable material combinations so that use of marginal concrete for paving can be avoided. A secondary goal of the study was to understand the mechanisms behind the observed behaviors.

Following is a list of the specific objectives for the research in this project:

- Develop or refine test procedures that can be used to evaluate the potential of materials and combinations of materials to contribute to early stiffening in concrete pavement mixtures. After test procedures are refined, develop test protocols and guidelines for evaluating job materials using the proposed procedures.
- Develop or refine test procedures that can indicate the potential for cracking of concrete mixtures including plastic shrinkage cracking and cracking resulting from restraint of drying shrinkage and temperature shrinkage. Develop test protocols and guidelines.
- Develop or refine tests to determine characteristics of the air void system in concrete, preferably while the concrete is still fresh.

A suite of phased tests has been developed into a protocol of relatively simple tests to assess the potential for incompatibility in a given set of concrete materials. If the results of these tests indicate possible problems, a more sophisticated set of tests can then be applied to more firmly establish the risk of problems and possible remedial actions.

Following is a list of components in the scope of this project:

- Conduct a literature review.
- Conduct the research in accordance with the approved work plan.

- Develop guidelines and test protocols for identifying the effects of incompatible concrete materials.
- Submit a final report documenting the work performed.
- Develop a comprehensive implementation and technology transfer plan.

## CHAPTER 2. LITERATURE REVIEW

### GENERAL

An extensive review of literature was conducted pertinent to the three areas of interest—early stiffening and retardation (rheology), premature cracking, and air void systems in concrete. The review focused on the following three objectives:

- Identify the extent of field problems and various manifestations of these problems.
- Determine if material incompatibility was the identified or suspected cause of these problems.
- Review test procedures identifying concrete material incompatibility.

In addition to the literature review, the study included a survey of highway officials, technical support staff from cement companies, and field office staff from the American Concrete Pavement Association (ACPA) to collect information on highway paving projects that was not reported in the literature. The following section summarizes responses and discusses construction materials and practices that may result in premature failures or unacceptable pavement and specific findings related to concrete rheology, premature cracking, and air void systems. A discussion on construction materials and practices distinguishes problems related to individual materials and construction practices from the problems related to use of incompatible materials.

### NEED FOR INFORMATION REQUEST RESPONSES

The following field problems were reported in response to a request for field experience information:

- Excessive void system caused by angular fine aggregate movement during placement and finishing operations.
- Longitudinal joint deterioration attributed to poor air void systems.
- Premature cracking in pavements, prestressed elements, and bridge decks, possibly related to incompatibility among admixtures, Class C fly ash, and cements.
- A mix exhibiting retardation attributed to incompatibility between the cement and water reducer, causing the no set in the concrete and cracking. The problems occurred in both cool and warm weather and disappeared with a change in the water reducer.
- Serious retardation in concrete that contained low-alkali Type I cement and 30 percent Class C fly ash. One Type-A lignosulfonate water reducer was used at a dosage of 2 ounces (59 milliliters) per 100 pounds (45 kilograms) of cement.

Testing indicated that the effect of the admixture on cement hydration was an important factor.

- Excessive slump loss and air loss within about 15 min at a paving site during November 2000. The concrete mix used 350 kilograms per cubic meter ( $\text{kg/m}^3$ ) (517 pounds per cubic yard (pcy)) of cement and no fly ash. The slump and air loss at the project and in the laboratory were attributed to the cement.
- Early stiffening problems such as excessive slump loss from the plant to the paving train resulted in poor strength results from field cast specimens. The water reducer used had no beneficial effect on the workability of the cement-Class C fly ash blend paste and, in fact, resulted in early stiffening. A change in the chemical admixtures was found to be effective.
- Material incompatibility may have caused some of the problems attributed to requirements for smoother pavements, high production placement, use of Class C fly ash, poor mixing cycles, and poor air void system.
- Early transverse shrinkage cracking in a concrete pavement and cracking were observed adjacent to several transverse joints during joint sawing. The early cracking was attributed to a retarded mix, possibly caused by overdosing the water reducer. The problem was corrected by increasing the cement content to 60 percent and reducing the slag and fly ash components to 30 percent and 10 percent, respectively.
- Low strength and air void clustering were observed frequently in one construction season. The problem was attributed to a lack of cement dispersion (measures to ensure effective dispersion of cement, use of water reducers, proper mixing action, and use of vinsol resin to achieve necessary air in relatively stiff mixes), cement composition (use of high dosage of air-entraining agent with low alkali cement), aggregates (use of blended aggregates and higher amount of fine aggregate to achieve required air void characteristics), and ambient temperature (routine use of water reducers and retarders under high ambient temperature conditions minimizes retempering the concrete with water when slump loss occurs). Clustering of air voids and low compressive strength can occur when concrete is retempered with water.
- Excessive slab warping and curling were observed in a pavement. A task force is looking at ways to specify reduced concrete shrinkage.
- Air void stability on a project where low alkali cement was used with high dosages of air-entraining admixtures.

## **CONSTRUCTION MATERIALS AND PRACTICES**

A survey of highway officials, technical support staff from cement companies, and field office staff from ACPA collected information on highway paving projects not reported in the literature. The survey also provided insights into current construction practices. The Pooled Fund Study, a statistical analysis of the histories of pavements in several States, provided additional



information about combinations of materials and practices associated with premature deterioration.<sup>(5)</sup> The association between materials and practices on one hand and poor performance on the other was generally anecdotal from the people surveyed and statistical from the Pooled Fund Study.

## **Construction Materials**

### *Class C Fly Ash*

Jennings et al. cited the use of Class C fly ash as one of the factors most strongly associated with pavement deterioration.<sup>(5)</sup> Numerous respondents to the informal survey also implicated Class C fly ash as the cause of premature deterioration. One State highway department no longer allows the use of fly ash in highway pavements because of this association. The exact causes of problems associated with certain combinations of portland cement and Class C fly ash are not known; however, the possibilities include available alkalis, CaO, and aluminates.<sup>(1)</sup> Free lime increases water demand, contributing to the loss of workability of the fresh concrete. Alkalis, CaO, and aluminates all affect setting. Alkalis accelerate the hydration reactions of the cementitious materials. Cement contains sulfates to control the hydration of the aluminates; however, if fly ash is added at the batch plant, the sulfates in the cement may not be sufficient to control the hydration of the additional aluminates from the fly ash. Several respondents to the survey associated the combination of Class C fly ash and hot weather placements with early stiffening.

### *Cement*

Alkalis in fresh concrete accelerate the hydration of the cementitious materials, and thus the setting of the concrete, making it difficult to place and consolidate the concrete. In addition, the loss of slump causes a loss of entrained air. Jennings et al. correlated incidents of premature deterioration with alkali contents of the cementitious materials.<sup>(5)</sup>

Sulfate is added to the cement to control the hydration of the aluminates (C<sub>3</sub>A) to prevent early stiffening. The department of transportation in one State limits the sulfate content of the cement to a maximum of 3 percent, regardless of the C<sub>3</sub>A content. The ASTM C 150 (2004) specification sets maximum sulfate contents of 3 percent for Type I cements with C<sub>3</sub>A contents up to 8 percent, and 3.5 percent for contents exceeding 8 percent. The specification allows higher sulfate contents provided that the mortar-bar expansion (ASTM C 1038) remains below acceptable limits. Lower limits set by some departments of transportation may result in cements in which control of the hydration of the C<sub>3</sub>A is only marginal. Additional aluminates from supplementary cementing materials would only increase the possibility of early stiffening.

### *Aggregate Grading*

In a well-graded aggregate, the smaller particles efficiently fill up the spaces between the larger particles so that the void space remaining is minimized. Gress also emphasized the importance of using the largest maximum aggregate size compatible with other requirements.<sup>(1)</sup> A continuous uniform aggregate grading minimizes the content of cement paste, which in turn minimizes the cost of the concrete, the heat of hydration, the volume of entrained air required to achieve an acceptable air void system, and the shrinkage of the hardened concrete. With a poorly graded

aggregate, the concrete is difficult to mix, place, consolidate, and finish. Aggregates with insufficient fines may result in excessive bleeding.

Sometimes only poorly graded aggregates are available, or the larger aggregate particles must be removed because they are subject to D-cracking. In that case, adjustments must be made to the mix design to compensate. These adjustments may include increasing the quantity of cement, using supplementary cementing materials, and increasing the volume of entrained air.

## **Construction Practice**

### *Concreting in Hot Weather*

Hot weather or high placement temperatures were cited by several respondents to the survey, as well as by Jennings et al.<sup>(5)</sup> Because the construction season spans the summer months, hot weather placements are unavoidable. In times of high demand for cement, it is shipped immediately after it is produced, still warm from the plant, increasing the temperature of the concrete. Elevated mix temperatures make mixing, placement, consolidation, and finishing more difficult. Loss of slump is associated with loss of entrained air. Rapid hydration of the cement increases the rate of heat evolution. Thermal gradients within the concrete may cause early cracking. Hot windy weather may result in plastic shrinkage cracking. The rapid loss of slump may tempt the crew to add water to the concrete, reducing strength and durability and increasing the risk of air void agglomeration. Increasing mix temperatures means that additional air-entraining admixture will be required to achieve the same air content.

### *Mixing*

If concrete is mixed briefly and subsequently not remixed, it may exhibit stiffening known as “brief mix set.”<sup>(6)</sup> Several survey respondents mentioned very short mixing times as a potential cause of early pavement distress. The low slumps (typically 1 inch or less) of today’s pavement concretes would make them difficult to mix thoroughly. Air-entraining admixtures need sufficient time to develop an adequate air void system. Because most pavement concretes are transported to the site in dump trucks, the only mixing they receive is at the central batch plant. Whiting and Nagi found greater variations in air content with short mixing times, and recommended that concrete be mixed at least 75 seconds (s) to obtain an adequate air void system.<sup>(7)</sup>

### *Delays in Placement*

Long haul times or delays in placement also contribute to the loss of entrained air. Whiting and Nagi reported that the loss of air content is typically 0.5 to 1 percentage points per hour, but that the rate of loss is greater for air contents higher than 6 percent.<sup>(7)</sup> When concrete is transported to the site in nonagitating trucks, the loss of air content ranges from 1 to 4 percentage points, depending on the haul time and consistency of the concrete. Placement techniques also can cause loss of air content. Whiting and Nagi recommended that the exact loss for equipment and techniques be established by test to compensate for the loss of air. One survey respondent cited this practice as a remedy for low air contents in the pavements in his State.

### *Vibration*

Vibration to consolidate the concrete also can result in loss of air, as seen in vibrator trails along the length of the pavement. Stutzman found that the air void systems of deteriorated pavements were worst in the vibrator trails.<sup>(8)</sup> Stark found that higher vibration frequencies had the most pronounced effect.<sup>(3)</sup> Concretes with low water-to-cement ratios (w/c) lost less air than those with higher w/c. Resistance to frost damage was related to both spacing factor (thus vibration) and w/c. Simon et al. also found that near the vibrator, the total volume of air was reduced by removal of the entrapped air and a portion of the entrained air, which was not necessarily detrimental to frost resistance.<sup>(9)</sup> Whiting and Nagi recommended that for slip-form paving, vibration frequency should be limited to 8,000 vibrations per minute (vpm) for paver speeds greater than 0.9 m/min (3 ft/min), and frequencies should be reduced for lower speeds.<sup>(7)</sup> Tymkowicz and Steffes identified excessive vibrator frequency at 12,000 vpm in one project, and excessive vibration locally when the paver speed was reduced to half that of normal with a vibrator frequency of 8,000 vpm.<sup>(4)</sup> Two survey respondents indicated that vibration frequencies are monitored continuously in their States.

### *Control Joints*

Concrete is subject to drying shrinkage and thermal expansions and contractions. A pavement slab will crack when such contractions occur unless contraction joints (also known as control joints) are provided as appropriate. Kosmatka et al. indicate that control joints should extend to a depth of one-fourth of the slab thickness.<sup>(10)</sup> Control joints may be formed in the fresh concrete with hand groovers or by placing strips of wood, metal, or preformed joint material at the joint locations. Control joints also may be cut into the concrete as soon as it is strong enough to resist damage from the saw blade, usually 4 to 12 h after the concrete hardens. Supplementary cementing materials generally slow the early strength gain of the concrete. Thus, they may necessitate longer waits before the joints can be cut. Four of the survey respondents reported cracking resulting from delayed or improper cutting of control joints.

### *Curing*

Curing provides the conditions of moisture and temperature that allow the concrete to develop strength and water-tightness. Senbetta and Malchow<sup>(11)</sup> found that proper curing could increase the abrasion resistance of concrete by 50 percent or more compared to air-drying. When curing cannot be applied sufficiently early, plastic shrinkage cracking may develop. It is essential to prevent moisture loss (e.g., by fogging, monomolecular layer, or—after finishing—application of a curing compound). Effective curing methods reduce the rate and magnitude of early shrinkage. For paving projects, the most practical method of curing is the application of a membrane-forming curing compound. These compounds prevent loss of water from the concrete.

## **FINDINGS ON RHEOLOGY, CRACKING, AND AIR VOID SYSTEM**

Many practices in the construction of highway pavements are less than ideal. Placement during hot weather, short mixing times, transport in nonagitating trucks, excessive or insufficient vibration, and poor timing of control joint sawing all contribute to unsatisfactory performance. Some materials and combinations of materials are more sensitive to these practices than others.

In particular, combinations of cement with Class C fly ash and cementitious materials with chemical admixtures have the potential for incompatibility, leading to early stiffening, increased cracking, and inadequate air void systems. The information collected on these issues is highlighted in the following paragraphs. The test program discussed later takes into account the findings from the literature review and the conditions encountered in pavement construction.

## **Rheology Findings**

The workability of fresh concrete is defined as the ease and homogeneity with which concrete can be mixed, placed, consolidated, and finished. Concrete loses workability, consistency, and other attributes with time. The rate of this loss is of paramount interest in paving because the concrete is usually mixed at the plant and transported to the site in nonagitating trucks. Interactions between concrete constituents can contribute to loss of workability.

### *Cementitious Materials and Early Stiffening*

When slump loss is so rapid as to interfere with the normal placing and finishing of concrete, it is often described as “early stiffening.” The stiffening of concrete could result from either the excessive amounts of calcium sulfate as hemihydrate (plaster) in the cement (false or plaster set) or the uncontrolled early hydration reactions of the aluminate component (early stiffening or “flash set”). False set is generally associated with short concrete mixing times and delivery without subsequent agitation. Although false set can be overcome by continued mixing of concrete through the stiffening phase, stiffening caused by inadequate control of aluminate hydration is not recoverable. Early stiffening is encountered more frequently in the presence of water-reducing and set-controlling admixtures.

Two ASTM standard test methods, ASTM C 451 and C 359, are intended to identify the early stiffening behavior of portland cement.

Depending on the chemistry of the system, the severity of false set or early stiffening may vary. Dehydration of the gypsum during milling may result in severe false setting. Hansen provided an extensive discussion of false set in portland cement. Lost plasticity is often regained on further mixing.<sup>(12)</sup>

Early stiffening depends on several factors. The form, size, distribution, and type of sulfate source control the release of sulfate ions in the pore solution. A balance is usually achieved through the reaction between the sulfate ions and  $C_3A$ . Although this reaction controls the reactivity by forming ettringite around the  $C_3A$  grains, analysis of the cement oxide composition does not provide any information on sulfate solubility characteristics of a cement.<sup>(13)</sup>

A proper  $C_3A$ -sulfate control is critical to hydrating cement paste and the performance of admixtures addition.<sup>(14)</sup> Improper aluminate control typically results in poor admixture efficiency, workability loss, and reduced strength. Wadso demonstrated the use of a multichannel conduction calorimeter for detecting cement-admixture incompatibility and to quantify retardation in hydrating cements in the presence of added sulfates and chemical admixtures.<sup>(15)</sup> He concluded that this device was efficient, easy to use, and required small size samples.

Marginally controlled and sometimes uncontrolled cements are sometimes encountered. Uncontrolled cements exhibit early stiffening tendencies even in the absence of admixtures. Marginally controlled cements generally do not exhibit abnormal stiffening behavior in the absence of chemical admixtures; however, in the presence of admixtures, the delicate balance between the soluble sulfate and  $C_3A$  may be disturbed. Well-controlled cements in general exhibit improved workability in the presence of water-reducing admixtures.

Water-reducing admixtures improve workability through the absorption of organic molecules on the surface of cement particles, reducing the interparticle forces and increasing dispersion. While the sugar content of the lignin-based, water-reducing admixtures may result in set retardation and air entrainment, a higher dosage of water-reducing admixtures may also affect strength development.<sup>(16)</sup> Type F high-range water-reducing admixtures have less effect on cement hydration and setting. The occurrence of cement-admixture incompatibility with high-range water-reducing admixtures is less than with water-reducing admixtures. In some combinations of cement with high-range water-reducing admixtures, severe slump loss has been encountered at higher dosages.<sup>(16)</sup> Because high-range water-reducing admixtures generally are not used in paving concrete, emphasis is given in this project only to water-reducing admixtures. In many cases, the incompatibility between some cements and water-reducing admixtures can be overcome by delaying the addition of the admixture by as little as half a minute. In some cement-admixture combinations, air-entraining admixtures may lead to early stiffening.

Supplementary cementing materials such as fly ashes and ground, granulated blast-furnace slag may also affect stiffening. Fly ash may contain reactive aluminate phases such as  $C_3A$  and Klein's compound (calcium sulfoaluminate), which may not be adequately controlled by the sulfates in the cement. If there is an incompatibility, the stiffening can be severe. Slag generally does not contain any such fast hydrating phases; however, jagged slag particles may reduce workability. On the other hand, fly ash may improve workability.<sup>(17,18)</sup>

False setting, if not overcome by remixing, and early stiffening of concrete, may affect the performance of concrete in the plastic and hardened states. If concrete is mixed briefly, and it is not remixed subsequently, it may also stiffen. This stiffening is also known as "brief-mix-set," which is different from early stiffening.<sup>(6)</sup> When cement incompatibility leads to stiffening, the water demand increases. The problems generally associated with early stiffening are related to workability, bleeding, setting time, and finishability of the plastic concrete. Subsequently, strength development and durability of the hardened concrete are also affected. For paving concrete with slump less than 50 mm, the incompatibility may cause inefficient consolidation, which may lead to honeycomb and lower strengths. In addition, durability may also be affected because the air content and the spacing factor may be adversely affected.<sup>(16)</sup>

### *Incompatibility between Materials*

Incompatibility between materials may arise from chemical and physical causes. When the incompatibility is of chemical origin, it is generally caused by some combination of cement, supplementary cementitious materials, and chemical admixtures, often at elevated temperatures. Physical incompatibility may arise from the mix proportions of the concrete. For example, a cement with normal setting characteristics may show stiffening behavior depending on the amount of cement and the type of aggregates used.<sup>(19)</sup> When chemical incompatibility is

combined with physical incompatibility, the early stiffening behavior may be compounded. Chemical incompatibility may be evaluated in cement paste and physical incompatibility in concrete. The paste can be evaluated before testing the concrete for physical incompatibilities. The concrete can be tested both at the plant and in the field, providing quality control measures before and during the paving job.

### *Techniques to Measure Workability of Cement Paste and Concrete*

Workability of concrete is most indicated by slump; however, if the slump is less than 50 mm, measurement of workability loss will lack the precision needed to diagnose incompatibility. In recent years several researchers applied rheological principles and methods to concrete for better characterization of the concrete workability. Rheological measurements determine the relationship among shear stress, shear strain, and time. For a simple (Newtonian) liquid, the shear stress is directly proportional to the shear rate, and the constant of proportionality is called the “coefficient of viscosity.” A Bingham fluid flows only when a certain shear stress is overcome, after which it flows at constant rate with increasing shear rates. This rate, or the slope of the curve, is called “plastic viscosity.”<sup>(20)</sup> In general, concrete exhibits a behavior similar to that described by the Bingham model.

### *Rheological Evaluation of Cement Paste System*

Kantro developed a minislump cone test as a rapid, simple method for evaluating the influence of water-reducing admixtures on the workability of neat cement paste.<sup>(21)</sup> A high-intensity mixer is used to make cement paste that is rheologically similar (i.e., comparable shear history) to that found in a typical concrete mix.<sup>(19,22)</sup> Researchers familiar with the minislump test routinely use the mixing protocol developed by Helmuth<sup>(22)</sup> and Tang and Bhattacharja<sup>(19)</sup> to evaluate cement paste rheology.<sup>(18,23)</sup> To predict the behavior of concrete, the cement paste should be mixed with high shear. (See references 18, 19, 22, 23.)

Ferraris and her collaborators have been evaluating cement paste using viscometers with parallel plate geometry.<sup>(18,23,24)</sup> Rheology of concrete depends on the gap between the aggregates, and parallel plate geometry allows them to vary the gap to simulate different interaggregate spacings in concrete. The interaggregate distance modifies the shear environment during concrete mixing, and it depends on the volume of the paste fraction. To avoid slippage, the faces of the parallel plate rheometer used by Ferraris and coworkers were serrated. Parallel plate rheometers are commonly used in asphalt laboratories at State departments of transportation (DOTs), commercial asphalt testing facilities, and asphalt concrete contractors. With some modification of the software and perhaps the hardware, this viscometer can be used to evaluate cement paste rheology.

### *Rheological Evaluation Methods*

To test the flow characteristics of concrete, it is necessary to apply shear stress. The schemes that have been used to generate shear stress in the existing methods can be divided into four categories: (1) free flow, (2) free flow under confinement, (3) rotational, and (4) vibrational.<sup>(20)</sup> These rheometers and the associated physical principles have been discussed at length by Ferraris et al.<sup>(18,25)</sup> and Wong et al.<sup>(26)</sup> The stiffness of concrete commonly used in pavement

applications is far above the application range of rheometers. The limitations of these rheometers have been discussed in several papers. (See references 18, 25, 27, 28.) Vibration has been used to test concretes with stiffness similar to that used for pavements. Some of these are Ve-Be time or remolding test (ASTM C 1170), and vibrating slope apparatus.<sup>(26)</sup> Vibration is commonly used during paving operations, and the concrete flows when the vibrational force transferred exceed the yield stress of the concrete.

Even though vibration makes it flow, low-slump paving concrete cannot be assumed to behave like a fluid. The calculation of a plastic viscosity from measurements taken under vibration is complex. Vibration also alters the rheological characteristics to such an extent that the behavior of vibrated concrete is very different from that of unvibrated concrete.<sup>(29)</sup> Only one rheometer is capable of measuring the rheological parameters while concrete is vibrated.<sup>(30)</sup> Because only a limited number of tests using vibration were performed with this instrument, the results may not correlate with field performance.

#### *Thermal Methods for Evaluating Cement-Admixture Incompatibility*

A proper aluminate control is critically related to the performance of admixture in the early age behavior of hydrating cement paste. Insufficient aluminate control often results in reduced admixture efficiency, loss of workability, and poor strength development. Cement-admixture interaction is often complicated and difficult to predict by current standards. Sandberg and Roberts reviewed the application of isothermal calorimetry for cement hydration related to aluminate-sulfate interaction in the presence of admixtures.<sup>(14)</sup> They found the heat signatures to be suitable for observing the hydration characteristics of combinations of additional soluble sulfates, supplementary cementing materials, and chemical admixtures.

Earlier, Wadso (2004) also demonstrated the use of conduction calorimetry as a convenient method for detecting cement-admixture incompatibility and to quantify retardation in hydrating cements in the presence of added sulfates and chemical admixtures.<sup>(15)</sup> The calorimeter used was designed to have multichannels for simultaneously testing 14 samples of cement pastes and mortars. This device had advantages over the semi-adiabatic calorimeters because it requires small-size samples, effectively makes use of the heat released, and is easier to use.

### **Early Stiffening Tests**

#### *Cement Paste Tests*

To diagnose incompatibility, the rheological measurements should be performed on cement pastes similar to those found in a typical concrete mix. This will require high-shear mixing of cement paste under controlled temperature conditions. Cement paste rheology can be tested using either parallel plate or coaxial cylindrical viscometer. Both perform reasonably well for cement paste.

Although parallel plate viscometers are generally available at DOT laboratories, the coaxial cylindrical viscometer is very common. During experimental development, the gap in the parallel plate viscometer may be modified to simulate the interaggregate spacing between aggregates. For industry to use such a method, the gap must be standardized to avoid any misleading results and conclusions. The gap between the spindle and cup in a coaxial cylindrical viscometer is

generally not varied. To minimize the effect of bleeding, a parallel plate viscometer is used with lower w/c ratios. Some chemical admixtures and supplementary cementing materials may increase bleeding, which may interfere with the rheological measurements. This is of less concern for a coaxial cylindrical viscometer, but the results can still be influenced by a concentration of particles at the bottom of the container; nevertheless, these two well-established rheological tools are best suited to evaluate cement paste.

### *Concrete Tests*

In paving operations, concrete is generally mixed in a batch plant and transported to the job site in a dump truck. If concrete suffers from false set or plaster set, the little agitation generated during transport and dumping may not be adequate. During unloading at the job site, the agitation may be adequate to regain some plasticity, but the concrete is likely to lack uniformity. After unloading, the concrete sits idle until the paver reaches it. The concrete is thoroughly agitated when the paver passes it through the auger. At this stage, the agitation is adequate, and false setting concrete may regain its plasticity. Considering this sequence of paving operations, false set appears not to be a problem. The stiffening behavior becomes an important issue if the concrete cannot be properly consolidated even with vibration.

Because vibration is always used for placement and consolidation of pavement concrete, concrete that does not achieve the desired quality under these conditions must be identified. The effect of combinations of the vibrational parameters (frequency and amplitude within the range practiced in the field) on the consolidation characteristics of concrete must be evaluated. If a concrete cannot be consolidated within the available range of vibrational parameters, it may be identified as early stiffening.

A concrete testing techniques that appears appropriate for paving concrete is the vibration testing apparatus, in which remolding or consolidation characteristics of the concrete are measured.<sup>(31)</sup> The settlement of the concrete is measured from the loss of concrete height as a function of vibration time.

### **Cracking Findings**

In several reported cases of cracking in pavement concrete, incompatibility between two or more of the concrete ingredients contributed to cracking. In other cases, the influence of other factors such as weather, design factors, and construction practices caused, or at least contributed to, the cracking. It is not always appropriate to examine these factors in isolation because a particular combination of ingredients may work well at some temperatures and not in others. Also, a particular combination of materials may be more sensitive to construction variables such as mixing time or curing practices.

### *Importance of Cracking*

Permeability of concrete is the key to durability. One of the most important strategies in protecting concrete from the action of aggressive agents is not to prevent deterioration (which may be impossible), but to retard it by limiting the ability of these agents to enter the concrete. Cracking dramatically increases permeability. Aldea et al. measured the permeability of concrete loaded under controlled conditions and found that the coefficient of permeability increased with



increasing crack width by several orders of magnitude.<sup>(32)</sup> While concrete having cracks less than 100 micrometers ( $\mu\text{m}$ ) (0.004 inch) wide exhibited a decrease in permeability over time, the permeability of concrete with cracks 200  $\mu\text{m}$  (0.008 inch) or higher remained unchanged.

Early cracks widen over time because of mechanical- and environment-induced stresses. The cracks become channels for the ingress of water and other harmful species; therefore, minimizing early cracking is important to the service life of the concrete. Chatterji identified four mechanisms responsible for cracking in concrete at early ages: (1) differential plastic shrinkage, (2) self desiccation, (3) desiccation, and (4) temperature differences between the interior and surface concrete.<sup>(33)</sup> Frequently the conditions that give rise to one of these mechanisms also favor another, and the combined effect is greater than the sum of individual effects.

Springenschmid et al. pointed out that cracks do not occur because of high temperatures, but because of the thermal stresses caused by the heat of hydration and the restrained deformations of the concrete.<sup>(34)</sup> In addition, strains unrelated to thermal effects (for example, self desiccation) often have an important influence. Springenschmid and Breitenbücher cited two parameters that must be considered in the assessment of cracking potential.<sup>(35)</sup>

- Cracking sensitivity of a concrete mix that depends on constituents, mix composition, and fresh concrete temperature.
- Boundary conditions (dimensions of a member, degree of restraint, temperatures).

#### *Cracking from Autogenous, Plastic, and Drying Shrinkage*

When the evaporation rate is higher than the rate of bleeding, the air-water interface penetrates into the concrete. Capillary menisci form, compressing the concrete mix and causing plastic shrinkage. Because of differential rates of plastic shrinkage in different parts of a concrete section, cracks appear. Plastic shrinkage cracking can be avoided by preventing the formation of menisci, that is, by preventing the evaporation of water from the surface.<sup>(33)</sup>

Long before cracks are visible, extensive microcracking occurs even on relatively mild drying. Drying can occur even in cold temperatures if the concrete temperature is considerably warmer than the ambient temperature. With the passage of cold air over the warm surface, air temperature is raised, lowering the relative humidity. The reduction in relative humidity dries the concrete surface, possibly enough to cause cracking. In this situation, covering the concrete with a plastic sheet prevents evaporation without affecting the thermal behavior.<sup>(33)</sup> Powers et al. subjected hydrated cement paste specimens to extended drying at 93 percent relative humidity (RH), followed by further drying at 79 percent RH and then resaturation.<sup>(36)</sup> They found that the water permeability of these specimens increased by a factor of about 70 compared with companion specimens, which were never dried. Chatterji<sup>(33)</sup> attributes this behavior to the formation of microcracks in the paste on drying.

Krauss and Rogalla found that drying shrinkage could be reduced by reducing the total paste volume and the water content, maximizing the aggregate volume, using Type II cement, and using an aggregate with low shrinkage.<sup>(37)</sup> They also found that extended moist curing does not necessarily decrease the total shrinkage, but may reduce the rate of shrinkage.

During the hydration of cement, the volume of the cement paste decreases. The change in volume depends on the original w/c and the degree of hydration. Continued hydration after the concrete sets can result in self-desiccation, in some cases causing cracks even before forms are removed.<sup>(33)</sup> Holt emphasized the importance of early-age shrinkage in the development of cracks.<sup>(38)</sup> Standard test methods measure the shrinkage of concrete from an age of 24 hour (h) onward. However, Holt reported that shrinkage in the first 24 h might exceed all shrinkage that takes place after that time.

### *Heat of Hydration and Thermally-Induced Cracking*

Traditionally, temperature differences between surface and interior have been limited to minimize the stresses (and cracking) due to thermal gradients. However, as Bernander pointed out, “there is no generally valid proportionality between temperature difference and stress.”<sup>(39)</sup> Stress calculations which take into account the nonuniform development of maturity in the concrete at different locations within a section show that the assumption of a linear relationship between the temperature distribution and the resulting stress distribution is simply not valid. However, in practice the assessment of risk of cracking is often based solely on temperature criteria.

Initially, the heat of hydration of the cement generates thermal expansion in the concrete. However, at early ages the modulus of elasticity is low, so that the restraint of this expansion does not generate significant compressive stresses. In addition, such compressive stresses that do develop are reduced by a high degree of relaxation. By the time the concrete cools off, the modulus of elasticity increases and the tendency to creep reduces, so that the tensile stresses generated by the restraint of thermal shrinkage are higher to begin with and do not relax as much.<sup>(35)</sup>

Thermal cracks may appear either in the heating or the cooling phase after the concrete is placed. Very early cracks that appear during the heating phase tend to close at the end of the cooling period. These cracks are generally surface cracks, which may or may not adversely affect performance. Cracks that occur in the cooling phase generally extend through the thickness. Depending on the geometry and the environmental conditions, these cracks may appear weeks, months, or even years after placement.<sup>(39)</sup>

Bernander recommended the use of cement with a low cracking sensitivity.<sup>(39)</sup> When this property cannot readily be determined, the use of low heat cements would be appropriate. In addition, the cement content can be reduced by the use of water reducers (which reduce the amount of paste required for good workability), replacement of some of the cement by supplementary cementing materials, and the use of a large maximum size of aggregate. In hot weather, Krauss and Rogalla recommended avoiding placement temperatures greater than 27 °C (80 °F), maintaining the placement temperature of the concrete at least 11 °C (20 °F) lower than ambient, placing the concrete during late afternoon or evening rather than morning or early afternoon, minimizing solar radiation during placement, and allowing lower early strengths by specifying 56- or 90-day strengths.<sup>(37)</sup>

### *Factors Affecting the Tendency of Concrete to Crack*

Analytical studies performed by Krauss and Rogalla showed that the modulus of elasticity of the concrete, adjusted for the effects of creep, affects both thermal and shrinkage stresses more than any other property of concrete.<sup>(37)</sup> The higher the modulus of elasticity, the higher the stresses associated with a given thermal or shrinkage strain. The use of aggregates with low modulus of elasticity, increased paste contents, and reduced concrete strengths would all reduce the modulus of elasticity of the concrete. These measures would also increase the total shrinkage.

Krauss and Rogalla recommended the following measures to reduce the tendency of concrete to crack: low modulus of elasticity at early ages; low early strength; high early creep; low cement content; good quality, low-shrinkage aggregates; low hydration temperatures; pozzolans with low heat of hydration; low coefficient of thermal expansion; minimum paste volume and free shrinkage; Type II cement; shrinkage-compensating cement.<sup>(37)</sup> The use of fine cement, silica fume, and other admixtures that give high strength and modulus of elasticity should be avoided.

Springenschmid and Breitenbücher summarized the relative effectiveness of measures that might be taken to reduce the tendency of concrete to crack.<sup>(35)</sup> Following the European practice, these are quantified in terms of their effects on the cracking temperature of the concrete. Measurement of the cracking temperature is described below. Simultaneous use of more than one of these measures generally results in effects that are less than the sum of the individual effects. Both the net effectiveness and the costs must be evaluated case-by-case. Springenschmid et al. considered it unreasonable to specify the maximum cracking temperature acceptable for a concrete.<sup>(34)</sup> Rather, the measures required to prevent cracking should be specified.

As Bernander pointed out, measures designed to avoid early-age cracking are directed primarily toward reducing the cement content. Such measures may jeopardize the mentioned materials requirements with regard to strength and durability.<sup>(39)</sup> As these requirements may vary with type of structure and environment, different measures for controlling cracking are necessary. The selection of a specific strategy for control of cracking in a given project will depend on the associated costs and benefits.

**Construction Variables.** The tendency of concrete to crack increases with the placement temperature of the fresh concrete. Springenschmid and Breitenbücher cited two reasons for this: (1) A high placement temperature will accelerate hydration of the cement, which generates heat and increases the temperature of the interior of the member, so that the temperature gradient is increased, and (2) high curing temperatures result in lower tensile strengths resulting from the type of microstructure that develops under these curing conditions.<sup>(35)</sup>

The placement temperature and the ambient temperature strongly influence the temperature distribution in the concrete. The interaction between them can be decisive for the tendency to crack at early ages. A suitable choice of placement temperature in relation to ambient temperature allows the possibility of optimizing prestress in the surface layers as well as of avoiding adverse conditions that cause surface cracking.<sup>(39)</sup>

Some measures used to control temperature are not always compatible with the goal of reducing cracking.<sup>(39)</sup> For example, a very low placement temperature on a hot summer day may actually

favor the formation of surface cracks caused by nonuniform maturity of the concrete through the thickness of the section. The warmer surface concrete develops strength and stiffness first, while the cooler interior concrete hydrates more slowly. When the interior portion of the concrete does begin to hydrate, generate heat, and expand, the surface concrete is already starting to cool and contract, generating tensile stresses at the surface. For pavement slabs, Bernander recommended reducing the placement temperature of the concrete, using cement with low cracking sensitivity, and optimizing the cement content to control the temperature rise. Control of drying shrinkage by the use of moist curing or curing compounds is essential. Joint spacing should be determined to minimize restraint. The concrete should be protected from solar radiation.

Cracking at early ages may be exacerbated by simultaneous exposure to low ambient temperatures, high surface temperatures (from solar radiation), and drying shrinkage. The risk of cracking caused by thermal expansion of the interior is greatest during the heating phase, when avoidance of exposure to drying and low temperatures is critical. For this reason, curing with water or curing compounds and protecting from direct sun are recommended.<sup>(39)</sup>

Van Breugel pointed out that the effect of wind on temperature development could exceed that of solar radiation.<sup>(40)</sup> Rapid cooling of the surface because of wind may result in steep temperature gradients between surface and interior. He warned that ignoring the effect of wind on temperature might completely invalidate the interpretation of otherwise sophisticated calculations. Holt measured the shrinkage of concrete specimens from the time of casting and found that if the concrete were allowed to dry with no wind, the shrinkage for the first 24 h was equal to the shrinkage in the next 3 months.<sup>(38)</sup> In the case of concrete allowed to dry with wind, the shrinkage during the first 24 h was seven times that of the long-term shrinkage. Thus, it is essential to begin curing as soon as possible.

Roper and Anderson observed that in slabs on grade the permeability of the base material has an important effect on cracking.<sup>(41)</sup> Their experiments showed that bleed water remained on the surface of concrete cast on an impermeable base far longer than for the same concrete cast on a granular base, making it less susceptible to plastic shrinkage cracking; however, tests of the quality of the concrete placed showed it to be inferior to that of the concrete cast on a permeable base.

**Materials Factors.** Krauss and Rogalla summarized the material properties of concrete that affect cracking tendency: cement content and composition, modulus of elasticity at early ages, creep, aggregate type, placement temperature, heat of hydration, and drying shrinkage.<sup>(37)</sup> They found that mix design factors affecting the tendency to crack include aggregate type and grading, cement type and amount, water content, supplementary cementing materials, silica fume, and chemical admixtures.

Aggregate with a low coefficient of thermal expansion will provide less restraint for the concrete, reducing its cracking sensitivity. Springenschmid and Breitenbücher considered crushed aggregates to be advantageous because their rough surface improves the tensile strength of the concrete.<sup>(35)</sup> A high maximum size reduces the amount of cement paste required for workability. The reduced cement content results in reduced temperature rise caused by the heat of hydration. With a high maximum aggregate size, the tensile strength may be somewhat reduced.

Cements that develop a modulus of elasticity relatively quickly would reduce the sensitivity of concrete to cracking because the concrete could develop some compressive prestress during the initial thermal expansion. As Springenschmid and Breitenbücher pointed out, it is not known how to implement this theoretical requirement.<sup>(35)</sup> It is clear that different cements give different sensitivities to cracking. Springenschmid and Breitenbücher reported that portland cements with low cracking sensitivity have relatively low alkali contents and high sulfate contents in relation to their C<sub>3</sub>A contents, and they are not too fine.<sup>(35)</sup> Also, high early strength results in increased tendency to crack.

Thomas and Mukherjee found that slag is effective in reducing the initial rate of heat development and the maximum temperature rise.<sup>(42)</sup> These effects increased with the slag content; however, these benefits are at least partially offset by concomitant reductions in the tensile strength and tensile strain capacity of slag concrete at early ages. Thus, the replacement of portland cement by slag may not be effective in mitigating thermal cracking without the use of additional measures. Chan et al. found that the presence of slag in the concrete increased the autogenous shrinkage, while the presence of fly ash reduced it.<sup>(43)</sup> Ternary concretes containing both supplementary cementing materials behaved similarly to the slag concretes.

Thomas et al. investigated the effects of 12 different fly ashes on the temperature rise and early-age tensile strain capacity of concrete.<sup>(42)</sup> They found that the rate and amount of heat evolved increased with the calcium content of the fly ash; however, increasing fly ash contents reduced the heat evolved for all of the fly ashes tested. Thus, even high-calcium fly ashes are effective in reducing the heat evolved if used in sufficiently large doses. The flexural strength of the concrete decreased with higher dosages of fly ash. The strain capacity at one day was reduced for many of the fly ash concretes compared to the control. The strain capacity of the fly ash concretes was similar to or slightly higher than that of the control concrete at 3 and 7 days. Thus, the beneficial effect of the fly ash in reducing temperature rise is not necessarily offset by reductions in the capacity to resist thermal strains. The authors did not consider the effects of creep and stress relaxation in their analysis.

Springenschmid et al. recommended that concrete strengths higher than necessary be avoided because high strengths often lead to higher cracking tendency.<sup>(34)</sup> Specifiers may prefer to specify a 56- or 90-day strength rather than a 28-day strength to reduce cementitious content, and therefore, the cracking tendency.

Ziegeldorf et al. tested the mechanical properties of cement pastes at early ages and found that those with lower w/c exhibited a rapid increase in tensile strength at about 7 h and little change in tensile strength between 15 and 75 h.<sup>(44)</sup> The compressive strength increased rapidly at first and continued to increase at later ages. The development of the modulus of elasticity was similar to that of the tensile strength. The development of strain to fracture was not uniform. Pastes with higher w/c showed a steep decrease with age up to 10 h, with a minimum at about 30 h. Pastes with lower w/c also showed a minimum at about 7 h.

To reduce the stresses caused by drying shrinkage, the water content should be kept as low as possible. A large maximum size aggregate and optimized particle size distribution of the aggregates, particularly for the sand, will minimize the amount of cement paste (and water)

needed for good workability. Further reductions in water content can be achieved by the use of water reducers, and by keeping the placement temperature low.<sup>(34)</sup>

Springenschmid and Breitenbücher reported that air entrainment increases the ultimate tensile strain by about 20 percent and reduces the modulus of elasticity and the consequent stresses caused by restraint.<sup>(35)</sup> Both effects reduce the cracking sensitivity of the concrete.

#### *Test Methods for Evaluating the Tendency of Concrete Mixtures to Early Cracking*

**Cracking Rings.** Krauss and Rogalla developed a test method in which concrete is cast in the annulus between a stiff inner steel ring and an outer steel ring.<sup>(37)</sup> The restraint supplied by the inner ring to the shrinkage of the concrete is comparable to that encountered in full-depth bridge decks, while the outer ring provides little restraint to expansions. Water is ponded on the concrete surface. At the end of the curing period, the water and the outer steel ring are removed, and heavy plastic sheeting attached to the top surface to prevent loss of water. Strain gauges attached at the quarter points on the inside of the inner ring indicate when the concrete cracks. Sellevold et al. have used a similar test apparatus.<sup>(45)</sup>

This test method provides a close approximation of the conditions encountered in concrete bridge decks; however, it is impossible to simulate the effects of delayed or negligent curing within the first hours (before final set). The test can be of long and highly variable duration; Whiting and Detwiler found that their silica fume concrete specimens took from 18 to 51 days to crack, and some did not crack at all.<sup>(46)</sup> More important, it is not clear what constitutes a good or acceptable result in terms of performance in the field; one can simply conclude that one concrete is more or less prone to crack than another.

The ASTM International has published a test method (ASTM C 1581) to determine the age of cracking in mortars and concrete under restrained shrinkage. The procedure can be used to determine the relative effects of cementitious materials properties on the risk of drying shrinkage cracking.

**RILEM Cracking Frame.** The International Union of Testing and Research Laboratories for Materials and Structures (RILEM) cracking frame consists of a closed insulated frame with two crossheads and two invar steel bars 100 mm (4 inches) in diameter. The fresh concrete is placed directly into the formwork of the frame. Thus, deformations are restrained from the beginning, with the degree of restraint being at least 75 percent. Strain gauges on the steel bars allow for continuous measurement of the deformations, and thus, the forces in the bars and in the concrete specimen.<sup>(47)</sup>

The information provided by the cracking frame data, that is, the stresses developed under conditions of restraint, is probably more useful than the time required to crack the concrete. This test method has the additional advantage of allowing for simulation of a wider variety of conditions of curing, including drying conditions beginning at the time of casting. The main disadvantage of this method is the high cost of the invar steel bars.

**ICBO Method: Cracking of Slab Under Restraint.** The International Conference of Building Officials (ICBO) Test Method for Evaluating Plastic Shrinkage Cracking of Restrained Concrete with Synthetic Fibers specifies a test panel 356 by 559 by 102 mm (14 by 22 by 4 inches) deep.

Immediately following casting and screeding, the finished surface is subjected to a wind generated by a fan. Internal restraints and a stress riser are cast into the panel to initiate cracking. This test provides a reasonable simulation of conditions likely to be encountered in the field on hot, windy days when cracking is most problematic; however, because it includes all of the conditions at once, it does not provide insights into the causes of cracking in a particular concrete.

**Japan Concrete Institute Method: Unrestrained Shrinkage.** The tendency to crack is closely related to shrinkage. If the concrete is completely unrestrained, it may shrink or expand freely and no stresses develop. If the concrete is restrained from shrinking, tensile stresses develop. This is particularly critical at early ages because the concrete has little or no tensile strength to resist the stresses, and thus, it is vulnerable to cracking. Tests such as ASTM C 157, Standard Test Method for Length Change of Hardened Hydraulic-Cement Mortar and Concrete, can be used to measure the free shrinkage of concrete at later ages (normally after 28 days curing), but ignore the critical first few days.

The Technical Committee on Autogenous Shrinkage of Concrete of the Japan Concrete Institute (JCI) reported on a new test method that measures the autogenous shrinkage or expansion of concrete specimens from the time of casting.<sup>(48)</sup> The specimens are 100 by 100 by 400 mm (4 by 4 by 16 inches). Gauge plugs are cast into each end to allow for measurement of any changes in length using dial gauges or other sensors. The bottom plate of the mold is covered with a polytetrafluoroethylene sheet and all surfaces of the mold are then covered with polyester film to prevent any restraint of the concrete specimen. After 24 h, the specimens are removed from the mold and sealed on all sides with aluminum adhesive tape. Length changes are monitored up to 28 days.

Holt and Leivo pointed out a difficulty inherent in this test method in relation to anchoring gauge plugs in fresh concrete.<sup>(49)</sup> At very early ages, the concrete may settle under its own weight. Because the embedded gauge plugs move with the concrete, the sensors could register settlement as a length change; however, this problem is expected to be minimized in the case of the low- or no-slump concretes used for paving. This test has the advantage that test conditions such as temperature and curing could be modified as needed to simulate conditions in the field.

Researchers who have used the test have indicated that precision and reliability of the test was poor.

### **Fundamental Properties of Concrete Related to Cracking**

For modeling, heat of hydration curves indicate the rate and amount of heat developed over time. These can be used to predict the temperature of the concrete at different locations and different times. Van Breugel considered that the various types of hydration curves—adiabatic, semi-adiabatic, or isothermal—to be equally useful for modeling.<sup>(40)</sup> The selection depends on the experimental difficulties in obtaining the data and the size of the concrete elements to be analyzed. Adiabatic curves for the first 72 h of hydration can be determined accurately using an adiabatic calorimeter. These have the advantage of being possible to determine for the concrete mix to be used on site, and they are most appropriate for simulating conditions in mass concrete. Semi-adiabatic curves are generally easy to determine for concrete. In smaller sections from

which some heat loss can be expected, these would simulate the hydration conditions reasonably well. Isothermal hydration curves usually apply to cement paste rather than concrete, and thus, they may not fully represent the hydration of cement in concrete. In any case, isothermal hydration would not be expected in concrete structures. The data generated from these tests can be used in modeling to predict the thermal history of the concrete at early ages.

The times of initial and final set can be determined by ASTM C 403, Standard Test Method for Time of Setting of Concrete Mixtures by Penetration Resistance. In this test, mortar is sieved from a representative sample of concrete, placed in a container, and stored at a specified ambient temperature. The resistance of the mortar to penetration by a set of standard needles is measured at regular time intervals. From a plot of penetration resistance versus elapsed time, the times of initial and final set are determined. This test has distinct advantages over tests on cement paste or mortar made expressly for the measurement of setting times. Testing cement paste is inappropriate because the shearing experienced by cement paste in concrete is very different from that imposed by the standard mixing procedure. Shearing has a significant effect on the rate of hydration of the cement at early ages, so it is essential to simulate the mixing conditions as closely as possible. The mortar test is preferable from the standpoint of mixing, but it is somewhat different from that of mixing in concrete. In addition, a large batch of concrete can be used to cast several types of test specimens, so that the data from different tests can be directly compared. Setting times could be determined for more than one ambient temperature to simulate different weather conditions in the field.

The basic mechanical properties of the concrete—compressive and tensile strength and modulus of elasticity—change rapidly within the first 24 h. The modulus of elasticity determines the stress developed when a volume change such as autogenous shrinkage, thermal expansion, or contraction is restrained. The tensile strength measures the ability of the concrete to resist cracking under these stresses; thus, it is essential to measure these properties at frequent intervals from the time of final set, particularly within the critical first 24 h. Standard ASTM tests for all of these properties are well established. As with the other tests, different specimens should be maintained at different temperatures so that the effect of weather can be included as a variable.

The mechanical properties of concrete would be difficult to monitor in the field by the methods described in the previous paragraph; however, they can be correlated with appropriate nondestructive test data for field use. Ultrasonic pulse velocity measurement has not been successful in determining the quality of early-age concrete, principally because of the attenuation of signal strength through the relatively thick units. A more recent approach to record the evolution of fresh concrete while still in the formwork (or molds) is described by Rapoport et al.<sup>(50)</sup> This approach concentrates on the interface between the formwork or mold and the concrete, and relies on the ultrasonic shear wave reflection from this interface. The reflection energy is measured, and it has been shown to be directly related to properties such as setting action between 1 and 6 h and modulus of elasticity after 12 h. The equipment used in those studies operates at a much higher frequency range than the direct transmission method (between 1 and 10 megahertz (MHz)). This is in the frequency range normally applied to steel weld testing, and is made possible by the relatively small signal penetration depths required. Repeatability and sensitivity are thereby enhanced. Laboratory specimens in metal molds can be monitored at the same time intervals used for the conventional mechanical tests and the data correlated. For field monitoring, metal boxes could be cast as inserts into the concrete.



See et al. outlined a procedure to quantify concrete behavior under restrained shrinkage using a ring specimen.<sup>(51)</sup> Cracking resistance of concrete is a combination of shrinkage potential, shrinkage rate, tensile creep, and tensile strength. Tensile creep was shown to be important in evaluating the risk of cracking under restraining conditions. It was also realized that shrinkage-reducing admixtures significantly improved the cracking resistance of concrete by reducing the shrinkage potential and the shrinkage rate. The data also showed that tensile creep under restrained shrinkage was lower than under a constant stress—suggesting the data on tensile creep obtained under classical constant load may lead to nonconservative predictions on concrete performance.

Hossain et al. developed a simple stress solution for the ring test data as an attempt to make the ring test more quantitative.<sup>(52)</sup> Their procedure incorporates restrained ring test with acoustic emission, which can be used in evaluating stress development and cracking tendency for various concrete bridge decks, patching, or paving mixtures.

## **Air Void System Findings**

### *Purpose and Mechanism of Air Entrainment*

Concrete used in pavements in cold regions of the country, such as the Midwest and the Northeast, is exposed to severe winter conditions. This includes heavy snowfall, the application of large quantities of deicing agents, and many cycles of freezing and thawing while concrete is in a saturated condition. Concrete is susceptible to frost damage because it is porous. Porosity of concrete consists of an interconnected pore system (capillary pores) representing the space occupied by mix water that did not become part of the hydrated portland cement. When subjected to freezing, concrete may be degraded because of the pressure generated by the movement of water or ice through the internal pore system. The mechanisms of frost damage are driven by the freezing of water in the capillary pores; however, the exact mechanism of frost damage is still not completely understood, even though it has been extensively studied for more than 50 years. It has been established that concrete with a proper air void system will sustain many cycles of freezing and thawing without serious damage, as the inclusion of entrained air provides empty space within the paste to which the excess water can move and freeze without damage.

While a minimum amount of entrained air certainly is needed, the quality of the air void system in the hardened concrete is the most important factor in its ability to withstand a severe freezing and thawing environment. Theoretical work has indicated that the minute air voids introduced into the concrete during mixing must, in the final hardened state, be of such a size and spacing that disruptive forces induced by migration of water during freezing can be relieved so that the tensile strength of the concrete is not exceeded.<sup>(2)</sup> Spacing factor and specific surface are the main parameters of the concrete air void system controlling frost resistance. The spacing factor is a measure of the distance water must travel before reaching an air void.<sup>(36)</sup> Specific surface is a measure of air void size. Higher specific surfaces are associated with a system consisting of a large number of small voids. The air bubbles, if properly spaced, act as safety valves to protect all the paste.

Air-entraining agents have been used in concrete for more than 50 years to produce an entrained air system that protects the concrete from frost damage. Air on the surfaces of cement and aggregate particles is normally entrapped in concrete on mixing, but it is of limited value because the air voids are too large and widely spaced. The addition of a suitable surfactant entrains additional air in the form of a stable foam that persists in the hardened concrete as a system of finely divided air voids well dispersed throughout the cement paste. Taylor describes air-entraining admixtures generically as long-chain molecules with a polar group at one end, which becomes concentrated at the air-liquid interface with their polar parts in the liquid and nonpolar parts in the air.<sup>(53)</sup> The air-entraining agent lowers the surface tension of the water, stabilizing the air bubbles. The inner surfaces of the air bubbles are composed of hydrophobic material formed by the nonpolar parts of the molecules. This material acts as a barrier to the entry of water during mixing or placement of the fresh concrete, or when the hardened concrete is saturated.

Until the early 1980s the majority of air-entraining agents were based solely on the salt of wood resin (neutralized vinsol resin). This material is a by-product of a process for recovering various solvents and rosins from pine wood stumps. These were originally marketed as vinsol, short for “very insoluble,” and later were known as vinsol resin. Because they are highly insoluble, they are neutralized with sodium hydroxide to form a soluble sodium soap, which is the basis of commercial formulations.<sup>(2,7)</sup> Neutralization allows the admixture to form films around air bubbles immediately after addition to and subsequent agitation of the concrete mix because it does not require any further reaction with alkalis generated by cement hydration. For this reason, entrained air is generated quickly with vinsol resin air-entraining agents, and there is a temporary minor increase in air content with continued mixing, followed by air loss with prolonged mixing.

In addition to neutralized vinsol resin, several groups of air-entraining admixtures were available but not widely used in highway construction. However, because of the limited supplies of vinsol-based admixtures and their relatively high cost, other types of air-entraining admixtures have been used more frequently in highway construction in the last few years.

It is difficult to define the exact components of an air-entraining admixture because of their complexity and the proprietary nature of manufacturers’ formulations. In addition to vinsol resin, air-entraining admixtures available in the market generally include wood-derived acid salts such as tall oil, vegetable oil acids, synthetic detergents, and others. Each class of these admixtures will generate air void systems somewhat different from the others. For example, tall oil-based agents will generate very small air bubbles, while vegetable oil acid-based air-entraining agents will create coarser air bubbles. A complete evaluation of the air void system is important when any new air-entraining agent is used, even though all other materials in the mix have remained the same.

### *Factors Affecting Air Entrainment*

In addition to air-entraining agents, all materials used in concrete (portland cement, supplementary cementing materials, water, chemical admixtures, sand, and aggregate) to a certain degree influence the air void system.<sup>(7)</sup> Production procedures, construction practices and field conditions also affect the air void system of concrete. The effects of these factors on the air void system have been studied extensively over the years. Recently the focus of research has

been on specific issues such as the effect of chemical admixtures and their compatibility with air-entraining admixtures and supplementary cementing materials.

Certain combinations of water reducers and air-entraining admixtures can be incompatible, resulting in unacceptable air void systems. Plante et al. indicated that increasing the dosage of water reducers influences the air void system.<sup>(54)</sup> Doubling the recommended dosage of any of three water reducers in their study negatively influenced the stability of the air void system. There was no consistent relationship between the change in admixture dosage and the resulting air content.

Accelerating admixtures have a minor effect on the air void system. Stott et al. studied the effect of both calcium chloride and nonchloride accelerating admixtures on frost durability.<sup>(55)</sup> They found that the air content and spacing factor of mixes containing accelerating admixtures did not differ from those of the control mixes. Attiogbe et al. indicated that properly air-entrained concrete containing superplasticizer could have adequate frost resistance even if the spacing factors were relatively high.<sup>(56)</sup> Spacing factors exceeding the American Concrete Institute (ACI) recommended maximum values of 0.20 mm (0.008 inch) were determined in their concretes, yet the frost resistance was acceptable.

Increases in the water content will increase the air content up to a point as the workability increases, but air may be lost from very fluid concrete. While increasing the cement content produces a greater number of smaller air bubbles, an increase in water generates coarser bubbles. Because air-entraining admixtures are surfactants (surface-active agents), the fineness of the cement influences the air content of the concrete. The introduction of more surface area with increasing fineness of the cement increases the required dosage of air-entraining admixture. Air content is decreased by increasing the cement content of a given concrete mix; therefore, a higher dosage of air-entraining agent (per unit mass of cement) is needed to maintain the required air content.

An overview also summarized the basic principles and influences of pore formation, manufacturing, and evaluation of air-entraining concretes.<sup>(57)</sup> Resin-based soaps and mixtures of both nonionic and ionic tensides are commonly used in developing air-entraining agents for concretes. The influence of cement type, additives, and aggregates, and a number of other factors needs to be considered for producing air-entrained concrete.

The chemical and mineralogical compositions of cement types (for example, intermixed substances, sulfate carriers, grinding aids) play a role in the air pore characteristics. Each cement needs to be evaluated for the amount of air-entraining agent to be used for a specific application. Fine particle additives can have detrimental effect on the formation and stability of air voids. Particle size and shape (spherical or pointed) of the additives also play a role. It is pointed out that additives that are not compatible with air-entraining agents may not develop the air pores at all, or they may destroy the already existing air pores.

Also, a change in aggregate sources such as sand and gravel pits can lead to variation in particle size distribution—especially in the range < 1 mm (0.04 inch) can have a pronounced effect on air void system. A large proportion of < 0.25-mm (0.01 inch) particles make formation of air voids difficult, whereas the presence of a high proportion of particles between 0.25 and 1 mm (0.01

and 0.04 inch) favors the formation of air voids. It is also recommended that only fresh water be used as mix water for concrete because the recycled water containing fine particle suspensions can cause uncontrollable changes in air void systems.

Pigeon et al. indicated that an increase in the soluble alkali content of the cement significantly improved the stability of the air void system, especially when superplasticizer is used.<sup>(58)</sup> They also found that the use of superplasticizer with a low-alkali cement can increase the spacing factor. Whiting and Nagi reported that alkalis allow more of the air-entraining agent to remain in solution during the mixing process, making it more effective.<sup>(7)</sup> The higher the alkali content of the cement, the lower the required dosage of air-entraining admixture.

Air content increases with increasing sand content; therefore, the dosage of air-entraining agent needs to be decreased as the sand content is increased to maintain the same air content. Coarse sand also increases the air content; however, spacing factors may be higher than acceptable. Pavements in Nebraska and Kansas, where coarse sands were used in concrete mixtures, exhibited freeze-thaw failure (in the form of scaling) even though the air contents were higher than specified.<sup>(59)</sup>

The use of supplementary cementing materials in concrete will affect its air void system. High carbon content in fly ash decreases the air content because carbon adsorbs the air-entraining agent and prevents it from acting to stabilize the air bubbles in fresh concrete; therefore, higher dosages of air-entraining agent are needed to form stabilized air void systems. Gebler and Klieger indicated that the air void system of concrete containing ASTM C 618 Class C fly ash is generally more stable than that of concrete containing Class F fly ash.<sup>(60)</sup> Their study showed that while fly ash affects the volume of air, it has less influence on the air void system parameters (spacing factor and specific surface). Studies showed that concretes containing up to 50 percent fly ash (percent by mass of total cementitious material) can have adequate frost resistance.<sup>(61)</sup> Their research indicated that different sources of fly ash did not have a significant effect on the concrete air void system. It has been found that silica fume does not have a significant influence on the production and stability of the air void system, but because of its fineness, higher amounts of air-entraining agent are needed.

Construction practices such as retempering (adding water to restore consistency), working in high temperatures, prolonged vibration (or over-vibration), and pumping may lead to alterations in the air void system of concrete. Compared with other construction factors, placement temperature can be more critical and difficult to control. Higher temperatures will require higher dosages of air-entraining admixtures to maintain a given air content.<sup>(7)</sup> However, Saucier et al. found that, while changes in temperature lead to changes in the total air content, the spacing factor of the hardened concrete is not significantly affected.<sup>(62)</sup> It has been observed recently that at high placement temperatures, some new air-entraining admixtures can cause the air bubbles to accumulate at the surfaces of aggregate particles, weakening the concrete. This phenomenon is discussed in the next section in more detail. If considerable air is lost because of any of the above factors, there may be insufficient air bubbles left to achieve the necessary spacing factors that are required to ensure good freeze-thaw durability.

Gardner and others have attributed several effects of elevated temperature on concrete.<sup>(63)</sup> This may include rapid setting because higher temperature facilitates faster formwork turnover;

elevated mix temperatures results in higher 28-day compressive strengths; elevated mix and curing temperatures lead to increase in pore diameter.

Pang and others developed a modified lignosulfonate superplasticizer to positively influence the hydration temperature and the resulting microstructure. It was found that the admixture could remarkably retard the cement heat of hydration.<sup>(64)</sup> With the dosage of 0.35 percent, the temperature dropped by 13 °C; thus, the amount of thermal crack reduced and the population of smaller pores increased. The growth of ettringite became refined as the crystal size turned small, which made the concrete denser, less permeable, and more corrosive resistant.

Khayat and Assaad evaluated the influence of mix proportioning on the stability of air void system in self-consolidating concrete (SCC) when subjected to agitation.<sup>(65)</sup> Several samples were tested at different time intervals to analyze the variation in air void system upon agitation. A modified point-count method was used to determine the air voids. The corresponding parameters evaluated were Bingham rheological parameters (plastic viscosity and yield stress), slump flow, filling capacity, V-funnel flow time, and surface settlement. Data indicated that the air void characteristics in SCC could be similar to those in normal-slump concrete. Greater air void stability could be achieved when the SCC had a higher content of cementitious materials and a lower water-to-cementitious materials ratio (w/cm). For mixtures with a relatively low cementitious material content and a high w/cm, air void stability may still be obtained by incorporating a viscosity-modifying admixture. It was pointed out that to avoid coalescence of small air bubbles during agitation, the plastic viscosity and yield stress values should not exceed 10 N·m·s (88.5 lbf·in·s) and 2 N·m (17.7 lbf·in·s), respectively. Such limits also yield greater air void stability in occasionally agitated concrete.

#### *Recent Problems With Air-Entrainment in Concrete Pavements*

A survey conducted by Nagi and Whiting, found that 85 percent of the respondents indicated having experienced some problems with control of air content.<sup>(66)</sup> Over the years concrete users have learned to overcome most of these problems. In the last 10 years, numerous incidents related to use of air-entraining agents in highway concrete were reported in many States. The most common problem was the loss of strength associated with the use of synthetic air-entraining agents. Loss of air caused by excessive vibration of concrete during paving procedures was also reported.

**Air Void Clustering.** Loss of strength associated with the use of new air-entraining admixtures (mainly synthetic admixtures) was noticed in several States in the last few years. Interviews with DOT personnel, researchers, and concrete producers in the Midwestern and Eastern States confirmed the occurrence of such problems. Strength reductions of 20 percent or more have been observed in concrete pavements. The strength loss is usually manifested when the 28-day compressive strength is found to be less than the design strength.

An increase in air content by a percentage point leads to an average reduction of 3 to 5 percent in compressive strength. Strength reductions recently have been noted in concretes having normal air contents. When neutralized vinsol resin air-entraining agents were replaced by synthetic admixtures, the 28-day compressive strengths dropped even for comparable air contents. Most of the States reported more than usual debonding of aggregate particles during compression testing.

A failure mode of mostly shear at the interface between aggregate and paste was noticed, with very few fractured aggregate particles. Microscopic examination indicated accumulations of air voids around the aggregate particles. The presence of excessive voids around the aggregate obviously reduces the bond strength between the aggregate and surrounding mortar, leading to this type of failure.

The effect on strength of clustering air voids around aggregate particles is not a new concept; however, few cases were reported in the past. Hover reported a case study in which the accumulation of air bubbles at the mortar/coarse aggregate interface led to debonding of aggregate particles and reduction in strength.<sup>(67)</sup> The South Dakota DOT conducted a comprehensive investigation to define the causes of compressive strength reduction observed during the construction season of 1997.<sup>(68)</sup> The strength reduction was caused by poor bond between paste and aggregate, and it was attributed to the change from the traditional vinsol resin air-entraining agents to new synthetic admixtures. The report stated that the incompatibility between low-alkali cement and synthetic admixtures, along with high summertime temperatures aggravated the problem. Thinner-walled air bubbles formed by these admixtures caused more flocculation than would be observed with vinsol resin admixtures. As a result of this study, the South Dakota DOT banned the use of synthetic air-entraining admixtures.

A research project sponsored by the New Jersey DOT is studying similar strength loss problems associated with the use of the new generation of air-entraining admixtures. The New York State DOT (NYSDOT) has experienced similar problems. During summer construction when certain synthetic air-entraining admixtures were used, the compressive strengths went down even though the air contents remained within the normal range. As a result, NYSDOT banned the use of some these admixtures. The State of Delaware also encountered strength reductions on one pavement project. Personnel in the Delaware DOT materials laboratory indicated difficulties with synthetic air-entraining admixtures in passing the strength requirements of ASTM C 260. ASTM requires the concrete strength when the new admixture is used to be at least 90 percent of that of a reference concrete. In some cases compressive strengths of 80 percent or less were obtained when synthetic air-entraining admixtures were used. Based on these observations, the State of Delaware banned the use of synthetic air-entraining admixtures. A representative of the Michigan DOT indicated that the State had had problems with incompatibility among synthetic air-entraining admixtures, cement, and water reducers. Strength loss associated with aggregate debonding was observed. On the other hand, this problem was not a major concern in Illinois, Kentucky, Maryland, Missouri, and Ohio.

The effect of the use of synthetic air admixtures was more noticeable at higher air contents. As mentioned, an increase in air content by 1 percent decreases the strength by 3 to 5 percent, but, when a synthetic air-entraining agent is used, the strength reduction may be greater.

Admixture manufacturers have indicated that the problem with air void systems and the associated strength loss may be caused by short mixing times. At least one manufacturer recommended the use of neutralized vinsol resin in concrete pavements. Other factors such as the condition of aggregate (e.g., moisture content) and mixing speed may also contribute to the problem. In applications other than pavement, synthetic air-entraining admixtures did not appear to be problematic. Some ready-mix suppliers prefer to use synthetic admixtures. Air loss

resulting from haul time and agitation is lower when synthetic air-entraining admixtures are used. Air contents are sometimes increased by the longer mixing times.

Kozikowski et al. investigated the factors causing the air void clustering.<sup>(69)</sup> They studied mix design variations, mode of mixing, slump, and strength in concrete samples prepared with a variety of cements, aggregates, admixture types, and w/c. Microscopic means were used to assess the degree of clustering. Following is a summary of the results:

- A late addition of water to concrete mixes using nonvinsol admixtures would result in air void clustering. Retempering concrete mixes containing these types of admixture will exacerbate the clustering problem. The severity of clustering increases when the retempered concrete is mixed for longer periods. A later addition of water enhances the formation of air content regardless of the admixture type used.
- The potential for air void clustering may be greater in finer air void systems.
- The timing of air-entraining admixtures (AEA) addition (i.e., before or after cement is added) did not influence the air void clustering.
- Moisture in aggregate did not influence the formation of air void clustering.

Based on the data obtained, a useful rating system was developed to relate the severity of air void cluster to the strength of concrete.

**Consolidation.** Normally consolidation is carried out by vibration, which reduces the friction between the aggregate particles and makes the concrete more flowable.<sup>(7)</sup> For slip-form paving, internal vibrators are usually spaced at a maximum of 450 to 600 mm (18 to 24 inches) and operate at frequencies from 5,000 to 10,000 vpm. The purpose of vibration is to remove pockets of entrapped air generated in fresh concrete; however, vibration also can cause a loss of entrained air from fresh concrete, especially if the vibrator is held in place for extended periods. The loss of air content caused by vibration depends on the concrete slump, initial air content, vibration frequency, and amount of vibration. Studies have shown that for a given vibration frequency and vibration time, the loss of air increases with slump.<sup>(70)</sup> An increase in vibration frequency also has a significant effect on the air void system. The spacing factor significantly increased for concrete subjected to 20 s of vibration at frequencies of 11,000 and 14,000 vpm; however, for frequencies of 8,000 vpm or less, even though the air content is decreased, the spacing factor remains relatively unchanged.

In some cases of concrete pavement construction, scaling caused by cycles of freezing and thawing is observed in paths following the vibrator heads on the paving machine. This is to the result of excessive vibration. The Iowa DOT has observed an increase in premature deterioration in concrete pavements related to overvibration. This problem has been noticed on several portland cement concrete pavement projects across the State. Tymkowicz and Steffes reported that cores taken from longitudinal cracks in I-80 in Iowa contained 3 percent air in the top half and 6 percent in the bottom half.<sup>(4)</sup> Iowa DOT attributed this behavior to excessive vibration, saying that excessive vibration occurred at lower paver speeds even though the frequency was at middle range (8,000 vpm). As a result, Iowa DOT recommends that for vibration frequencies

from 5,000 to 8,000 vpm, the paver speed should be greater than 1 meter per minute (m/min) (3 feet per minute (ft/min)). The investigation indicated that the radius of effective consolidation of the vibrator was smaller than is commonly believed. Cores taken between vibrator trails showed significant entrapped air within 4 inches of the vibrator location. Stutzman conducted a similar study on Iowa pavements and found that the air void systems of deteriorated pavements were worse in the visible vibrator trails.<sup>(8)</sup>

### *Test Methods for Air Void System*

The preceding discussion summarizes the many factors that can influence the air void systems of concrete and lead to changes in its air content from design values. All highway agencies specify limits for air contents of concretes. These limits account for the possible changes in air content resulting from the factors mentioned above; however, all current specifications are based on measuring the air content of fresh concrete.

**ASTM C 231, Air Content of Freshly Mixed Concrete by Pressure Method.** This is the most commonly used test. This test serves as a very good quality control tool to assure frost resistance of millions of cubic meters ( $m^3$ ) (cubic yards ( $y^3$ )) of concrete each year used in pavements and other infrastructure; however, the total air content in itself does not guarantee frost resistance. One reason is that the total air content includes entrapped air, which does not contribute to frost resistance. In addition, many contractors target the lower limit of air content to maximize strength. This sometimes may not leave enough entrained air to protect the concrete, especially in severe exposures. As mentioned above, some concretes with high air content will not tolerate repeated cycles of freezing and thawing because of high spacing factors. Much of the air may exist in larger entrapped voids, which can protect only a small portion of the paste. The number of air voids in concretes having the same air content may vary dramatically. In one experiment, 5 to 6 percent air was incorporated into concrete by using each of five different air-entraining agents.<sup>(71)</sup> The resultant numbers of were 24,000, 49,000, 55,000, 170,000, and 800,000 voids per cubic centimeter (390, 803, 900, 2,790, and 13,100 million air voids per cubic inch).

**ASTM C 457, Microscopical Determination of Parameters of the Air void System in Hardened Concrete.** The measurement of the air void system parameters, as opposed to total air content, is a more realistic prediction of concrete performance under repeated cycles of freezing and thawing. It would be desirable to have a rapid test that could give concrete users a quick indication of the air void system so that corrections could be made without incurring extensive delays in the construction process. The only ASTM method for such measurements is ASTM C 457, Microscopical Determination of Parameters of the Air void System in Hardened Concrete. In this method, entrained air is measured microscopically on a cut and polished section of concrete. While modern computer-assisted techniques make the measurement somewhat more efficient, it is still time consuming and tedious, and concrete must be sufficiently mature to withstand polishing for examination. It may be possible to accelerate the hydration by heat curing the specimens.

Torrens and Ivey developed a test in which the air in a mortar sample is displaced by excess water in a conical glass container.<sup>(72)</sup> By tracing the area of bubbles that adhere to the glass plate, an estimate of the surface area can be obtained to compute a void-spacing indicator. The relationship between the void-spacing indicator factor and the spacing factor depends on the ratio



between the air contents of the fresh and hardened concrete. Because this ratio cannot be known in advance, predicting the spacing factor from the void-spacing indicator factor is difficult.

**ASTM Type A Air Meter.** Another technique to evaluate fresh concrete air void system has been developed by Norwegian investigators using an ASTM Type A air meter.<sup>(73)</sup> The meter is filled with concrete and subjected to external vibration. The rate of air loss with time is determined. From the rate of air loss and certain assumption related to the rheological properties of concrete, the void size distribution is calculated. The test assumes ideal behavior of air bubbles regarding their movement through the cement paste.

**Air Void Analyzer.** A more promising technique was developed in Europe in the mid 1980s to measure the air void parameters of concrete. The equipment for this test, known as an Air Void Analyzer (AVA), is commercially available. The main advantage of this technique is that the test is conducted on fresh concrete and takes less than 30 min to complete.<sup>(74)</sup> The method is based on Stoke's Law. Large bubbles rise through a column of liquid faster than small bubbles do, and therefore, bubble size can be accurately inferred from the time it takes the bubble to rise. Mortar is extracted from a concrete sample taken from the as-placed concrete and injected by means of a syringe into the base of the AVA. The mortar sample is stirred into a viscous liquid to release the air voids. The bubbles rise through the viscous liquid and water in the glass cylinder, and then, they are gathered on a petri dish suspended from a bracket attached to a sensitive balance. From the viscosity of the system and using Stoke's Law, the sizes of the air bubbles with time are computed and the air void parameters are calculated. The parameters obtained with this method are the air content, spacing factor, and specific surface.

Since 1993, the AVA has been used commercially in Denmark, Sweden, Iceland, Germany, Belgium, Switzerland, Italy, and Spain. Recently the AVA was used on the E6 Motorway in Sweden.<sup>(75)</sup> In this project, approximately 1,453 m<sup>3</sup> (1,900 y<sup>3</sup>) of concrete were produced daily. The concrete was transported on trucks and placed using a slip-form paver. The AVA was used for quality assurance to achieve frost resistance. In addition, cores were taken for ASTM C 457 test. The specific surface and spacing factor results of the two methods to determine the were almost identical.

Magura evaluated the practicality of the AVA and compared it to ASTM C 457.<sup>(76)</sup> He listed several disadvantages of some parts of the AVA procedure such as the sensitivity of the test to vibration and changes in temperature.

An evaluation of the AVA also was conducted by the Maine DOT. The equipment was evaluated during the 1998 construction season. Redmond reported, "this is a remarkable technology and should definitely be developed further."<sup>(77)</sup> When comparing AVA data with ASTM C 457 measurements, the report stated that the difference in the readings occurred when air voids larger than 3 mm (0.12 inch) (mostly entrapped air) were included in the ASTM C 457 measurement but excluded from the AVA data. The report mentioned the sensitivity of equipment to vibration and temperature.

More recently, an automated linear traverse system has also been developed by Zhang et al. to determine entrained air void in hardened concrete.<sup>(78)</sup> The technique has several analytical components including an image analysis system for surface images through a microscope,

methodology for detecting and identifying the air voids, and a computer-controlled two-dimensional actuator for bringing the sampling points in line with the microscope. The technique requires pigmenting of the sample for color contrast between the voids and matrix. Data are analyzed automatically, and air void parameters for air content, specific surface, spacing factor, void frequency are displayed and stored. After the sample is prepared for analysis, the process for the complete determination of air void parameters takes approximately 15 min.

### *Test Methods for Air Void Stability*

In a search for simpler techniques to evaluate the air void stability of concrete, most researchers looked into the use of foam theories. Several testing procedures were developed over the years to evaluate the effectiveness of an admixture or effect of combinations of materials on air void system stability. The earliest technique was used by Bruere in the 1950s.<sup>(79)</sup> He used the cylinder flotation test to evaluate the stability of foams produced by different air-entraining admixtures.

**Foam Index Test.** The foam index test<sup>(80)</sup> has been successfully used by various researchers.<sup>(7)</sup> Gebler and Klieger used the test to evaluate the stability of the air void system of concrete containing different types of fly ashes and measure the relative air-entraining admixture requirements for fly ash concretes.<sup>(60)</sup> The stability of the air bubbles formed during mixing a paste suspension may be an indication of the air void stability in concretes made with the same materials. In this test, 50 milliliters (mL) (1.7 fluid ounces (fl oz)) of water are placed in a 500 mL (17 fl oz) wide-mouth jar. Then, 20 grams (g) (0.7 oz) of the appropriate proportions of cement and fly ash are hand-blended and added to the water. The jar is capped and vigorously shaken for 15 s. A quantity of air-entraining admixture is then added, and the jar is shaken for an additional 15 s. The jar is then placed upright for 45 s, and then the cap is removed. The foam index is the minimum amount of air-entraining admixture (in mL or oz) needed to produce a stable foam, which is defined as the state where bubbles exist over the entire surface of solution in the jar. An unstable state is recognized by discontinuities in the foam, where a stable state is indicated by no breaks in the foam. The foam index has been used as a relative indication of the amount of air-entraining agent needed in the concrete, assuming that the dosage for a comparable concrete without fly ash has been determined. This dosage is then multiplied by the ratio of the foam index for the fly ash mix to the foam index of the control concrete to estimate the dosage needed for the fly ash concrete.

**Foam Drainage Test.** A more promising technique known as foam drainage test, has been selected by Cross et al.<sup>(68)</sup> in the recent South Dakota study to evaluate the stability of air void system. The foam drainage test was originally used by Gutmann.<sup>(81)</sup> He used a kitchen blender to mix air-entraining admixtures with water and then poured the foam into a graduated cylinder. The level of water drained from the foam was measured after 1 h. In the Gutmann test, only water and admixtures were used; the test did not include cement. Also, as indicated by Cross et al., the single measurement at 1 h does not allow the determination of the kinetic nature of the foam drainage.<sup>(68)</sup>

By contrast, Cross et al. included cement in their mixture. 300 mL (10 oz) of water is mixed with 10 mL (0.3 oz) of air-entraining admixture and 5 g (0.18 oz) of cement in a blender.<sup>(68)</sup> The resultant foam is poured into a 1,000 mL (34 oz) graduated cylinder. The amount of water drained as a function of time is fit to kinetic equations and the values of  $V_0$  and  $-1/k$  are

calculated.  $V_0$  is the amount of liquid in the foam at the start of drainage and  $-1/k$  is a mixture parameter. The percent of water drained and the percent of water in the foam are also calculated. These three parameters define the stability of void system formed by a given air-entraining admixture. The test data presented by Cross et al. indicate that the foam drainage test provides a rapid method for screening air-entraining admixtures.

## **SUMMARY**

Concrete mix designs are becoming more complex with the use of supplementary cementing materials and combinations of chemical admixtures. The likelihood of incompatibility among cementitious materials and admixtures increases with the number of ingredients added to the mix. Incompatibility may manifest itself as early stiffening, retardation of setting and strength gain, coalescence of entrained air voids, loss of air, or early-age cracking. These problems in turn reduce the durability of the pavement, increasing the life-cycle cost that must ultimately be borne by the taxpayer and imposing costly delays on the driving public.

Because of the complexity of concrete, it is not possible to predict incompatibility from tests of the individual materials. Combinations of the specific materials to be used on the job must be tested using methods that appropriately simulate job conditions. Numerous test methods already available could lend themselves to the prediction of various aspects of incompatibility. Some of these methods are established ASTM standards, while others are in various stages of development.



## CHAPTER 3. PROJECT TASKS

### TASK 2.1.1—EARLY SETTING OR EXCESSIVE RETARDATION

#### Introduction

One of the greatest difficulties experienced by the paving construction industry is when a concrete does not stiffen and set at the right time. Early stiffening makes it impossible to move the concrete through a slipform paving machine, resulting in poor consolidation and an unacceptable surface finish. This is particularly prone to occur during hot weather and when certain combinations of cementitious materials and chemical admixtures are used in the concrete mixture. Early setting may result in cracks appearing because of drying shrinkage before saw-cuts can be made. At the other extreme, slow strength gain and setting can also result in a higher risk of cracking because of plastic shrinkage, and difficulties with applying curing compounds, which should be conducted soon after texturing but after bleeding has stopped.

Systems that exhibit unpredictable stiffening and setting are therefore a matter of serious concern, and methods to detect such problems well before the concrete is batched are needed. The work conducted in this task was to develop such methods, as well as to better understand the mechanisms behind the observed problems.

The work conducted is described first, followed by the data collected and a discussion of its meaning and application.

Six portland cements were tested in this program, with a wide range of  $C_3A$  and alkali contents. Three different supplementary cementing materials (SCM) were included, a slag, and two fly ashes including a Class C with a high  $C_3A$  content. Two Type A water-reducing admixtures (WRA), one lignin and one sugar-based, were included in the matrix. All of these materials are discussed in more detail in the following sections.

A large suite of tests was conducted on a matrix of the materials to assess the ability of the tests to detect early stiffening and retardation type incompatibility. Some of these tests were conducted at 10 °C (50 °F) and 32 °C (90 °F) as well as at the standard 21 °C (70 °F).

Following is a summary of the rounds of the test matrix:

- Round 1. Every cement, with a single dose of every SCM and a single dose of the lignin-based WRA (24 mixtures), all at 21 °C (70 °F).
- Round 2a. Selected cement/SCM combinations (Early Stiffening) with no WRA, and at a double dosage of the lignin-based admixture (7 mixtures) at 21 °C (70 °F).
- Round 2b. Selected cement/SCM combinations (Normal and Early Stiffening) with sugar-based WRA at a single dose (6 mixtures), 21 °C (70 °F).

- Round 3. Selected cement/SCM/WRA combinations (Normal and Early Stiffening) (8 mixtures) at 32 °C (90 °F).
- Round 4. Selected cement/SCM/WRA combinations (Normal and Delayed Stiffening) (8 mixtures) at 10 °C (50 °F).

In addition, concrete mixtures were prepared and tested using selected cementitious/admixture systems at all three temperatures (36 mixtures).

Details of the materials and the selections of combinations for the various rounds are discussed in the next two sections. Discussion of the test methods and results follows.

### Materials Selection and Characterization

To cover a reasonable number of material combinations, six commercial portland cements, described in table 1, were identified based on analyses of samples received from manufacturers. North American cements contain different proportions of gypsum and hemihydrate, and the cements in table 1 provide a representative selection. To address the solubility of natural anhydrite and gypsum, cements containing anhydrite were incorporated in the program. Both retarding and early stiffening characteristics of these cements were evaluated with and without WRAs. One cement from Task 2.1.2 was also used in this task as indicated in table 1. The cements came from six plants and five manufacturers.

**Table 1. Commercial portland cement characteristics used in Task 2.1.1.**

Cement Type	Percentage of C <sub>3</sub> A Content (High is > 6)	Percentage of Alkali Content (High is > 0.6%)	Gypsum-to-Hemihydrate Ratio (High is > 1)	Comment
Type I	High	High	Low	Contains natural anhydrite
	High	High	Low	–
	High	Low	High	–
	High	Low	Low	–
Type II	Low	Low	Low	From Task 2.1.2
	Low	Low	Low	Contains natural anhydrite

A Class C fly ash was selected with a relatively high C<sub>3</sub>A content (11.4 percent) based on the experiences reported from the field that this type of material is most commonly associated with setting and stiffening problems.

The Class F fly ash used was selected with moderate to high loss-on-ignition (LOI) content (4 percent).

A commercially available ASTM C 989 grade-100 slag was selected from a local supplier.

Type A WRAs generally are made using three basic chemical forms: (1) lignins with set-balancers, (2) sugars or polymers, and (3) combinations of 1 and 2. Most of the work was

conducted using a lignin-based material (WRA A), but some mixtures were prepared using a sugar-based system (WRA B).

### Materials Characterization

The procured cements and SCMs were characterized for their phase and oxide compositions and fineness as shown in tables 2, 3, and 4. The analytical tools used were X-ray diffraction, X-ray fluorescence, differential scanning calorimetry (DSC), and thermogravimetric analysis (TGA).

Analysis and characterization of the materials used in the study involved the use of X-ray diffraction analysis and selective dissolution techniques, some of which were specially developed at the contractor's laboratory for this project. The six portland cements used for this study consisted of Type I and Type II cements with compositions ranging from low to high C<sub>3</sub>A and varying alkali contents. The supplementary cementing materials used in preparing the cement blends were Class C and Class F fly ash, and granulated slag. Both fly ashes were used at a replacement level of 20 percent by mass, while the blend made with the slag was at 40 percent.

**Table 2. Oxide analyses of cements.**

Analyte	Percentage of Mass					
	Cement 1	Cement 2	Cement 3	Cement 4	Cement 5	Cement 6
SiO <sub>2</sub>	20.51	19.06	20.29	19.48	19.22	20.83
Al <sub>2</sub> O <sub>3</sub>	4.46	6.03	5.48	5.95	5.56	4.20
Fe <sub>2</sub> O <sub>3</sub>	3.19	2.13	2.8	2.68	2.66	3.3
CaO	63.43	62.45	65.59	64.42	61.63	62.55
MgO	2.99	2.67	1.02	0.85	2.34	3.23
SO <sub>3</sub>	2.72	3.87	2.63	3.32	4.42	2.75
Na <sub>2</sub> O	0.13	0.23	0.19	0.18	0.27	0.13
K <sub>2</sub> O	0.65	1.25	0.3	0.53	0.99	0.65
TiO <sub>2</sub>	0.23	0.26	0.26	0.51	0.29	0.30
P <sub>2</sub> O <sub>5</sub>	0.07	0.31	0.16	0.24	0.21	0.09
Mn <sub>2</sub> O <sub>3</sub>	0.07	0.07	0.06	0.04	0.18	0.53
SrO	0.1	0.25	0.16	0.24	0.07	0.05
Cr <sub>2</sub> O <sub>3</sub>	<0.01	<0.01	<0.01	0.01	<0.01	<0.01
ZnO	<0.01	<0.01	0.01	0.02	0.04	0.22
L.O.I. (950 °C)	1.44	1.23	0.9	1.41	2.11	1.45
Total	99.99	99.82	99.86	99.88	99.99	100.24
Alkalies as Na <sub>2</sub> O	0.56	1.06	0.38	0.53	0.92	0.56
Gypsum plaster ratio	1.5	0.08	0.07	1.05	4.11	0.58
Anhydrite	Yes	No	No	No	No	Yes
<b>Calculated Compounds per ASTM C 150-02a</b>						
C <sub>3</sub> S	60	55	65	61	51	56
C <sub>2</sub> S	13	13	9	10	17	18
C <sub>3</sub> A	6	12	10	11	10	6
C <sub>4</sub> AF	10	6	9	8	8	10
Blaine Fineness, m <sup>2</sup> /kg	392	395	411	442	431	392

**Table 3. Oxide analyses of supplementary cementing materials.**

Analyte Material	Percentage of Mass		
	Slag	Class C Fly ash	Class F Fly ash
SiO <sub>2</sub>	37.6	32.26	52.56
Al <sub>2</sub> O <sub>3</sub>	7.95	17.38	20.26
Fe <sub>2</sub> O <sub>3</sub>	0.87	6.06	11.46
CaO	38.91	26.8	4.29
MgO	10.87	7.87	1.00
SO <sub>3</sub>	2.49	2.65	0.64
Na <sub>2</sub> O	0.33	2.03	1.32
K <sub>2</sub> O	0.37	0.35	1.92
TiO <sub>2</sub>	0.84	1.37	0.97
P <sub>2</sub> O <sub>5</sub>	<0.01	0.90	0.28
Mn <sub>2</sub> O <sub>3</sub>	0.53	0.04	0.05
SrO	0.04	0.47	0.08
Cr <sub>2</sub> O <sub>3</sub>	0.01	0.02	0.02
ZnO	<0.01	0.01	0.04
L.O.I. (950 °C)	-0.99	0.24	4.22
Total	99.84	98.47	99.1
Alkalies as Na <sub>2</sub> O	0.58	2.26	2.58
<b>Thermogravimetric Analysis (as-received basis)</b>			
Free moisture (Ambient -105 °C)		0.06	0.08
L.O.I. (105 °C-750 °C)		0.21	4.26
L.O.I. (750 °C-950 °C)		0.03	-0.04

**Table 4. Particle size distributions of cementitious materials.**

Size (micron)	Percentage Passing								
	Cement 1	Cement 2	Cement 3	Cement 4	Cement 5	Cement 6	Slag	Class C	Class F
45	90.22	87.42	87.74	89.15	88.53	90.20	97.97	74.47	84.14
30	77.51	72.49	72.43	74.71	73.58	77.74	90.96	64.51	74.09
10	41.24	36.30	34.81	37.79	36.94	37.90	56.21	39.00	40.38
7	32.05	28.67	27.46	29.96	29.34	28.62	44.93	31.71	30.34
3	16.47	14.58	14.27	15.69	15.23	13.75	23.07	16.73	12.48
1	5.41	4.72	4.73	5.17	4.99	4.03	7.11	5.12	3.10

*Cement 1*

This cement had low free lime (CaO) and moderate to high level of periclase (MgO) with high ferrite phase (C<sub>4</sub>AF) and low C<sub>3</sub>A. Alite (C<sub>3</sub>S) and belite (C<sub>2</sub>S) were present in normal amounts with only slight prehydration as indicated by the presence of small amounts of Ca(OH)<sub>2</sub>. The total alite and belite was estimated at 78 percent by mass of the cement using selective dissolution techniques. Anhydrite (CaSO<sub>4</sub>) was the predominant form of calcium sulfate present in the cement, followed by hemihydrate or plaster (CaSO<sub>4</sub>·½H<sub>2</sub>O) and gypsum (CaSO<sub>4</sub>·2H<sub>2</sub>O). The clinker sulfate was mainly present in the form of K<sub>3</sub>Na(SO<sub>4</sub>)<sub>2</sub>.



### *Cement 2*

In contrast to Cement 1, Cement 2 contained high  $C_3A$  and low ferrite phase. It was also with low free lime and moderate amounts of periclase. The alite and belite were present in normal proportions with an estimated total of 73 percent. There was slight prehydration of the silicates, as indicated by the presence of small amounts of  $Ca(OH)_2$ . Hemihydrate or plaster was the predominant form of calcium sulfate present in the cement, mixed with only a small amount of gypsum. Alkali sulfates in the form of both  $K_2SO_4$  and  $K_3Na(SO_4)_2$  were present in significant amounts in this cement.

### *Cement 3*

This high  $C_3A$  cement contained both low free lime and periclase. Again, alite and belite are present in normal proportions with an estimated total of 77 percent. No indication of prehydration was found in this cement. Hemihydrate or plaster was the predominant form of calcium sulfate form present in this cement mixed with small amount of gypsum.  $K_2SO_4$  and  $K_3Na(SO_4)_2$  were also detected in the cement but only in small amounts.

### *Cement 4*

This cement was high in  $C_3A$  content and low in both free lime and periclase contents. Alite and belite also appeared to be present in normal proportions with an estimated total of 74 percent. No indication of prehydration was found in the cement. Gypsum was the predominant form of calcium sulfate present in the cement mixed with small amounts of hemihydrate or plaster. Both  $K_2SO_4$  and  $K_3Na(SO_4)_2$  in moderate amounts were detected in the cement.

### *Cement 5*

This cement was moderately high in  $C_3A$  with low free lime and moderate amount of periclase. The alite and belite in the cement appear to be present in normal proportions with an estimated total of 72 percent. There was slight prehydration of the  $C_3S$  as indicated by the presence of small amounts of  $Ca(OH)_2$  in the cement. Gypsum was the predominant form of calcium sulfate present in the cement mixed with very small amounts of anhydrite and hemihydrate or plaster. High amounts of clinker sulfate in the form of arcanite, aphthitalite, and calcium langbeinite were detected in the cement. This cement had been received from the field (see section on cracking), and it had been in sealed storage for some time before testing.

### *Cement 6*

As with Cement 1, this cement had a high ferrite content and the lowest level of  $C_3A$  of the six cements. It also had low free lime and contained moderate amounts of periclase. As in the case of the other five cements, alite and belite were also present in normal proportions at an estimated total of 78 percent. No indication of prehydration of the silicates was found. Anhydrite was the predominant form of calcium sulfate form present, followed by hemihydrate or plaster and gypsum. The only clinker sulfate detected in the cement was  $K_2SO_4$  in small amounts.

### *Granulated Slag*

The granulated slag was completely amorphous (glassy). The characteristic amorphous peak in the diffractogram was at about 0.29 nanometers (nm), a significantly lower D-spacing than that found in Class C fly ash. The slag had an estimated glass content of 99 percent as obtained using an acetic acid selective dissolution method.

### *Class C Fly Ash*

The Class C fly ash consisted mainly of an amorphous phase (glassy phase) along with crystalline compounds that include alpha-quartz ( $\text{SiO}_2$ ),  $\text{C}_3\text{A}$ ,  $\text{MgO}$ ,  $\text{CaO}$ ,  $\text{CaSO}_4$ ,  $\text{C}_2\text{S}$ ,  $\text{C}_2\text{AS}$ , and ferrite. Further testing of the fly ash gave the following additional information:  $\text{C}_3\text{A}$  = 11.4 percent,  $\text{CaSO}_4$  = 4.0 percent, and acid insoluble residue = 28 percent. The acid insoluble residue was primarily composed of alpha-quartz ( $\text{SiO}_2$ ), anorthite ( $\text{CaSi}_2\text{O}_7$ ), sillimanite ( $\text{Al}_2\text{SiO}_5$ ), coesite ( $\text{SiO}_2$ ), cristobalite ( $\text{SiO}_2$ ), and a glassy phase that was not acid-soluble.

### *Class F Fly Ash*

As with the Class C fly ash, the Class F fly ash also was composed primarily of an amorphous phase and some crystalline components that include alpha-quartz,  $\text{Fe}_3\text{O}_4$ ,  $\text{Al}_2\text{SiO}_5$ ,  $(\text{Mg,Fe})_2\text{SiO}_4$ , and  $\text{CaO}$ . The main difference was that Class F fly ash contains no reactive crystalline reactive component such as  $\text{C}_3\text{A}$ . The acid-insoluble residue (89 percent) of the fly ash consisted virtually of the same phases detected before treatment except for  $\text{CaO}$ .

### *Chemical Admixtures*

The chemical admixtures used for this study are identified according to ASTM C 494 as Type A. Water-reducer Type A was reported by the manufacturer to be lignin-based and water-reducer Type B was reported by the manufacturer to be sugar-based. Both products were obtained from the same manufacturer.

## **TEST MATRIX FOR PASTE AND MORTAR SYSTEMS**

Fifty-two sets of cement pastes and mortars were tested in four rounds. For each of the mixtures prepared in the four rounds described below, a number of tests were conducted as summarized in table 5 (described below). All of the paste tests were conducted in duplicate. Details of the methods are provided in the discussion in the next section.

Following is a list of labeling conventions used:

- First character=cement number (1 through 6).
- Second character=SCM added (P=plain, C=Class C fly ash, F=Class F fly ash, S=slag).
- D (where present) indicates a double dose of admixture.
- A or B identifies water-reducing admixture. (No label means no admixture.)

**Table 5. Tests conducted on paste systems in all rounds.**

<b>Information to Obtain</b>	<b>Test Method</b>
Yield stress and plastic viscosity to diagnose stiffening characteristics	Minislump (Contractor, National Institute of Standards and Technology (NIST)) Rotational rheometer (NIST)
Heat generation behavior of the cementitious system	Isothermal conduction calorimetry
Setting behavior	Penetration of 2 mm diameter vicat needle (AASHTO T 131)( Contractor, NIST)
Bleeding	Mass and volume of water decanted after initial set from a known volume and mass of cement paste (NIST)
Mortar cube strength	ASTM C 109 (Contractor)
Mortar air content	ASTM C 185 (Contractor)
Mortar stiffening	ASTM C 359 (Contractor)
Pore solution chemistry	Periodically up to 24 h. Analyses were conducted for sulfate, calcium, alkali and hydroxyl ion concentrations, and pH (Contractor)

Supplementary cementing materials were dosed at the following cement replacement levels: 20 percent for Class C and Class F fly ash, and 40 percent for ground granulated blast furnace slag (GGBFS). All paste and mortar tests were prepared at a fixed w/cm of 0.5, unless otherwise indicated. Admixture dosages were fixed as 325 and 650 mL/100 kg (5 and 10 oz/cwt) for WRA A at single dose and double dose, respectively, and 163 mL/100 kg (2.5 oz/cwt) for WRA B.

Discussion of the test methods and their data interpretation is given in a later section.

### **Round 1**

**Mixtures.** Mixtures made with the six cements shown in table 1 were tested at room temperature with and without a single dosage of each of the three supplementary cementing materials. The fly ashes were used at 20 percent cement replacement, and the slag at 40 percent cement replacement. All of the mixtures were made with a lignin-based Type A lignin-based WRA, and they were dosed at the manufacturer’s maximum recommended dosage (24 mixtures). All tests were conducted in duplicate.

**Data.** All results have been consolidated into a single table (table 6). Limiting values were selected to indicate early stiffening systems, and those outside these limits are shaded. The limits were selected based on the following criteria:

- Where current specifications provide pass/fail limits, these were used.
- For some test methods, the experience and expertise of the team were used.
- For other tests, values were selected that flagged a limited number of the tests in round 1.

The shaded cells in table 6 indicate potentially rapid stiffening systems, while speckled cells indicate potentially delayed or retarded systems. The number of shaded cells for each system was counted, as shown in the right-most columns of table 6.

Based on the number of shaded cells, systems 2PA, 2CA, 4PA and 5PA were selected as “early stiffening” and 1PA, 1CA, and 6PA as “normal.”

**Discussion.** A significant difference between the approaches by the contractor and the National Institute of Standards and Technology (NIST) was that the contractor concentrated on the stiffening that occurs in the first few minutes as a result of  $C_3A$  and/or sulfate effects. These tests have indicated several cases of false set, and in Cement 2, a lot of apparent instability. NIST, which concentrated on the instability and  $C_3S$ -based stiffening effects, flagged Cements 3 and 4.

In reviewing the complete set of data, the contractor took the viewpoint of a user who observes something happening to the concrete, and who does not know or care about the chemical reactions that are causing the problem. It is, therefore, appropriate that the tests represent both types of problem and exclude cement 3 and 4 from the “normal” set. The systems without supplementary cementing materials that exhibited the least number of fast hits were 1P and 6P, and that 1C was selected as the system with Class C fly ash to pair with its control.

At least one system containing a SCM was included in both sets; therefore, the choice of 2C is appropriate because problems in the field often are associated with high  $C_3A$  Class C fly ash, depending on the cement with which it is combined.

Table 6. Summary of paste and mortar data from round 1.

	CTLGroup									CTLGroup Mortar			NIST					Fast Hits	Slow Hits
	Bleed	2-mm vicat final set	Calorimeter Set	Minislump False Set Index (A5/A2)	Minislump Stiffening (A30/A5)	Minislump Pat Area (A5-A30)	Max Heat Rate	Silicate Peak	Cumulative Heat, First Peak	Cubes	Air	C359	Minislump, Time to < 48mm	Initial Set, Vicat	Final Set, Vicat	Stress Growth Time	Stress Growth Slope		
	mL	Hr	Hr			mm <sup>2</sup>	J/gh	J/gh	J/g	MPa	%	Min	Min	Min	hrs	µNm/hrs			
Fast limit	6	6	7	1.3	0.85	14800	70.0	12.0	25.0			120	300	400	3	900			
Slow limit	0	8	9			22600			10.0			450	450		6	200			
1PA	5.0	5.5	6.5	1.2	1.0	17400	44.2	13.0	18.4	7.17	26.9	245	335	436	4.6	209	3	0	
1CA	5.0	8.5	9.0	1.1	0.9	19300	40.4	9.4	24.4	3.10	26.8	536	668	4.4	184	0	3		
1FA	7.0	6.5	7.0	1.1	0.9	17100	45.6	10.6	18.7	3.72	18.6	305	327	445	4.8	126	0	1	
1SA	8.0	7.5	8.5	1.2	1.1	17100	26.5	8.5	14.2	2.07	24.5	304	441	601	7.0	127	0	2	
2PA	10.0	6.5	8.0	0.9	0.6	7000	87.0	14.7	30.6	7.45	30.0	13	354	468	2.8	1091	8	0	
2CA	6.0	10.5	10.5	1.1	0.8	15600	77.3	12.0	33.4	1.86	31.7	64	582	697	6.9	343	4	4	
2FA	5.5	7.5	9.0	1.1	0.9	15500	75.4	11.1	25.2	3.59	24.2	197	417	608	3.7	408	2	0	
2SA	5.0	7.5	8.0	1.2	0.8	12400	48.1	10.2	18.7	2.28	26.7	123	405	538	4.6	505	2	0	
3PA	4.5	5.5	6.0	1.1	1.0	14200	65.2	10.4	22.3	5.38	21.2	185	259	380	2.9	295	7	0	
3CA	7.5	9.5	11.0	1.1	0.9	18600	61.0	9.9	29.0	2.83	22.7	307	466	634	6.1	248	3	4	
3FA	6.5	6.5	8.0	1.1	1.0	15100	73.4	9.0	23.6	4.55	12.9	183	290	440	2.5	469	4	0	
3SA	7.0	6.5	7.5	1.2	1.0	15100	45.9	8.6	16.5	2.41	21.2	243	327	453	2.0	525	2	0	
4PA	4.0	5.5	7.0	1.3	1.1	16600	84.0	12.2	26.0	10.48	22.5	94	211	401	2.6	1007	8	0	
4CA	6.5	7.5	10.0	1.2	1.0	18500	75.7	10.9	30.0	5.03	24.3	184	340	542	4.8	380	1	1	
4FA	6.5	6.5	9.5	1.2	1.1	16500	85.0	10.5	26.1	7.38	15.1	180	260	379	2.2	558	5	1	
4SA	6.5	6.5	8.5	1.4	1.3	15400	58.6	10.6	19.3	3.31	20.6	186	310	442	3.8	408	2	0	
5PA	5.0	5.0	6.5	1.1	0.8	14700	74.0	13.9	26.7	11.17	25.9	94	261	365	2.2	780	11	0	
5CA	5.0	7.5	8.0	1.1	0.8	16300	66.3	10.7	32.6	6.41	28.8	123	403	510	4.0	348	1	0	
5FA	5.5	6.5	7.5	1.1	0.9	15100	71.1	10.3	24.8	5.79	20.1	187	369	452	2.9	540	3	0	
5SA	6.0	7.0	7.5	1.3	1.0	14600	48.0	8.9	20.2	4.07	25.3	243	347	448	3.9	383	1	0	
6PA	5.0	5.5	7.0	1.3	1.1	16700	39.6	13.3	17.9	5.17	30.0	242	294	417	3.1	295	4	0	
6CA	4.0	8.5	10.0	1.3	1.0	18100	33.3	10.4	24.2	2.28	29.9	243	500	610	6.0	193	0	4	
6FA	7.5	6.5	9.5	1.2	1.0	17100	35.8	11.0	18.5	2.76	20.4	363	377	495	5.6	125	0	2	
6SA	6.0	8.0	9.5	1.3	1.1	15900	22.2	9.1	11.9	1.65	25.9	424	457	560	5.8	134	1	4	

Note: Shaded cells indicate potential rapid stiffening or setting.  
 Speckled cells indicate potential delayed or retarded stiffening or setting.

Unit conversions:  
 1mm = 0.0394 inch  
 1 mL = 0.0338 oz  
 1 mm<sup>2</sup> = 0.00155 in<sup>2</sup>  
 1 megapascal (MPa) = 145.0 pounds per square inch (psi)

## **Rounds 2a and 2b**

**Mixtures.** Four of the mixes that exhibited early stiffening in round 1 were repeated with no WRA and at double the manufacturer’s maximum recommended dosage using the same admixture (8 mixtures) (round 2a).

The early stiffening cementitious systems tested in round 2a, along with three that did not exhibit accelerated stiffening, were repeated using a second (sugar-based) WRA at the manufacturer’s maximum recommended dose (7 mixtures) (round 2b).

Fifteen combinations were tested at room temperature. The same tests were conducted in this round as in round 1.

**Data.** All of the results from this round are consolidated into table 7. As before, the same limiting values were used to indicate “Early Stiffening” systems, and those outside these limits are shaded. Again, the approach was to count the number of shaded cells for each system as shown in the last columns on the right.

Based on the number of shaded cells in tables 6 and 7, the following systems were selected for testing in rounds 3 and 4:

- Early stiffening: 2PA, 5PA, 5P, 5PB.
- Normal: 1PA, IPB, 1CA, 6PA.
- Delayed stiffening: 2CA, 2FA, 2CDA, 1CB.

**Discussion.** Cements 2 and 5 have indicated problems with early stiffening including when they contain different admixtures. Three versions of the Cement 5 system were selected as “Early Stiffening,” along with one from Cement 2.

As before, Cements 1 and 6 appeared to be the least prone to problems, and they were selected as the control materials: three from Cement 1 and one from Cement 6.

Selection of the “Delayed Stiffening” set was the most open-ended because there was no obviously retarded system in the materials tested. Class C fly ash appears to have slowed setting, despite its propensity to also cause slump loss, and therefore, it was included in three of the selected systems. One system with Class F fly ash was also chosen as a companion to one of the Class C fly ash selections.

The overlap of materials selected was considered desirable to help with comparing the effects of each component on the systems.

**Table 7. Summary of data from round 2.**

	Bleed	Set	Cal Set, curve	Minislump False Set Index (A5/A2)	Minislump Stiffening (A30/A5)	Minislump Pat Area	Max Heat Rate	Silicate Peak	Cumulative Heat, First Peak	Cubes	Air	C359	Minislump, Time to < 48mm	Initial Set, VICAT	Final Set	Stress Growth Time	Stress Growth Slope	Fast Hits	Slow Hits
	mL	Hr	Hr			mm <sup>2</sup>	J/gh		J/g	MPa			Min		Min	hrs	µNm/hrs		
2P		5.0	4.5	1.6	1.9	11900	66.3	14.5	23.2	16.82	15.1	False	123	250	360	2.9	789	9	0
2C		7.0	6.5	1.1	1.0	16700	65.1	13.3	28.7	24.13	15.4		305	396	535	4.9	268	2	0
4P		4.5	4.5	1.2	1.1	15900	87.3	14.7	25.1	13.79	15.7	False	183	187	301	3.0	2101	8	0
5P		4.5	4.5	1.1	0.9	14800	64.5	15.6	22.2	12.34	14.3	Rapid	125	189	276	2.1	1599	9	0
2PDA		10.5	9.5	1.9	1.0	11100	73.3	12.9	30.9	2.14	38.5		13	459	607	3.3	557	5	3
2CDA		11.5	14.0	1.2	0.8	7500	49.8	9.7	32.9	2.41	36.7		423	764	na	8.9	146	2	5
4PDA		7.0	10.0	1.6	1.1	13400	87.7	12.1	33.0	5.24	35.4	False	93	330	456	2.9	535	7	1
5PDA		6.5	8.0	1.3	0.7	9800	72.7	11.8	26.3	5.03	31.9	False	64	322	433	3.0	922	6	0
2PB		7.5	8.5	1.0	0.4	8800	78.3	15.6	28.7	15.31	16.9	False	13	348	464	2.8	2154	8	0
2CB		10.5	11.5	1.2	0.7	15900	58.7	12.1	34.2	10.82	17.8		64	641	736	6.5	437	3	4
4PB		5.0	8.0	1.2	0.9	14300	87.5	14.0	31.0	12.07	16.8	False	182	216	322	1.6	1400	9	0
5PB		6.0	6.5	0.9	0.4	8400	76.8	14.6	29.9	17.79	15.8	Rapid	124	278	327	2.1	1713	10	0
1PB		10.5	8.5	1.3	0.9	15900	45.9	13.0	23.0	11.10	17.2		304	312	393	4.6	173	2	2
1CB		14.0	10.5	1.1	0.9	19400	38.7	10.3	34.3	4.34	17.3		362	472	684	7.1	148	1	5
6PB		9.5	8.5	1.1	0.8	17200	37.3	14.7	21.8	7.79	20.4	False	304	331	434	3.6	222	3	1

Notes: Shaded cells indicate potential rapid stiffening or setting.  
 Speckled cells indicate potential delayed or retarded stiffening or setting.

Unit conversions:  
 1 mL = 0.0338 oz  
 1 mm<sup>2</sup> = 0.00155 inch<sup>2</sup>  
 1 MPa = 145.0 psi

## **Rounds 3 and 4**

Eight mixes were tested in round 3 at an approximate paste temperature of 32 °C (90 °F) to simulate hot weather conditions. The eight mixtures were selected based on the stiffening rates measured in rounds 1 and 2. Four were the fastest stiffening mixes from rounds 1 and 2, and the other four were those with intermediate stiffening rates. This set was selected to model the effect of high temperature on the risk of loss of workability and early setting (eight mixtures).

In round 4, eight paste mixes were tested at 10 °C (50 °F). The eight mixes were selected based on the stiffening rates measured in rounds 1 and 2. Four were the slowest stiffening mixes from rounds 1 and 2, and the other four were the same set as used in round 3 with intermediate stiffening rates. This set was selected to model the effect of low temperature on the risk of retardation (eight mixtures).

**Data.** The results from the last two rounds were consolidated into table 8. The same limiting values were used to indicate “Early Stiffening” systems, and those outside these limits are shaded. Based on the data from all four rounds of tests conducted on pastes, eight systems were selected for testing in concrete.

It was decided that the three selected for the “Delayed Stiffening” paste tests should also be used for concrete tests. Noting that 1C is in the “Delayed Stiffening” set, the remaining two were selected for the “Normal” concrete mixtures. The set of “Early Stiffening” systems in round 3 has only two materials; therefore, a third system was selected based on its performance in rounds 1 and 2:

- Early Stiffening: 2P, 5P, 4P.
- Normal: 1P, 6P.
- Delayed Stiffening: 2C, 2F, 1C.

**Discussion.** Again, the overlap of materials selected should help with the comparison of the effects of each component on the systems and concrete performance with paste and mortar.

All data from rounds 1 through 4 are summarized in table 9 in sets of cement type to allow comparison of the effects of chemical admixture types and dosages.



**Table 8. Summary of data from rounds 3 and 4.**

90	Bleed	Set	Cal Set, curve	Minislump False Set Index (A5/A2)	Minislump Stiffening (A30/A5)	Minislump Pat Area	Max Heat Rate	Silicate Peak	Cumulative Heat, First Peak	Cubes	Air	C359	Minislump, Time to < 48mm	Initial Set, VICAT	Final Set	Stress Growth Time	Stress Growth Slope	Fast Hits	Slow Hits
	mL	Hr	Hr			mm <sup>2</sup>	J/gh		J/g	MPa			Min		Min	hrs	µNm/hrs		
2PA	4.1	3.5		1.0	0.5	7100				15.24	21.7	Dry	12	312	424	2.6	1865	7	0
5PA	3.5	3.0		1.0	0.5	9200				6.69	30.2	False	187	249	345	3.1	918	7	0
5P	0.0	1.9		1.0	0.5	7900				15.72	12.6		184	158	271	2.1	1213	7	0
5PB	0.7	3.0		0.8	0.4	7100				11.79	19.3	False	124	247	327	2.2	998	8	0
1PA	5.6	3.2		1.2	1.0	16600				10.41	27.3		304	301	448	2.4	311	2	0
1CA	2.0	5.0		1.1	0.7	16000				6.07	22.5		304	495	648	5.0	303	2	1
1PB	5.6	3.5		1.1	0.8	15300				13.17	17.1		335	310	451	3.6	231	2	0
6PA	6.9	2.9		1.3	0.9	14600				9.31	28.9		184	186	331	2.8	469	5	0
50	Bleed	Set	Cal Set, curve	Minislump False Set Index (A5/A2)	Minislump Stiffening (A30/A5)	Minislump Pat Area	Max Heat Rate	Silicate Peak	Cumulative Heat, First Peak	Cubes	Air	C359	Minislump, Time to < 48mm	Initial Set, VICAT	Final Set	Stress Growth Time	Stress Growth Slope	Fast Hits	Slow Hits
	mL	Hr	Hr			mm <sup>2</sup>	J/gh		J/g	MPa			Min		Min	hrs	µNm/hrs		
2CA	2.3	12.0		1.2	1.1	20000					33.1		123	467		5.8	437	0	3
2FA	9.0	12.0		1.2	0.8	18500					27.7		183	413		3.7	448	1	2
2CDA	0.5	12.0		1.2	1.1	19000					39.3		365	714		8.3	252	0	4
1CB	3.5	12.0		1.1	1.0	22100				0.55	20.0		303	397		5.6	323	2	1
1PA	6.0	12.0		1.1	0.9	17500				1.24	28.4		244	239		2.9	174	2	2
1CA	5.0	12.0		1.0	0.9	17200				0.34	27.2		302	424		6.2	143	0	3
1PB	8.0	12.0		1.4	1.2	22300				3.03	21.2		244	242		3.3	298	2	1
6PA	5.0	12.0		1.1	1.0	17900				0.55	32.2		186	186		2.0	126	2	2

Notes: Shaded cells indicate potential rapid stiffening or setting.  
 Speckled cells indicate potential delayed or retarded stiffening or setting.

Unit conversions:  
 1 mL = 0.0338 oz  
 1 mm<sup>2</sup> = 0.00155 inch<sup>2</sup>  
 1 MPa = 145.0 psi

**Table 9. Summary of all paste and mortar data.**

Round	Mixture	Temperature	Bleed	2-mm Vicat Final Set	Calorimeter Set	Minislump False Set Index (Area5/Area2)	Minislump Stiffening (Area30/Area5)	Minislump Pat Area	Initial Peak	Silicate Peak	24 Hour Cube Strength	Air Content	Stiffening (ASTM C 359)	Minislump, Time to < 48mm	Vicat Initial Set	Vicat Final Set	Rheology	Stress Growth Slope
		°C	mL	min	min			in <sup>2</sup>	J/gh	J/gh	MPa	%		Min	Min	Min	hrs	μNm/hrs
4	1PA	10	6.0	720		1.1	0.9	17480			1.24	28		244	239		2.9	3
1	1PA	21	5.0	330	390	1.2	1.0	17390	44.2	13.0	7.17	27		245	335	436	4.6	5
3	1PA	32	5.6	192		1.2	1.0	16650			10.41	27		304	301	448	2.4	2
4	1PB	10	8.0	720		1.4	1.2	22320			3.03	21		244	242		3.3	3
2	1PB	21		630	510	1.3	0.9	15950	45.9	13.0	11.10	17		304	312	393	4.6	5
3	1PB	32	5.6	210		1.1	0.8	15290			13.17	17		335	310	451	3.6	4
C	1PDA	10																
C	1PDA	21																
C	1PDA	32																
4	1CA	10	5.0	720		1.0	0.9	17160			0.34	27		302	424		6.2	6
C	1CA	10																
1	1CA	21	5.0	510	540	1.1	0.9	19280	40.4	9.4	3.10	27			536	668	4.4	4
C	1CA	21																
3	1CA	32	2.0	300		1.1	0.7	16000			6.07	23		304	495	648	5.0	5
4	1CB	10	3.5	720		1.1	1.0	22060			0.55	20		303	397		5.6	6
2	1CB	21		840	630	1.1	0.9	19450	38.7	10.3	4.34	17		362	472	684	7.1	7
C	1CDA	10																
C	1CDA	21																
1	1FA	21	7.0	390	420	1.1	0.9	17070	45.6	10.6	3.72	19		305	327	445	4.8	5
1	1SA	21	8.0	450	510	1.2	1.1	17130	26.5	8.5	2.07	25		304	441	601	7.0	7
2	2P	21		300	270	1.6	1.9	11910	66.3	14.5	16.82	15	False	123	250	360	2.9	3
1	2PA	21	10.0	390	480	0.9	0.6	6980	87.0	14.7	7.45	30	False	13	354	468	2.8	3
C	2PA	21																
3	2PA	32	4.1	210		1.0	0.5	7100			15.24	22	Dry	12	312	424	2.6	3
C	2PA	32																
2	2PB	21		450	510	1.0	0.4	8800	78.3	15.6	15.31	17	False	13	348	464	2.8	3
2	2PDA	21		630	570	1.9	1.0	11080	73.3	12.9	2.14	39		13	459	607	3.3	3
C	2PDA	21																
C	2PDA	32																

**Table 9. Summary of all paste and mortar data (continued).**

Round	Mixture	Temperature °C	Bleed mL	2-mm Vicat Final Set min	Calorimeter Set min	Minislump False Set Index (Area5/Area2)	Minislump Stiffening (Area30/Area5)	Minislump Pat Area in <sup>2</sup>	Initial Peak J/gh	Silicate Peak J/gh	24 hour Cube Strength MPa	Air Content %	Stiffening (ASTM C 359)	Minislump, Time to < 48mm Min	Vicat Initial Set Min	Vicat Final Set Min	Rheology hrs	Stress Growth Slope μNm/hrs	
2	2C	21		420	390	1.1	1.0	16680	65.1	13.3	24.13	15		305	396	535	4.9	5	
4	2CA	10	2.3	720		1.2	1.1	20000				33		123	467		5.8	6	
C	2CA	10																	
1	2CA	21	6.0	630	630	1.1	0.8	15570	77.3	12.0	1.86	32		64	582	697	6.9	7	
C	2CA	21																	
2	2CB	21		630	690	1.2	0.7	15940	58.7	12.1	10.82	18		64	641	736	6.5	7	
4	2CDA	10	0.5	720		1.2	1.1	18970				39		365	714		8.3	8	
C	2CDA	10																	
2	2CDA	21		690	840	1.2	0.8	7520	49.8	9.7	2.41	37		423	764		8.9	9	
C	2CDA	21																	
4	2FA	10	9.0	720		1.2	0.8	18450				28		183	413		3.7	4	
C	2FA	10																	
1	2FA	21	5.5	450	540	1.1	0.9	15530	75.4	11.1	3.59	24	False	197	417	608	3.7	4	
C	2FA	21																	
C	2FDA	10																	
C	2FDA	21																	
1	2SA	21	5.0	450	480	1.2	0.8	12380	48.1	10.2	2.28	27		123	405	538	4.6	5	
1	3PA	21	4.5	330	360	1.1	1.0	14180	65.2	10.4	5.38	21	False	185	259	380	2.9	3	
1	3CA	21	7.5	570	660	1.1	0.9	18580	61.0	9.9	2.83	23		307	466	634	6.1	6	
1	3FA	21	6.5	390	480	1.1	1.0	15070	73.4	9.0	4.55	13	False	183	290	440	2.5	3	
1	3SA	21	7.0	390	450	1.2	1.0	15050	45.9	8.6	2.41	21	False	243	327	453	2.0	2	
2	4P	21		270	270	1.2	1.1	15930	87.3	14.7	13.79	16	False	183	187	301	3.0	3	
1	4PA	21	4.0	330	420	1.3	1.1	16610	84.0	12.2	10.48	22	False	94	211	401	2.6	3	
C	4PA	21																	
C	4PA	32																	
2	4PB	21		300	480	1.2	0.9	14300	87.5	14.0	12.07	17	False	182	216	322	1.6	2	
2	4PDA	21		420	600	1.6	1.1	13360	87.7	12.1	5.24	35	False	93	330	456	2.9	3	
C	4PDA	21																	
C	4PDA	32																	
1	4CA	21	6.5	450	600	1.2	1.0	18490	75.7	10.9	5.03	24		184	340	542	4.8	5	

**Table 9. Summary of all paste and mortar data (continued).**

Round	Mixture	Temperature °C	Bleed mL	2-mm Vicat Final Set min	Calorimeter Set min	Minislump False Set Index (Area5/Area2)	Minislump Stiffening (Area30/Area5)	Minislump Pat Area in <sup>2</sup>	Initial Peak J/gh	Silicate Peak J/gh	24 hour Cube Strength MPa	Air Content %	Stiffening (ASTM C 359)	Minislump, Time to < 48mm Min	Vicat Initial Set Min	Vicat Final Set Min	Rheology hrs	Stress Growth Slope μNm/hrs
1	4FA	21	6.5	390	570	1.2	1.1	16520	85.0	10.5	7.38	15	False	180	260	379	2.2	2
1	4SA	21	6.5	390	510	1.4	1.3	15400	58.6	10.6	3.31	21	False	186	310	442	3.8	4
2	5P	21		270	270	1.1	0.9	14800	64.5	15.6	12.34	14	Rapid	125	189	276	2.1	2
3	5P	32		114		1.0	0.5	7940			15.72	13		184	158	271	2.1	2
1	5PA	21	5.0	300	390	1.1	0.8	14730	74.0	13.9	11.17	26	False	94	261	365	2.2	2
C	5PA	21																
3	5PA	32	3.5	180		1.0	0.5	9160			6.69	30	False	187	249	345	3.1	3
C	5PA	32																
2	5PB	21		360	390	0.9	0.4	8390	76.8	14.6	17.79	16	Rapid	124	278	327	2.1	2
3	5PB	32	0.7	180		0.8	0.4	7100			11.79	19	False	124	247	327	2.2	2
2	5PDA	21		390	480	1.3	0.7	9810	72.7	11.8	5.03	32	False	64	322	433	3.0	3
C	5PDA	21																
C	5PDA	32																
1	5CA	21	5.0	450	480	1.1	0.8	16290	66.3	10.7	6.41	29		123	403	510	4.0	4
1	5FA	21	5.5	390	450	1.1	0.9	15110	71.1	10.3	5.79	20	False	187	359	452	2.9	3
1	5SA	21	6.0	420	450	1.3	1.0	14560	48.0	8.9	4.07	25		243	347	448	3.9	4
4	6PA	10	5.0	720		1.1	1.0	17940			0.55	32		186	186		2.0	2
1	6PA	21	5.0	330	420	1.3	1.1	16730	39.6	13.3	5.17	30		242	294	417	3.1	3
3	6PA	32	6.9	174		1.3	0.9	14580			9.31	29		184	186	331	2.8	3
2	6PB	21		570	510	1.1	0.8	17170	37.3	14.7	7.79	20	False	304	331	434	3.6	4
C	6PDA	10																
C	6PDA	21																
C	6PDA	32																
1	6CA	21	4.0	510	600	1.3	1.0	18090	33.3	10.4	2.28	30		243	500	610	6.0	6
1	6FA	21	7.5	390	570	1.2	1.0	17070	35.8	11.0	2.76	20		363	377	495	5.6	6
1	6SA	21	6.0	480	570	1.3	1.1	15860	22.2	9.1	1.65	26		424	457	560	5.8	6

Unit conversions:  
 1 mL = 0.0338 oz  
 1 mm<sup>2</sup> = 0.00155 inch<sup>2</sup>  
 1 MPa = 145.0 psi

## TESTING CONCRETE

The matrix of concrete mixtures and tests is given in tables 10 and 11.

**Table 10. Test plan for early stiffening and normal concrete systems.**

Mix Behavior	Cementitious System	WRA	Test Temperature	Tests
Early Stiffening	2P, 5P, 4P	WRA A at 2 dosage levels, 325 and 650 mL/100 kg (5 and 10 oz/cwt)	Nominal temperatures of 21 and 32 °C (70 and 90 °F)	Slump and flow time (vibrating-slope apparatus) immediately, 30-min, and 60-min after mixing.
Normal	1P, 6P	WRA A at 650 mL/100 kg (10 oz/cwt)		Extracted mortar to perform AASHTO T 197 for setting time and mortar flow following ASTM C 230 flow table. Change in temperature of concrete in adiabatic cell with time.

**Table 11. Test plan for retarding and normal concrete systems.**

Mix Behavior	Cementitious System	WRA	Test Temperature	Tests
Retarding	2C, 2F, 1C	WRA A at 2 dosage levels, 325 and 650 mL/100 kg (5 and 10 oz/cwt)	Nominal temperatures of 21 and 10 °C (70 and 50 °F)	Change in temperature of concrete in adiabatic cell with time.
Normal	1P, 6P	WRA A at 650 mL/100 kg (10 oz/cwt)		Setting time.

Coarse aggregate used in the concrete mixtures was a crushed limestone from the Chicago area. Fine aggregate was a siliceous river sand also from the Chicago area. The physical properties of the materials are given in table 12. The nominal concrete mix proportions used for all the mixes are given table 13.

**Table 12. Physical properties of aggregates.**

	<b>Limestone Coarse Aggregate</b>	<b>Siliceous Fine Aggregate</b>
<b>Sieve Analysis</b>		
<b>Sieve</b>	<b>Percentage Passing</b>	
2.54 cm (1 inch)	100.00	
1.9 cm (0.75 inch)	92.30	
1.27 cm (0.5 inch)	46.50	
0.95 cm (0.375 inch)	25.10	
number 4	8.70	100.00
number 8		90.70
number 16		71.30
number 30		49.30
number 50		16.20
number 100		3.00
number 200		0.60
Pan	0.00	0.00
Fineness Modulus		2.69
<b>Density</b>		
Bulk Specific Gravity (SSD)	2.69	2.67
Absorption	1.40	1.77
Dry Rodded Unit Weight, kg/m <sup>3</sup>	1,633.00	1,794.00

Unit conversions:

$$1 \text{ kg/m}^3 = 1.69 \text{ pcy}$$

**Table 13. Nominal concrete mix proportions (SSD).**

Material	Mass (kg/m <sup>3</sup> )	Mass (pcy)
Cementitious Materials	335	564
Fine Aggregate	994	1,676
Coarse Aggregate	961	1,619
Water	141	237

All concrete materials were conditioned in rooms controlled at the target temperatures for 24 h before mixing. Mixes were prepared in a 0.056 m<sup>3</sup> (2 ft<sup>3</sup>), Type SW counter current mixer in a room controlled at 21°C (70 °F). Immediately after samples were made they were transported back to the appropriate temperature-controlled rooms.

The following tests were conducted on samples of the concrete mixtures:

- Slump loss in concrete every 15 min up to 60 min, ASTM C 143. Samples were all molded as soon as mixing was complete, covered with plastic sheeting, and left until the cones were lifted at the designated times.
- Slump loss of mortar sieved from the concrete every 15 min up to 60 min, Modified ASTM C 1437.
- Unit weight, ASTM C 138.
- Air content, ASTM C 231.

- Temperature, ASTM C 1064.
- Setting time, ASTM C 403.
- Consolidation monitoring.
- Ultrasonic P-wave monitoring.
- Temperature monitoring using a semi-adiabatic cell.

Concrete slump, unit weight, air content, and temperature measurements for every concrete mix are presented in table 14. Slump loss and mortar flow determinations conducted on some (rapid stiffening and control mixtures) are shown in table 15. Setting time results, as well as data obtained from nondestructive testing (NDT) measurements and the semi-adiabatic cell, are combined in table 16.

**Table 14. Temperature, air content, unit weight, slump, and impedance results.**

<b>Cementitious System</b>	<b>WRA A Dosage (mL/100 kg)</b>	<b>Mix Temperature (°C)</b>	<b>Air content (%)</b>	<b>Unit Weight (kg/m<sup>3</sup>)</b>	<b>Initial Slump (mm)</b>	<b>Impedance, Initial (Ω)</b>	<b>Impedance, Final (Ω)</b>
Cement 1 No SCM	650	21.7	7.0	2342	70	220	190
	650	33.9	4.8	2396	20	300	150
	650	13.6	9.0	2284	120	300	220
Cement 1 20%C-Ash	325	20.0	5.2	2380	65	160	140
	650	19.5	8.5	2291	135	390	220
	325	15.0	5.0	2390	50	170	110
	650	14.6	7.8	2307	100	170	150
Cement 2 No SCM	325	23.0	4.6	2385	5	260	190
	650	23.9	5.2	2355	15	185	110
	325	35.3	6.0	2243	0	340	320
	650	34.6	4.0	2451	0	245	130
Cement 2 20% C-Ash	325	23.1	4.2	2411	20	245	140
	650	23.6	6.7	2315	85	150	115
	325	14.2	5.5	2364	65	165	120
	650	14.3	6.7	2331	70	210	160
Cement 2 20% F-Ash	325	22.9	3.5	2409	5	250	180
	650	22.1	4.0	2358	15	130	80
	325	15.2	3.4	2396	20	250	160
	650	14.8	4.8	2355	45	200	150
Cement 4 No SCM	325	21.7	3.5	2428	5	340	140
	650	23.5	4.2	2409	25	390	220
	325	33.6	4.9	2352	5	405	275
	650	35.7	5.1	2302	0	455	305
Cement 5 No SCM	325	23.1	4.9	2364	0	200	140
	650	23.9	6.0	2361	15	130	80
	325	32.7	5.3	2368	15	180	140
	650	33.7	5.4	2390	40	130	80
Cement 6 No SCM	650	21.7	8.5	294	160	220	190
	650	32.3	5.3	2377	30	230	170
	650	13.4	8.5	2319	75	220	190

Unit conversions:

$$1\text{ }^{\circ}\text{C} = (X - 32)/1.8\text{ }^{\circ}\text{F}$$

$$1\text{ mL}/100\text{ kg} = 0.0154\text{ oz}/\text{cwt}$$

$$1\text{ kg}/\text{m}^3 = 1.69\text{ pcy}$$

$$1\text{ mm} = 0.0394\text{ inch}$$



**Table 15. Slump loss and mortar flow loss.**

Cementitious System	Mix Temp. (°C)	WRA Dosage, (mL/100 kg)	Slump (mm)	Percentage Slump Loss (at time, m)				Percentage Mortar Flow Loss (at time, m)		
				0	15	30	60	15	30	60
Cement 1 No SCM	21	650	70	0	27	64	82	0	12	26
	32	650	20	0	100	100	100	0	5	24
	10	650	120	-	-	-	-	-	-	-
Cement 2 No SCM	21	325	6	0	0	100	100	0	-5	-15
	21	650	15	0	100	100	100	0	4	13
	32	325	0	0	0	0	0	0	0	0
Cement 4 No SCM	32	650	0	0	0	0	0	0	-4	30
	21	325	5	0	100	100	100	0	22	14
	21	650	25	0	50	100	100	0	6	3
Cement 5 No SCM	32	325	5	0	100	100	100	0	36	54
	32	650	0	0	0	0	0	0	10	45
	21	325	0	0	0	0	0	0	62	94
Cement 6 No SCM	21	650	15	0	50	50	100	0	33	39
	32	325	15	0	100	100	100	0	22	51
	32	650	40	0	83	100	100	0	11	21
Cement 6 No SCM	21	650	160	0	84	92	100	0	11	22
	32	650	30	0	100	100	100	0	15	32
	10	650	75	-	-	-	-	-	-	-

Unit conversions:

1 mL/100 kg = 0.0154 oz/cwt

1 kg/m<sup>3</sup> = 1.69 pcy

1mm =0.0394 inch

**Table 16. Setting time, NDT, and semi-adiabatic cell results.**

Cementitious System	Temp (°C)	WRA Dosage (mL/100kg)	Max Temp (°C)	Impedance (Ω)		Setting Time (min)				
						ASTM C 403		Ultrasonic P-Wave		Semi-Adiabatic Cell
				Initial	Final	Initial	Final	Initial	Final	Initial
Cement 1 No SCM	21	650	34.3	220	190	398	486	325	685	378
	32	650	50.3	300	150	277	348	175	455	282
	10	650	20.4	300	220	673	880	733	1293	612
Cement 1 20%C-Ash	21	325	32.2	160	140	450	556	460	820	468
	21	650	31.8	390	220	486	625	589	1029	660
	10	325	21.5	170	110	513	728	512	832	480
	10	650	21.1	170	150	716	963	707	1147	654
Cement 2 No SCM	21	325	40.6	260	190	235	350	215	190	255
	21	650	41.1	210	130	340	436	231	811	330
	32	325	53.3	340	320	124	204	220	438	174
	32	650	53.9	245	130	196	263	230	430	210
Cement 2 20% C-Ash	21	325	38.7	245	143	429	496	345	746	360
	21	650	37.1	150	115	541	597	576	996	516
	10	325	21.7	165	123	776	886	758	1390	777
	10	650	20.8	210	163	1081	1447	1115	1752	1041
Cement 2 20% F-Ash	21	325	36.8	250	180	283	410	314	594	258
	21	650	37.7	130	80	368	497	383	663	396
	10	325	20.6	248	160	534	832	630	1330	510
	10	650	21.0	203	150	735	1015	626	1005	687
Cement 4 No SCM	21	325	37.3	340	140	251	332	270	510	258
	21	650	39.0	390	220	328	419	388	868	372
	32	325	51.5	405	275	186	221	184	564	210
	32	650	52.9	455	305	232	298	211	591	315
Cement 5 No SCM	21	325	38.0	200	140	263	338	297	577	228
	21	650	40.5	130	80	237	303	245	525	306
	32	325	52.6	180	140	174	227	158	558	180
	32	650	53.3	130	80	246	297	n/d	727	246
Cement 6 No SCM	21	650	34.5	220	190	435	539	378	708	468
	32	650	48.3	230	170	247	344	304	574	288
	10	650	20.2	220	190	642	869	691	1231	642

Unit conversions:

1 °C = (X - 32)/1.8 °F

1 kg/m<sup>3</sup> = 1.69 pcy

1 mL/100 kg = 0.0154 oz/cwt

1mm =0.0394 in.

## TEST METHODS DISCUSSION

Each test method is discussed below, including details of the test method if it is not standardized, the relevance of the results to assessment of stiffening and setting, and how to interpret the data.

As indicated above, there is no single mechanism causing so-called incompatibility; therefore, no single test will determine if a problem exists. It was observed that all tests are effective for some mechanisms, but not for others. Another confounding issue was that no single incompatible system could be used as a reference point to calibrate the data from the 24 sets of test data collected. This meant that decisions regarding the validity of using a given test method were based on data from other test methods that were likewise being questioned.

A general observation is that in many test methods there is no simple threshold or pass/fail limit. A value obtained for one cementitious system may be satisfactory, but a clear indication of trouble for another. Rather, a change between batches of materials or between loads of concrete will act as the required warnings. This means that data must be collected for a given mix design to establish appropriate values for that concrete.

Many tests that are more suited to field application will be particularly useful in monitoring variability. Regular and frequent testing of materials and the concrete system will allow the user to develop a familiarity with the product. A sudden change in results of any test discussed below will clearly indicate that something has changed in the raw materials, the proportions, or the environment. Such a change may signal potential problems in the concrete, and test results will warn the user that changes may be required in proportioning or practice. Details of what to do will depend on the situation, and the situation may require additional investigation and possibly expert advice. A decision to proceed with work during this additional investigation will need to be based on balancing the risk of failure against the cost of stopping or changing materials or processes.

Selecting test methods also will be governed by equipment availability. For example, a number of methods can be used to assess initial setting time. Any of those tests would be appropriate if used consistently, depending on the circumstances at the site and the needs of the project.

This discussion begins with a brief summary of the hydration processes that are believed to occur in the first hours after mixing. The relative rates of these processes cause the observed effects, and it is necessary to be able to interpret the data presented in tables 9 through 16.

A technique used to review the data was to plot two different sets of results to observe whether a relationship existed between them. The plots, generated semi-automatically in a spreadsheet, were not saved. The plots compared 24 variables, but because the purpose was to see relationships, the plots were not generated with axis labels. An example plots with both a clear relationship and another with little relationship appear in figures 1 and 2. These plots are the basis of the discussion of the usefulness of data sets.

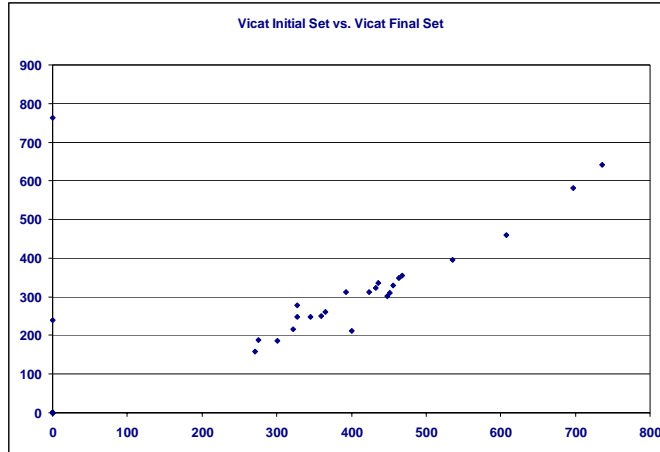


**Figure 1. Example plot with a strong relationship between data sets.**

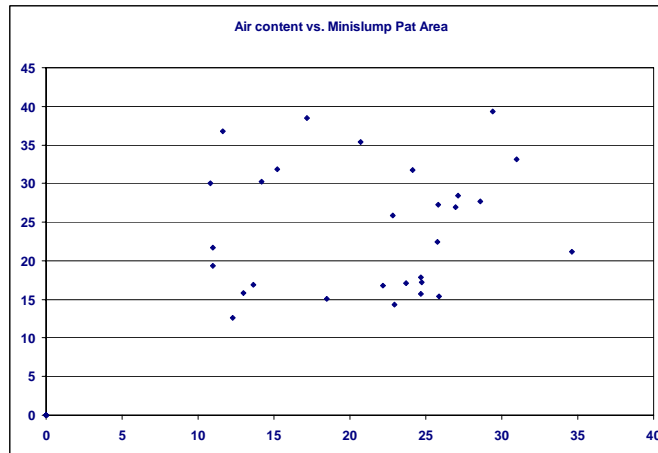


**Figure 2. Example plot of data sets with little or no relationship.**

### **Bleeding**

The total bleed water removed from 250-gram (g) (8.8-oz) paste samples was recorded for some of the systems. The mixtures used were the same as those prepared to make minislump samples.

Little useful information was obtained from the bleed tests. There was little correlation between these data and any other data collected.

### **Setting Time**

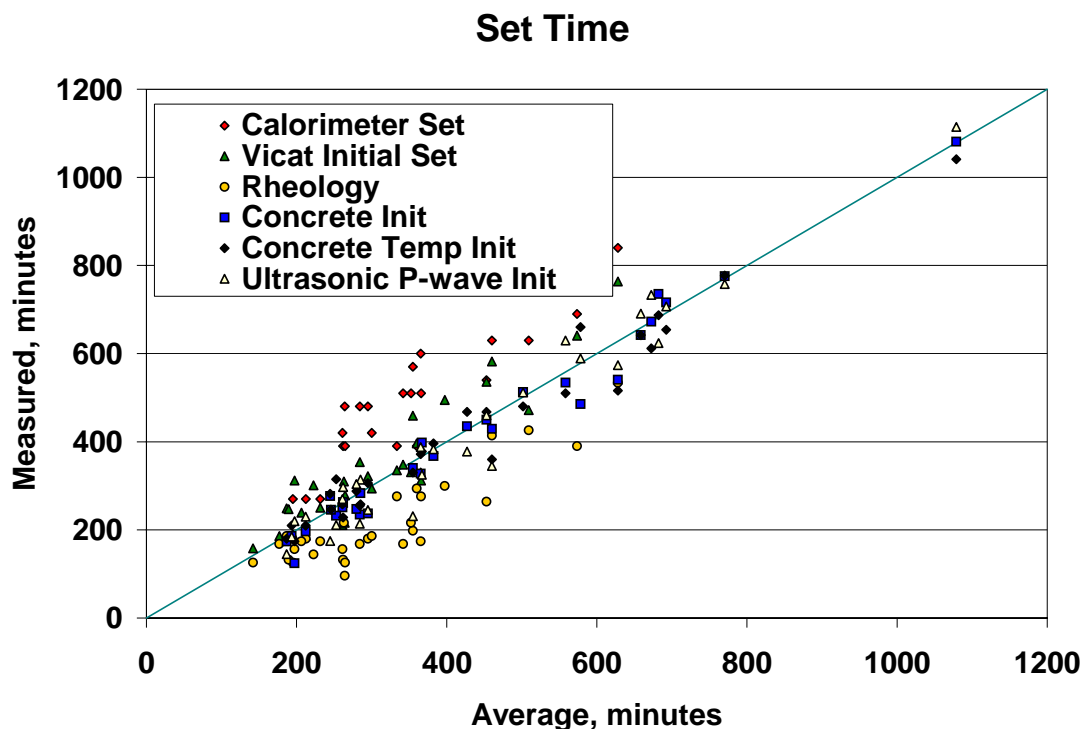
Setting time was determined in paste in the contractor’s laboratory using a 2-mm (0.08-inch) diameter needle attached to a vicat apparatus. The time to achieve a zero indentation was used to indicate the time of final set. The mixtures used were the same as those prepared for minislump tests. Tests were cut off at 12 h for systems that had not set in this time.

Setting time in paste was conducted at NIST in accordance with the ASTM C 191 standard using the same mixtures as the minislump tests. Data include both initial and final setting times.

Setting time was also determined using isothermal calorimetry in paste and penetrometer (ASTM C 403), ultrasonic P-wave, and semi-adiabatic temperature data in concrete. The initial set was taken to be the time when heat or stiffness started to increase after the dormant period.

Attempts were made to determine the final set based on some variation of when the rate of increase in temperature or stiffness flattened out, but, not surprisingly, a poor correlation with the penetrometer data existed because final set determined using ASTM C 403 is an arbitrary pressure value not necessarily related to the time when hydration rates slow.

Correlation of the various determinations of initial set was fair, as shown in figure 3.



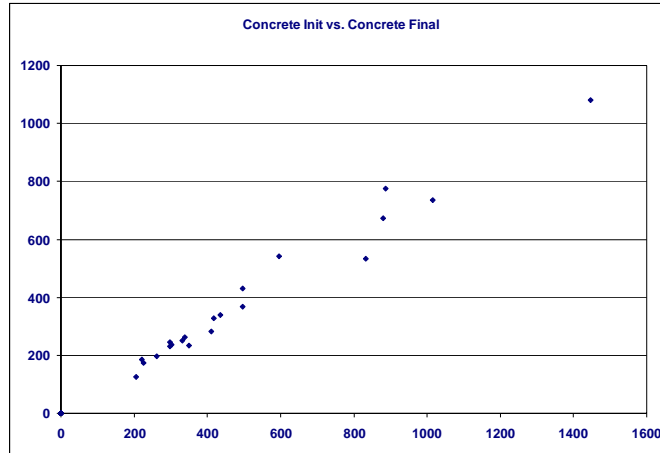
The horizontal axis is the average of the various methods for each mixture.

**Figure 3. A plot comparing sets of initial setting time measurements determined by different methods.**

Correlation between initial set and final set was also found to be reasonably good for any test method, as shown in figures 4 and 5. This means that final set can be estimated with some confidence after the initial set is determined using any of the described approaches. Following is a list of some of the general observations about the initial set:

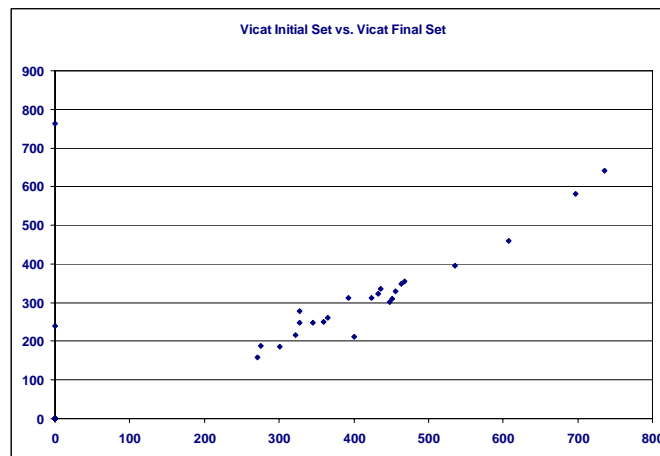
- Retarded with increasing dosage of WRA.
- Retarded with decreasing temperature.
- Retarded with the use of fly ash.
- Longer in concrete than in the equivalent paste systems.

These observations are consistent with reported trends.



Vertical axis is the first parameter in the heading, horizontal axis is the second. Both axes are in minutes.

**Figure 4. Correlation between initial and final set for concrete tests.**



Vertical axis is the first parameter in the heading, horizontal axis is the second. Both axes are in minutes.

**Figure 5. Correlation between initial and final set for paste tests.**

The most rapid setting times were observed in the systems containing cements 4 and 5. In these systems, the silicate reactions were fastest. The slowest setting times were associated with the systems containing fly ash, despite the cement reactivity, largely as a result of changes to the rate of silicate hydration. Measurement of this parameter indicates silicate hydration rate and its associated effects on concrete properties.

It appears that any of the tests would be applicable in the laboratory or in the field. Test selection depends on the availability of equipment and controlled environments. The cheaper field systems are prone to more scatter than more controlled laboratory-based sets.

Knowledge of the setting time is useful for a number of reasons. Changes in setting time from batch to batch or day to day can signal changes in the concrete system. Setting time of concrete is sensitive to the environment and the chemistry of the reactive materials, and therefore, it provides a useful means to flag changes that have occurred. Changes in setting also affect the timing of protecting, finishing, and curing activities, plus the critical activity of saw-cutting joints to prevent random cracking in unreinforced pavements. Knowledge of when setting has (or will) occur enhances the probability of achieving a crack-free durable structure or pavement.

## Calorimetry

**Introduction.** Isothermal conduction calorimetry was selected as a technique to monitor the cement hydration process. Cement hydration process is an exothermic reaction. Its intensity greatly depends on the cement composition, the w/c, the types of admixture added, and the fineness of tested material. The rate and amount of hydration of a hydraulic material, as a function of time, can be determined using conduction calorimetry. Conduction calorimetry also helps to understand the reactions that occur during the hydration process and their influence on strength development, setting time, and premature stiffening. This study used conduction calorimetry to assess the effect of supplementary cementing materials on the hydraulic properties of cement blends and investigate the effect of admixtures on cement hydration.

Strength development and setting properties of cement, and subsequently concrete, largely depend of the hydration of different cement minerals. Conduction calorimetry monitors cement hydration under isothermal conditions as a function of time from the moment water is added to cement and the hydration process is initiated.

Calorimetry is useful to track hydration of a cementitious system. The shape of the power/time plot can give clear indications of setting time, reactivity of the system, time when ettringite starts to be converted to monosulfate, and if slag or fly ash are present in the system in significant amounts. As with many test methods, calorimetry is most useful in detecting changes in the system. , The data are summarized as the magnitude of the silicate peak in table 9.

**Equipment.** The calorimetry testing was performed using a differential heat flow calorimeter designed to monitor the heat of cement hydration as a function of time. A control unit and a calorimeter block are two major parts of the instrument. The control unit provides electronic temperature control for the heating of the calorimeter block, measures voltage of the thermo-signal, and assists in calibration. The calorimeter block is actually a measuring cell that holds the specimen and the reference.

For the analysis, a test tube containing the specimen and a reference test tube containing inert material were placed inside the calorimeter block. A disposable syringe filled with mix water was placed above the specimen. At the beginning of the experiment, the syringe needle was embedded in the sample to deliver the mix water. After the thermal balance was reached, the specimen was injected with the mix water. The heat evolved after reactants were mixed was continuously measured, evaluated, and stored by a computer during the first 24 h after mixing.

Current thinking among experts is that it is more important to control the amount of mixing applied to the paste at the expense of losing the data for the first 15 to 30 min of the test. This is in agreement with the data from this work in which little correlation was observed between the initial (wetting/aluminate reaction) peak and the performance of the material. Consistent mixing will reduce the scatter in the output of the test.

**Results and Observations.** The conduction calorimetry analyses were performed using 5.0 g (0.18 oz) of a selected sample and a w/c or w/cm of 0.5. Tests were performed for 24 h at  $25 \pm 1^\circ\text{C}$  ( $77 \pm 2^\circ\text{F}$ ). The results for rounds 1 and 2 are discussed below. Tests were not conducted on rounds 3 and 4.

**Round 1—General.** The intensities of the induction period peaks closely follow the chemistry of the tested cements, specifically the tricalcium aluminate ( $\text{C}_3\text{A}$ ) content. The most intense peaks are attributed to sample 2PA and 4PA, samples with the highest amount of  $\text{C}_3\text{A}$ . Intermediate intensity peaks were observed for samples 3PA and 5PA, and the lowest intensity peaks are produced by samples 1PA and 6PA that contain the smallest amount of tricalcium aluminate.

The beginning of tricalcium silicate ( $\text{C}_3\text{S}$ ) reaction occurs essentially within the same time frame, that is, 2 and 2.5 h, for all samples except for sample 2PA. The onset of the  $\text{C}_3\text{S}$  reaction for this sample occurs almost 3 h after the start of the hydration process. The intensity of the  $\text{C}_3\text{S}$  reaction for this sample is also the highest, followed by the sample 5PA. The  $\text{C}_3\text{S}$  hydration profile for samples 1PA and 6PA is very similar; however, the  $\text{C}_3\text{S}$  for 1PA peaks a little earlier. Samples 3PA and 4PA display a double  $\text{C}_3\text{S}$  hydration peak normally occurring when there is an excess of  $\text{C}_3\text{A}$  over that required combining with the sulfate.

Calorimetry testing of this set of cements confirmed that hydration process significantly depends on the  $\text{C}_3\text{A}$  and  $\text{C}_3\text{S}$  content of the selected samples together with the sulfate form and content.

**Round 1—Cement and Fly Ash Blends.** The hydration process of cement with fly ash additions differs from hydration of cements only. Other factors affecting the hydration process of cement-fly ash matrix include glass content of fly ash, particle size, amount of sulfate and alkali content of cement. The addition of fly ash to cement results in a decrease in the amount of calcium hydroxide formed during the cement hydration process; this reduction is caused by the pozzolanic reaction with fly ash.

In this study, the addition of Class C fly ash overall had a retarding effect on all tested cements, with sample 3CA (highest  $\text{C}_3\text{S}$  content) affected the most and 5CA influenced the least (lowest  $\text{C}_3\text{S}$  content). For the rest of the samples, the intensity for  $\text{C}_3\text{A}$  peaks decreased only slightly compared to cement-only samples. The effect of Class C fly ash addition was more evident in the



hydration of  $C_3S$ , which was delayed for about 1 (sample 5CA) to 3 h (sample 3CA). Furthermore, the  $C_3S$  hydration peaks became broader and more diffused and exhibited noticeable secondary  $C_3A$  peaks, particularly for 5CA and 3CA samples.

Overall, the addition of Class F fly ash delayed the hydration process of the sample compared to the cement-only samples, but it had a less retarding effect compared to samples with added Class C fly ash. Compared to the cement-only samples, the  $C_3A$  peak intensity for 1FA and 3FA samples increased, and samples 4FA and 5FA showed about the same intensity. The  $C_3A$  reaction for 2FA and 6FA samples were affected the most by the Class F fly ash addition compared to the respective cements (i.e., it diminished noticeably). Compared to the cement-only samples, the onset of  $C_3S$  reaction was only slightly delayed for all samples with Class F fly ash except for 6FA. For this sample, the  $C_3S$  reaction was retarded by almost 2 h. None of the samples containing Class F fly ash exhibit the secondary  $C_3A$  peak evident in the calorimetry graphs for samples with Class C fly ash addition.

**Round 1—Cement and Slag Blends.** The hydration process of cement with addition of slag is influenced by slag composition, glass content, and fineness. Other important factors influencing hydration of cements with slag addition are the dosage of slag and temperature of curing. In this study, the addition of slag in general had a retarding effect on both  $C_3A$  and  $C_3S$  hydration. The intensity of  $C_3A$  and  $C_3S$  peaks diminished for all cements containing slag compared to cement-only samples. All slag-containing cement samples except for 1SA exhibit a secondary  $C_3S$  peak, which is most prominent in sample 4SA.

**Round 2a—Selected Cements and Blends with and without Admixture A.** The effect of WRA on the hydration process of samples exhibiting early stiffening is assessed when comparing the hydration profiles of the same samples tested without admixture addition. It was evident that the use of admixture A noticeably enhanced the  $C_3A$  reactivity for samples 2PA, 2CA, and 5PA. In the case of sample 4P, the use of admixture had very little effect on  $C_3A$  hydration.

In the hydration of  $C_3S$ , the retarding effect of admixture addition appears to be very prominent for all tested samples, especially for sample 2CA. For this sample, the use of admixture considerably inhibits the rate of  $C_3S$  hydration, extending the initial setting time by almost 2 h.

The addition of a double dose of admixture A had a significant retarding effect on all tested samples; with sample 2CDA affected the most. The onset of the  $C_3S$  reaction for this sample is delayed by almost 3.5 h.

Based on the results obtained during round 2a testing phase, it is evident that for a given dosage, the added admixture enhances the  $C_3A$  hydration reaction in the early stages of cement hydration. The use of the admixture considerably retards the  $C_3S$  hydration, especially in cements with high alkali and  $C_3A$  content.

The addition of a double maximum recommended dosage of admixture A had a detrimental effect on  $C_3S$  hydration, significantly inhibiting the hydration process of all tested samples.

**Round 2b—Selected Cements and Blends with Admixture B.** In round 2b of testing, calorimetry analysis was applied to evaluate the effect of sugar-based admixture on the hydration

process of the selected samples. For normal-setting cements, the addition of admixture B at the maximum recommended dosage had a considerable retarding effect on  $C_3S$  hydration, especially for sample 1CB. Furthermore, the addition of this admixture enhanced the rate of  $C_3S$  hydration for samples 1CB and 6PB compared to the  $C_3S$  hydration of the same samples tested with additions of admixture A.

In the case of early-stiffening cements, both 2P and 2C cements, the retarding effect of the admixture B is similar to the effect of addition of a single dose of admixture A. The addition of admixture B enhanced the  $C_3A$  reaction of the 2PB sample compared to the 2P cement, but it is less intense than the  $C_3A$  reaction of the 2PA sample. The intensity of the  $C_3A$  reaction for sample 2CB decreased when compared to the  $C_3A$  reaction of both samples 2C and 2CA. The use of this admixture considerably increased the rate of  $C_3A$  hydration of sample 4PB, and had almost the similar effect as admixture A on the  $C_3A$  hydration for sample 5PB.

The addition of admixture B had a similar retarding effect on  $C_3S$  hydration for samples 2CB and 5PB as for the samples with a single dose of admixture A. In the case of sample 4PB, the addition of admixture B had a more pronounced effect on  $C_3S$  hydration, where the onset of the  $C_3S$  hydration occurred almost 2.5 h later than in the samples with a single dose addition of admixture A; however, the rate of  $C_3S$  hydration is considerably enhanced compared to sample 4PA, and only slightly less than for sample 4P.

The calorimetry testing of sample 2PB with the addition of admixture B shows the increased rate of  $C_3A$  hydration when compared to samples 2P and 2PDA, but less intense than for sample 2PA. The onset of  $C_3S$  hydration for this sample occurs almost at the same time as for sample 2PA, but the rate of  $C_3S$  is higher than for samples 2P, 2PA, and 2PDA.

## **OBSERVATIONS**

The following list of observations resulted after examining the data obtained from the calorimetry tests:

- Little relationship was observed between the initial (wetting) peak and other measured parameters in the pastes. This is not surprising because the data collected is governed by both the heat of wetting (dissolution) and the heat of reaction of the  $C_3A$ , and it was not possible to separate the two mechanisms.
- The data collected provided a reasonable indication of initial setting times as illustrated in figure 3. Early hydration rates (particularly silicates) and the effects of supplementary cementitious materials are clearly indicated. This method is useful in assessing silicate-based reactions.
- Based on the work reported by Sandberg, the method has the potential to indicate the sufficiency of sulfate in the system as indicated by the position of the sulfate depletion hump.<sup>(14)</sup> Undersulfated systems exhibit a secondary peak to the left (earlier than) the silicate peak, while systems with sufficient or slight excess of sulfate will show a peak to the right (later than) the silicate peak.

- Hydration initiation of supplementary cementing materials can be observed as a second peak some time after the silicate peak. The presence of such a peak is a clear indication of the presence of an SCM.
- As with many of the other methods considered, the method is useful for identifying change in a cementitious system to flag potential difficulties in the field.
- The data indicate that hydration is retarded and slowed with:
  - Increasing fly ash content.
  - Increasing WRA dosage (independent of WRA type).

ASTM is developing a procedure for running this test and providing a guide for interpreting the data.

Disadvantages of the method are that it requires use of a relatively expensive instrument (although many cement and admixture manufacturers have purchased it), and it takes 24 h to run. This is a central laboratory test, but some similar, albeit less precise or sensitive, information can be obtained from a field-based semi-adiabatic temperature measurement system. This is discussed in a later section.

### **Minislump**

The minislump cone test (MSCT) was developed to assess the early stiffening of cement paste resulting from false set, uncontrolled C<sub>3</sub>A hydration (flash set), and cement-admixture interactions, that is, the reactions occurring in the first 30 min of hydration. The method is being used for troubleshooting problems being observed in the field. The approach is to adjust parameters such as admixture dosage between mixes and observe changes in behavior. Recommendations based on these observations are often successful in reducing problems in the field. The test is somewhat more sensitive than can be observed in concrete, meaning that a system indicated as potentially problematic in the test may be satisfactory in the field.

In the procedure, 500 g (17.6 oz) of cement or cement-blend is slowly introduced into the mixing jar of a blender containing 250 ml (8.5 oz) of de-ionized water and mixed at a blender speed of 10,000 revolutions per min (rpm). The blender was equipped with a cooling system designed to maintain a final paste temperature of  $23 \pm 1$  °C ( $73 \pm 2$  °F). In cases where chemical admixtures were used, they were added with the aid of a dropper into the mix along with cement as it was slowly introduced into the mix water. A mixing schedule of 30-s mix/rest/60-s mix was adopted to enhance the detection of the false setting tendency of cement. After 30 s of mixing, a sample of the paste was immediately taken for the first test at 2 min. Next, the remainder of the paste was returned to the blender, and at about 3 min, the paste was mixed for another 60 s. After this mixing, samples of the resulting paste were taken for subsequent tests at 5, 10, and 30 min. The paste was given a low-intensity mixing in the blender 1 min before the 10- and 30-min tests. This was done to minimize the effects of bleeding.

The size of the paste pat formed after the minislump cone was lifted is expressed in the area of the pat ( $\text{mm}^2$  (inches<sup>2</sup>)), and the size is an indication of the cement paste workability and flow

property. The pat areas at ages 2, 5, 10, and, 30 min are reported averages of duplicate determinations. The false setting tendency of the cement or blend is reported in terms of a false set index (FSI) that is described as the ratio of the pat area obtained at 5 min to that of the 2-min test. High FSI values denote the severity of the false-setting tendency of the cement or blend. Experience has shown that a value above 1.3 indicates false set. An index of early stiffening was also calculated based on the area of the pat at 30 min over the area at 5 min. A value less than 0.85 was selected as being an indicator of rapid stiffening. The third value used in assessing the results was the average pat area between 5 and 30 min. Low values (less than 14,800 mm<sup>2</sup> (23 in<sup>2</sup>)) indicated a stiff mix caused by a high water requirement of the system. This value was used for these mixes that were all at a fixed cementitious content and a fixed w/cm.

The minislump tests in round 1 at the contractor's facility were conducted on mixtures with and without admixture A because it was important to establish the effect of the admixture on the performance of the systems. All of the tests in the main matrix were conducted twice. The average variation between pairs was 625 mm<sup>2</sup> (0.97 in<sup>2</sup>) with a standard deviation of 560 (0.87). All of the tests were conducted by the same operator. A limited number of tests were also conducted with one cement system at three different w/cm to observe the effect of w/cm.

The sequence applied at NIST was somewhat different. The same mixes as the main matrix of the project were used, but the sequence of mixing and testing was different. Paste was prepared in the blender and the initial minislump measured. Measurements were repeated at 30, 60, 90, and 120 min. Before each measurement, the cement paste was mixed for 10 s with the blender. The data were analyzed to interpolate the time at which a 48-mm (1.9-inch) pat diameter was achieved. This parameter is an indicator of the silicate-related stiffening of the paste. NIST has also developed a mechanical lifting device to remove variability between operators in this step of the procedure (figure 6).

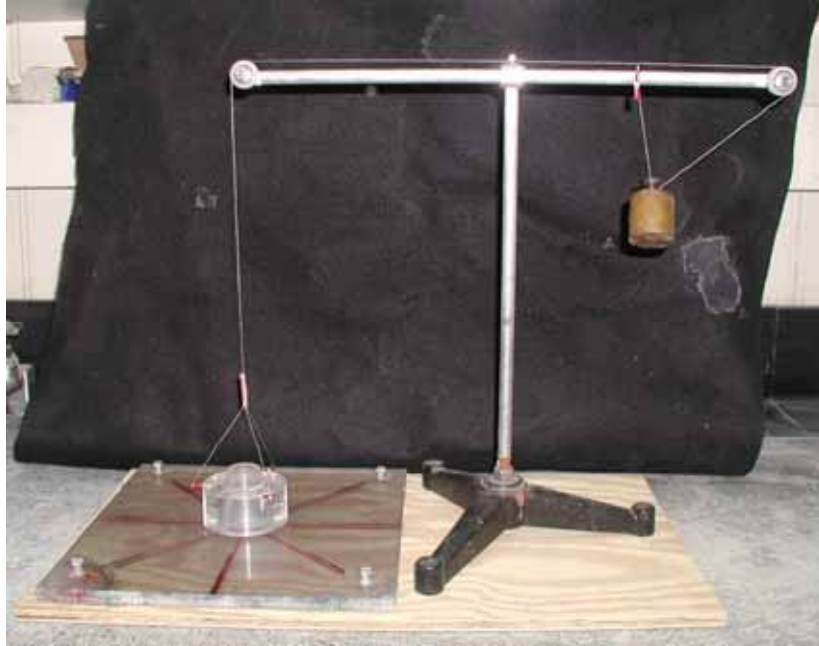
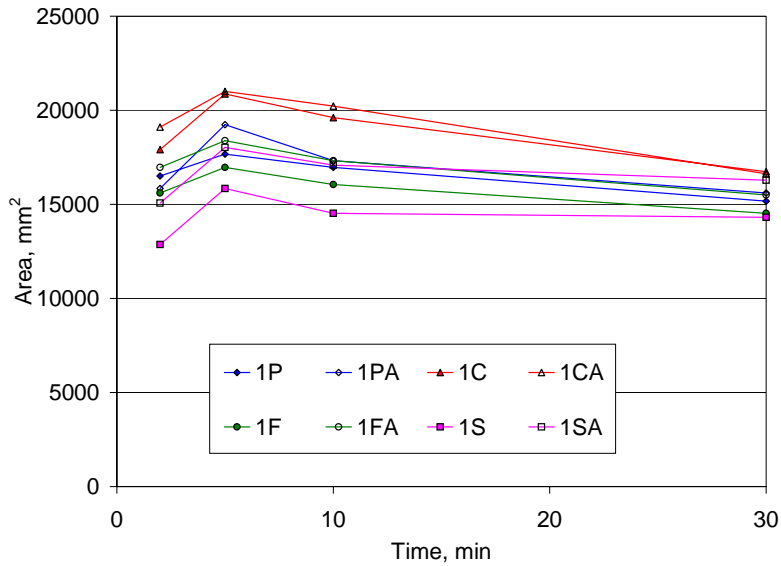


**Figure 6. Device used at NIST to lift the mold for the minislump test.**

**Test Results and Discussion.** The results for rounds 1 and 2 are presented in tables 17 and 18. The contractor's MSCT data for cement sample 1P and its blends show no indications of early stiffening tendency resulting from false set or  $C_3A$ -related stiffening reactions. The paste pat sizes from 2 to 30 min are on average about  $16,000 \text{ mm}^2$  ( $25 \text{ in}^2$ ), suggesting that the cement has a normal water demand (figure 7). The blend made with Class C fly ash produced the most workable paste as indicated by the significantly larger size of the pats in comparison with that of the pure cement or those of the other blends made with either Class F fly ash or granulated slag. The overall smaller size of the paste pats obtained with the slag blend appear to be reflective of the angular nature of slag particles, which has been reported to have a negative effect on the flow property of the paste.



Unit conversions:  
 $1 \text{ mm}^2 = 0.00155 \text{ inch}^2$

**Figure 7. A plot of minislump data for mixtures tested in round 1.**

**Table 17. Minislump test data for round 1.**

Mix	Pat Area (mm <sup>2</sup> at time, min)				False Set Index (Limit 1.3)	Stiffening Index (Limit 0.85)	Average Pat Size (mm <sup>2</sup> )
	2	5	10	30			
1P	16,520	17,680	16,970	15,160	1.1	0.9	16,580
1PA	15,810	19,230	17,290	15,610	1.2	1.0	17,420
1C	17,940	20,840	19,610	16,710	1.2	0.9	19,100
1CA	19,100	20,970	20,260	16,650	1.1	0.9	19,290
1F	15,610	16,970	16,060	14,520	1.1	0.9	15,870
1FA	16,970	18,390	17,290	15,480	1.1	0.9	17,100
1S	12,840	15,810	14,520	14,320	1.2	1.1	14,900
1SA	15,100	18,000	17,100	16,260	1.2	1.1	17,160
2P	5,810	8,520	12,260	12,260	1.5	2.1	11,030
2PA	10,580	9,480	5,100	6,390	0.9	0.6	6,970
2C	16,260	17,940	16,710	15,420	1.1	0.9	16,710
2CA	16,060	17,810	15,940	12,970	1.1	0.8	15,550

**Table 17. Minislump test data for round 1 (continued).**

Mix	Pat Area (mm <sup>2</sup> at time, min)				False Set Index (Limit 1.3)	Stiffening Index (Limit 0.85)	Average Pat Size (mm <sup>2</sup> )
	2	5	10	30			
2F	13,290	14,710	14,970	14,710	1.1	1.1	14,840
2FA	15,480	17,290	15,290	14,000	1.1	0.9	15,550
2S	8,320	13,680	12,840	12,840	1.6	1.5	13,160
2SA	12,190	14,710	12,390	10,000	1.2	0.8	12,390
3P	1,160	13,290	11,870	10770	11.7	9.5	12,000
3PA	13,810	13,610	14,650	14,320	1.1	1.0	14,190
3C	5,810	16,260	14,970	13,290	2.8	2.3	14,840
3CA	18,260	20,520	18,650	16,650	1.1	0.9	18,580
3F	1,230	13,290	12,450	10,970	10.6	8.7	12,260
3FA	13,870	15,290	15,610	14,320	1.1	1.0	15,100
3S	4,770	13,870	13,290	12,450	2.9	2.6	13,230
3SA	13,480	16,520	14,970	13,680	1.2	1.0	15,030
4P	14,520	18,130	16,520	14,970	1.2	1.0	16,520
4PA	14,190	17,940	16,710	15,160	1.3	1.1	16,580
4C	15,810	19,100	18,650	16,520	1.2	1.0	18,060
4CA	16,390	20,000	18,970	16,520	1.2	1.0	18,520
4F	13,680	16,520	16,060	14,710	1.2	1.1	15,740
4FA	14,320	17,230	16,970	15,420	1.2	1.1	16,520
4S	9,680	14,130	14,130	13,290	1.5	1.4	13,810
4SA	11,290	15,740	15,740	14,710	1.4	1.3	15,420
5P	14,970	16,970	16,520	13,870	1.1	0.9	15,810
5PA	14,710	16,840	14,970	12,390	1.1	0.8	14,710
5C	17,420	19,100	17,420	14,710	1.1	0.8	17,100
5CA	17,100	18,840	16,650	13,350	1.1	0.8	16,320
5F	14,320	16,520	15,160	13,480	1.2	0.9	15,030
5FA	15,290	16,840	15,420	13,100	1.1	0.9	15,100
5S	11,290	14,130	13,870	11,870	1.2	1.1	13,290
5SA	12,390	16,060	14,970	12,650	1.3	1.0	14,580
6P	5,680	18,390	17,940	15,810	3.2	2.8	17,350
6PA	13,870	18,130	17,230	14,840	1.3	1.1	16,710
6C	9,480	20,390	18,840	16,710	2.1	1.8	18,650
6CA	15,740	20,390	18,520	15,420	1.3	1.0	18,060
6F	7,100	17,680	16,260	14,970	2.5	2.1	16,320
6FA	15,610	18,390	17,420	15,420	1.2	1.0	17,100
6S	7,870	15,610	14,710	14,320	2.0	1.8	14,900
6SA	13,160	17,230	15,940	14,450	1.3	1.1	15,870

Unit conversions:

$$1 \text{ mm}^2 = 0.00155 \text{ inch}^2$$

**Table 18. Minislump test data for round 2.**

Mix	Pat Area (mm <sup>2</sup> at time, min)				False Set Index	Stiffening Index	Average Pat Size (mm <sup>2</sup> )
	2	5	10	30			
<b>Round 2a</b>							
2P	6,580	10,580	12,770	12,390	1.1	0.9	11,940
2C	16,060	17,550	16,970	15,480	1.2	1.0	16,710
4P	13,810	17,230	15,940	14,650	1.2	0.9	15,940
5P	14,320	16,390	15,290	12,710	1.1	0.9	14,770
2PDA	7,290	14,190	11,480	7,550	1.1	0.9	11,100
2CDA	13,940	16,580	13,940	10,710	1.1	0.9	13,740
4PDA	10,000	15,740	13,810	10,580	1.2	1.1	13,350
5PDA	9,940	13,290	9,480	6,650	1.2	1.1	9,810
<b>Round 2b</b>							
2PB	12,000	12,390	8,710	5,290	1.1	0.9	8,770
2CB	16,520	19,350	16,770	11,680	1.2	1.0	15,940
4PB	13,870	16,390	14,520	12,000	1.2	0.9	14,320
5PB	12,650	12,000	8,260	4,840	1.1	0.9	8,390
1PB	14,650	18,520	15,940	13,350	1.1	0.9	15,940
1CB	19,870	21,480	19,870	16,970	1.1	0.9	19,420
6PB	18,130	19,610	17,810	14,130	1.2	1.1	17,160

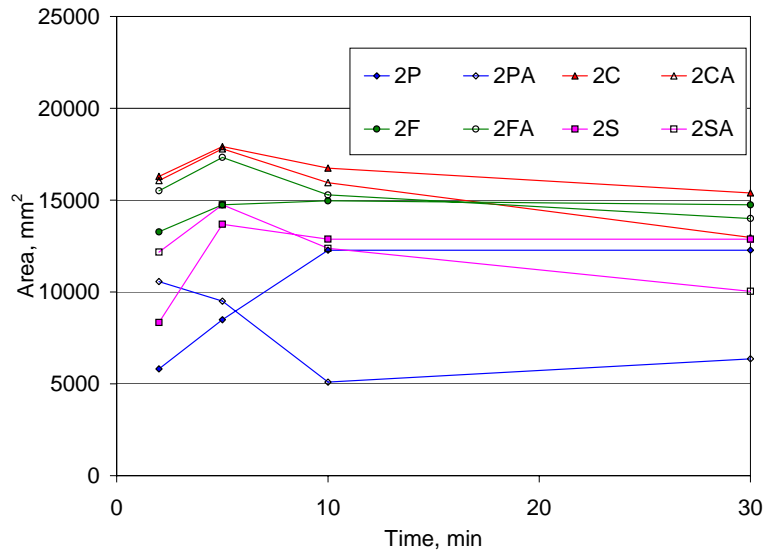
Unit conversions:  
1 mm<sup>2</sup> = 0.00155 inch<sup>2</sup>

As expected, sample 1P cement set much faster than the blends, and sample 1C blend showed the most extended setting by about 3 h. The amount of bleed water was about twice as much for the blends than it was for the pure cement.

Sample 2P was the first cement to indicate false set as a result of plaster converting to gypsum, which caused the 5- and 10-min pat areas to be smaller than the 2-min pat (figure 8). Previous analysis of the cement showed it to contain mostly plaster with very little gypsum (table 2). Judging from the increasing size of the paste pats from 2 to 30 min, it is apparent that this conversion was slow and appeared to reach completion after about 10 min. The overall size of the paste pats of the cement and the blends made from it were slightly smaller than that of sample 1P and its blends, suggesting higher water demand for sample 2P cement. The early stiffening tendency and higher water demand of sample 2P most likely results from its high plaster content, and also its high C<sub>3</sub>A and alkali contents. The blend made with Class C fly ash also appeared to show the most workable paste mix.

As with the previous cement, sample 2P cement set faster than its blend with sample 2C blend, which showed the most retardation. The bleeding capacity of the blends was similar to that of the pure cement.



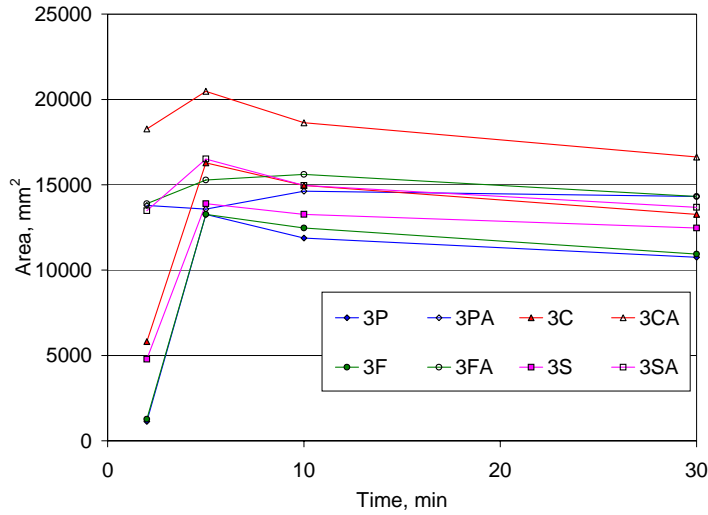


Unit conversions:  
 $1 \text{ mm}^2 = 0.00155 \text{ inch}^2$

**Figure 8. A plot of minislump data for mixtures tested in round 2.**

Sample 3P cement was another case of early stiffening resulting from plaster-to-gypsum conversion (figure 9). As with sample 2P cement, sample 3P cement also had a high plaster content; however, the conversion of plaster to gypsum in sample 3P cement appeared to occur much faster. It was completed in about 5 min (paste pat size is at maximum), and it appeared to be more severe than sample 2P cement, judging from its much higher FSI value.

The pastes made from the blends showed similar false setting trends as the pure cement. All pastes made with the blends were more workable, set longer, and bled more than the pure cement. The paste made with the blend containing Class C fly ash was again noticeably more workable than the other blends.



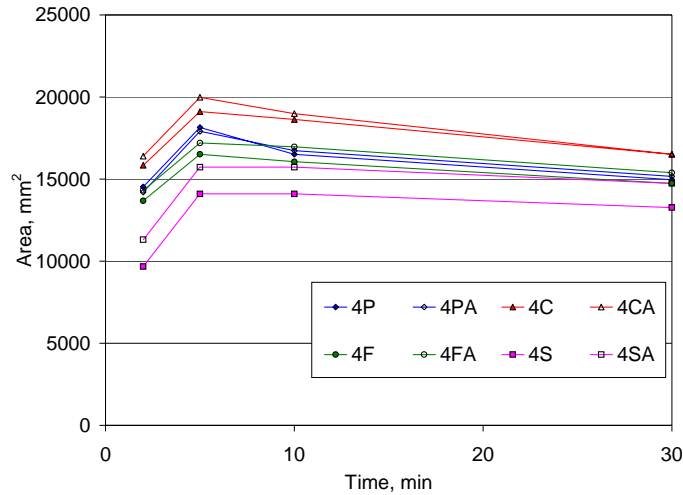
Unit conversions:  
 $1 \text{ mm}^2 = 0.00155 \text{ inch}^2$

**Figure 9. A plot of minislump data for mixtures tested in round 3.**

The minislump data for sample 4P cement gave all indications that the cement had a low water demand with practically no early stiffening tendency (figure 10). Analysis of the cement showed it to contain mainly gypsum as the calcium sulfate source present, with only minor amounts of plaster. The cement was also found to be high in  $C_3A$ , but it was apparent that its early hydration reactions were being properly controlled largely by gypsum.

Only the blend made with Class C fly ash gave a more workable paste than the cement. The other blends produced pastes of about the same workability, and in the case of the sample 4S blend, the paste was somewhat less workable.

As observed in the previous cements, sample 4P cement set sooner and bled less than its blends.

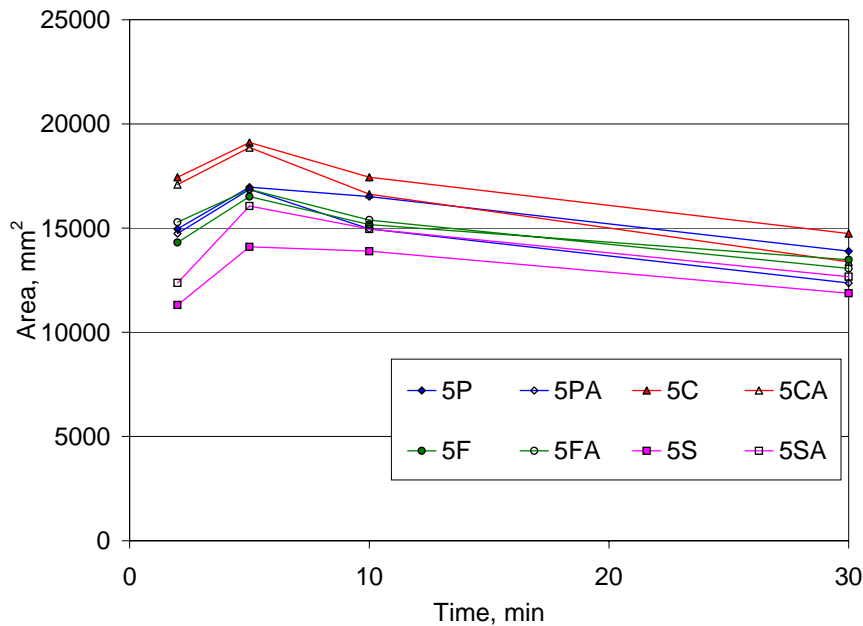


Unit conversions:  
 $1 \text{ mm}^2 = 0.00155 \text{ inch}^2$

**Figure 10. A plot of minislump data for mixtures tested in round 4.**

As with sample 4P cement, sample 5P cement showed no indications of early stiffening resulting from false set. The size of paste pats from 2 to 30 min suggested the cement had a normal water demand (figure 11). This is consistent with previous analysis showing the cement to contain a moderate amount of  $C_3A$  with mostly gypsum and very little plaster. As observed in previous cements, the blend made with Class C fly ash gave the most workable paste mix, and the one containing the granulated slag was the least workable.

Setting time was found to be earliest for the pure cement and latest for the blends containing Class C fly ash. Again, the pure cement bled the least with the blends showing about twice the bleeding capacity.

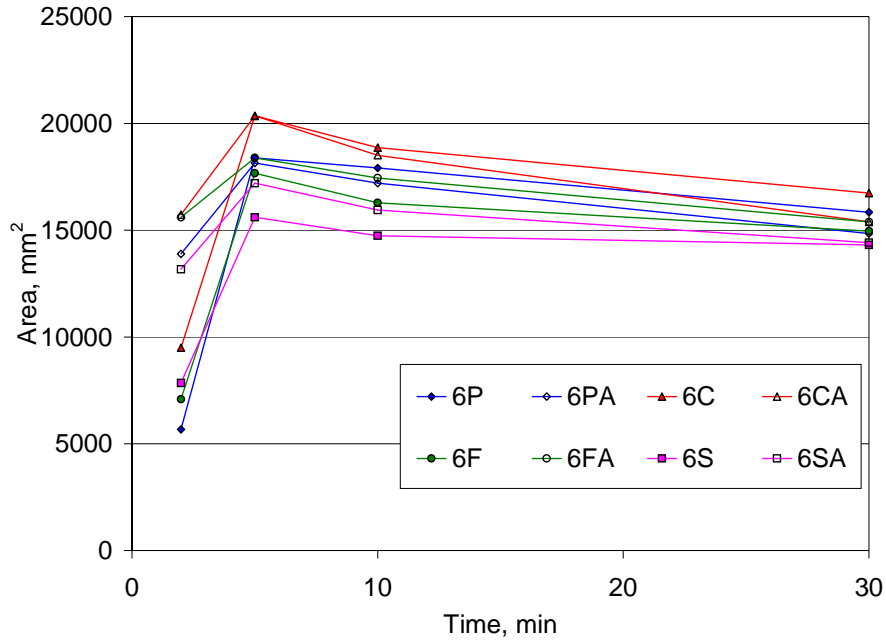


Unit conversions:  
 $1 \text{ mm}^2 = 0.00155 \text{ inch}^2$

**Figure 11. A plot of minislump data for mixtures tested in round 5.**

Sample 6P cement is another cement that shows indications of early stiffening resulting from false set because of the plaster-to-gypsum conversion (figure 12). However, after remixing, the cement paste became very fluid, indicating a normal water demand based on the very large pats from 5 to 30 min. Part of the reason for the very low water demand of sample 6P cement was likely its very low  $C_3A$  content. As observed in the previous cements, the blend made with Class C fly ash gave the most workable mix. Both blends made with Class F fly ash and granulated slag were somewhat less workable than the pure cement. The lower workability of the slag blend could be explained in terms of the angular nature of the slag particles. For the blend containing Class F fly ash, one explanation may involve its finer particle size and distribution.

As with the other previous five cements, sample 6P cement had shorter setting time and less bleed water than its blends.



Unit conversions:  
 $1 \text{ mm}^2 = 0.00155 \text{ inch}^2$

**Figure 12. A plot of minislump data for mixtures tested in round 6.**

**Effects of Chemical Admixtures.** The results of minislump tests conducted in rounds 3 and 4 are shown in table 19. The use of the lignin-based chemical admixture provided some benefit of water reduction to only samples 1P and 3P cements and their respective blends, estimated roughly at around 3 percent water reduction. The rest of the cement and blends were either unchanged or may have suffered slight loss in early workability. Of the three cements found to show rapid stiffening, two cements (2P, 6P) indicate incompatibility with the chemical admixtures, as shown by the paste slump loss from 5 to 30 min that more resembles flash set than false set. Sample 3P cement, which was found to have the most severe false setting tendency earlier, is shown to have the most benefit with admixture addition. The positive effect of lignin-based admixture on sample 3P cement may be explained as the result of (1) rapid conversion of plaster to gypsum taking place as the paste is being mixed, or (2) the admixture is causing a delay in the delay of this conversion process beyond 30 min. Further observation of the paste at later ages beyond 30 min favors explanation (1).

**Table 19. Minislump test data for round 3 and 4.**

Mix	Pat Area (mm <sup>2</sup> at time, min)				False Set Index	Stiffening Index	Average Pat Size
	2	5	10	30			
<b>Round 3</b>							
5P	10,390	10,390	8,190	5,230	1.1	0.9	7,940
5PA	12,260	12,060	9,100	6,390	1.2	1.0	9,160
5PB	9,160	7,420	4,840	3,810	1.2	0.9	5,350
2PA	9,740	9,740	6,130	5,350	1.1	0.9	7,100
1PA	15,100	18,390	16,900	14,650	1.1	0.9	16,650
1PB	16,260	18,000	15,610	12,190	1.1	0.9	15,290
1CA	17,680	19,740	16,650	11,550	1.2	1.1	16,000
6PA	13,100	17,680	14,900	11,160	1.2	1.1	14,580
2CA	13,810	13,810	10,060	5,680	1.5	2.1	9,870
2FA	12,900	12,060	9,480	6,840	0.9	0.6	9,480
2CDA	10,060	9,290	5,100	3,350	1.1	0.9	5,870
1CB	16,650	17,680	12,320	5,870	1.1	0.8	11,940
<b>Round 4</b>							
2CA	17,550	20,520	21,030	18,520	1.1	0.9	20,000
2FA	17,940	20,580	20,130	14,520	1.2	1	18,450
2CDA	15,610	19,290	19,870	17,810	1.2	0.9	18,970
1CB	21,030	23,230	22,320	20,710	1.1	0.9	22,060
1PA	17,100	18,390	18,130	15,810	1.1	0.9	17,480
1PB	17,230	17,810	17,940	15,740	1.1	0.9	17,160
1CA	17,230	23,350	22,710	20,840	1.2	1.1	22,320
6PA	13,100	17,680	14,900	11,160	1.2	1.1	14,580

Unit conversions:  
1 mm<sup>2</sup> = 0.00155 inch<sup>2</sup>

In general, the addition of lignin-based admixture caused longer setting times and more bleed water for the cements and their blends, which is a direct result of some retardation of the hydration reactions by the clinker phases, especially C<sub>3</sub>S. All blends made with Class C fly ash showed the longest setting time and the most bleed water.

Further testing was done on three cements and one blend that exhibited early stiffening tendency to evaluate the effect of double dose of the lignin-based admixture. The results are shown in table 19. As the results indicate, the double dose addition of lignin-based admixture did very little to prevent the early stiffening tendencies of the cements and the blend. In fact, it made the condition worse—the double dose addition resulted in greater slump loss from 5 to 30 min when compared with single dose admixture addition. The double dose addition also resulted in much longer setting times accompanied with excessive amounts of bleed water.

Sugar-based admixture at a dosage rate of 163 ml/100 kg (2.5 oz/cwt) was also tried on the same set of three cements and one blend. The results given in table 19 are very similar to those obtained with the lignin-based admixture. No benefit of water reduction was achieved by the addition of sugar-based admixture. All pastes containing sugar-based admixture showed longer setting times accompanied by more bleeding. When added to the normal sample 6P cement, the sugar-based admixture was also found to have very little benefit in providing water reduction.

**Effects of Temperature.** The study on the effects of temperature was carried out at 32 °C (90 °F) and 10 °C (50 °F), to simulate summertime and fall concreting (table 9). The cements and blends used for evaluation were selected on the basis of their rapid or normal stiffening tendencies, plus the slow setting properties found earlier. The results are shown in round 3 and round 4 test results. As expected, all pastes made at 32 °C (90 °F) are less workable than those prepared at 23 °C (70 °F). This is the result of accelerated hydration of the clinker phases, especially C<sub>3</sub>A. Conversely, hydration reactions are slowed at 10 °C (50 °F), resulting in pastes of high workability.

At 32 °C (90 °F), the pastes took much shorter times to set as a direct result of higher reaction rates and formation of more hydration products. In contrast, pastes prepared at 10 °C (50 °F) were slower to set and were accompanied with more bleeding, which resulted from the hydration process being slowed down by a lower temperature.

**Effects of Class C Fly Ash.** In all cases, the Class C fly ash-containing blend shows higher slump loss from 5 to 30 min than that of the pure cement, sample 1P. The greater slump loss of the blend that seems to become more severe at lower w/c ratios appears to be related to some early reactions outside of the cement clinker-phase hydration reactions. Earlier analysis of Class C fly ash showed it to contain reactive components that include C<sub>3</sub>A estimated as 11.4 percent by weight of the fly ash. Anhydrite (CaSO<sub>4</sub>) was also detected in the fly ash at an estimated amount of 4 percent. With this level of C<sub>3</sub>A in the Class C fly ash coupled with the form of calcium sulfate (anhydrite) present, the higher slump loss observed in all 1C blend pastes may be related to the inadequate control of C<sub>3</sub>A hydration.

**Effects of Water-to-Cementitious Materials Ratio.** Some mixes were added to address the issue of Class C fly ash reactivity in blends at lower w/c ratios. These paste mixes were prepared using w/cm=0.50, 0.42, 0.40, and 0.37. The results are shown in table 20.

**Table 20. Minislump test data for investigating effect of w/cm.**

w/cm	Pat Area (mm <sup>2</sup> at time, min)				False Set Index	Stiffening Index	Average Pat Size
	2	5	10	30			
Mix 1C							
0.37	8,840	7,420	6,390	3,420	1.1	0.9	5740
0.40	12,260	11,290	10,770	8,320	1.2	1.0	10,130
0.42	14,130	13,870	12,260	9,480	1.2	0.9	11,870
0.50	17,940	20,840	19,610	16,710	1.1	0.9	19,030

Unit conversions:  
1 mm<sup>2</sup> = 0.00155 inch<sup>2</sup>

### *NIST Minislump Test*

The minislump tests conducted at NIST aimed at identifying silicate-based stiffening effects indicate the following observations (tables 21 to 23):

- Extremely short times to reach a small (48-mm (1.9-inch) diameter) pat size were recorded for most combinations of Cement 2. The exceptions were with no admixture present and at high water-reducer dosage with Class C fly ash.
- Shortened times were reported for the combinations of Cements 4 and 5 containing water reducer at 21 °C (70 °F).
- Cements 1 and 6 showed normal/extended times.

These observations are consistent with other test methods that indicate stiffening caused by silicate reactions.

**Table 21. NIST test data for round 1.**

Mix	Pat Size (mm at time, min)					Time to reach 48 mm, (min)	Slope (mm/min)
	15	30	60	90	120		
1PA	79.5	71.3	67.3	60.5	57.9	*	-0.187
1CA	87.5	73.6	63.9	58.4	58.4	*	-0.340
1FA	83.1	76.5	71.4	69.4	63.1	305	-0.123
1SA	76.4	73.4	73.4	73.3	69.1	304	-0.102
2PA	46.0	44.0	44.0	44.0	*	13	-0.125
2CA	57.9	50.9	48.1	*	*	64	-0.198
2FA	50.1	53.4	49.5	51.3	53.3	197	-0.013
2SA	53.9	51.8	49.4	48.8	48.3	123	-0.072
3PA	64.9	60.0	57.4	54.5	53.3	185	-0.110
3CA	71.0	66.6	59.4	58.5	57.9	307	-0.071
3FA	71.0	66.5	62.0	53.6	54.9	183	-0.132
3SA	62.4	61.8	59.3	57.9	52.4	243	-0.073
4PA	64.3	58.0	50.5	48.5	*	94	-0.198
4CA	76.0	64.0	58.4	55.3	52.5	184	-0.144
4FA	71.5	65.0	56.9	52.4	51.4	180	-0.142
4SA	65.6	59.4	56.3	53.0	49.5	186	-0.103
5PA	61.9	53.6	49.0	48.1	*	94	-0.160
5CA	74.1	56.5	56.1	49.1	47.8	123	-0.206
5FA	65.1	61.0	55.3	53.4	51.5	187	-0.108
5SA	68.8	65.0	54.1	55.9	52.1	243	-0.094
6PA	78.4	65.6	61.6	59.9	54.0	242	-0.128
6CA	82.5	65.8	60.9	56.5	52.5	243	-0.129
6FA	81.5	70.5	69.1	69.9	65.6	363	-0.094
6SA	75.0	65.3	66.5	64.5	60.0	424	-0.064

Note - \* = No data recorded

Unit conversions:

$$1 \text{ mm}^2 = 0.00155 \text{ inch}^2$$



**Table 22. NIST test data for round 2.**

Mix	Pat Area (mm <sup>2</sup> at time, min)					Time to reach 48 mm (min)	Slope (mm/min)
	15	30	60	90	120		
<b>Round 2A</b>							
2P	52.3	51.3	49.0	48.1	47.0	123	-0.047
2C	69.9	65.5	60.6	58.1	56.0	305	-0.065
4P	76.3	69.3	62.8	56.5	51.3	183	-0.188
5P	70.6	63.0	60.0	53.4	48.9	125	-0.157
2PDA	47.0	47.8	47.1	45.8	*	13	-0.034
2CDA	74.9	70.5	61.9	56.0	52.5	423	-0.057
4PDA	56.9	50.6	48.9	45.8	*	93	-0.126
5PDA	57.3	48.4	46.3	*	*	64	-0.193
<b>Round 2B</b>							
2PB	46.1	44.5	*	*	*	13	-0.061
2CB	62.3	51.8	47.0	45.6	*	64	-0.273
4PB	66.9	59.6	52.8	50.8	49.5	182	-0.121
5PB	58.5	49.8	49.0	48.0	44.8	124	-0.104
1PB	78.3	70.4	66.5	64.8	63.0	304	-0.105
1CB	88.1	74.5	67.3	62.5	58.5	362	-0.101
6PB	78.8	65.8	61.0	57.6	57.0	304	-0.099

Note - \* = No data recorded

Unit conversions:

1mm =0.0394 inch

1 mm<sup>2</sup> = 0.00155 in<sup>2</sup>

**Table 23. NIST Test Data For Round 3 and 4.**

Mix	Pat Area (mm <sup>2</sup> at time, min)					Time to reach 48 mm (min)	Slope (mm/min)
	Round 3	15	30	60	90		
5P	69.9	59.6	55.3	51.3	48.5	184	-0.148
5PA	58.0	53.6	51.1	49.5	48.4	187	-0.065
5PB	60.0	50.8	49.5	48.3	46.4	124	-0.102
2PA	43.3	*	*	*	*	12	*
1PA	76.0	71.0	65.9	65.8	60.4	304	-0.110
1PB	77.0	71.0	68.6	65.8	64.8	335	-0.086
1CA	81.9	69.0	61.0	57.1	55.4	304	-0.082
6PA	78.3	69.8	67.5	56.1	51.5	184	-0.205
2CA	59.3	56.8	51.3	48.4	46.0	123	-0.123
2FA	50.5	51.3	49.6	49.3	48.8	183	-0.029
2CDA	*	*	*	*	*	*	*
1CB	91.5	75.8	70.0	64.1	61.3	363	-0.249
<b>Round 4</b>	<b>15</b>	<b>30</b>	<b>60</b>	<b>90</b>	<b>120</b>		
2CA	59.0	55.8	55.1	49.4	46.8	123	-0.100
2FA	64.0	53.8	54.4	52.5	50.8	183	-0.059
2CDA	93.6	84.8	77.6	68.5	61.4	365	-0.237
1CB	90.5	74.9	72.8	64.8	60.3	303	-0.111
1PA	81.0	75.9	72.3	66.5	60.1	244	-0.166
1PB	82.9	73.0	68.8	66.0	62.3	244	-0.142
1CA	93.5	82.9	71.1	67.3	62.6	302	-0.126
6PA	87.5	81.0	76.8	70.1	62.5	186	-0.199

Note - \* = No data recorded

Unit conversions:

1mm =0.0394 inch

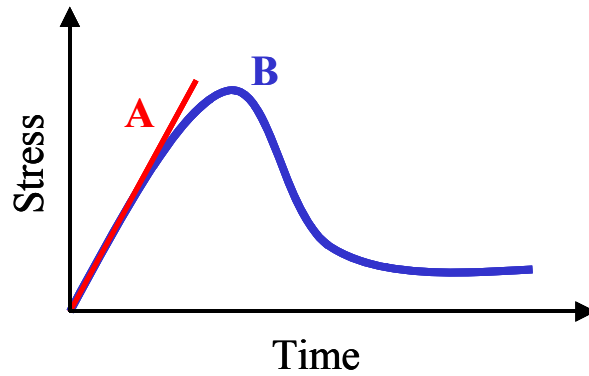
1 mm<sup>2</sup> = 0.00155 in<sup>2</sup>

## Rheology

Rheological methods for cement paste were investigated for their potential to identify incompatibilities between pavement materials. The logic behind this approach is that the main incompatibility problems occur between the cement, chemical admixtures, and supplementary cementitious materials. The advantage is that cement paste testing needs small amounts of materials, and it is less labor intensive than tests performed on concrete.

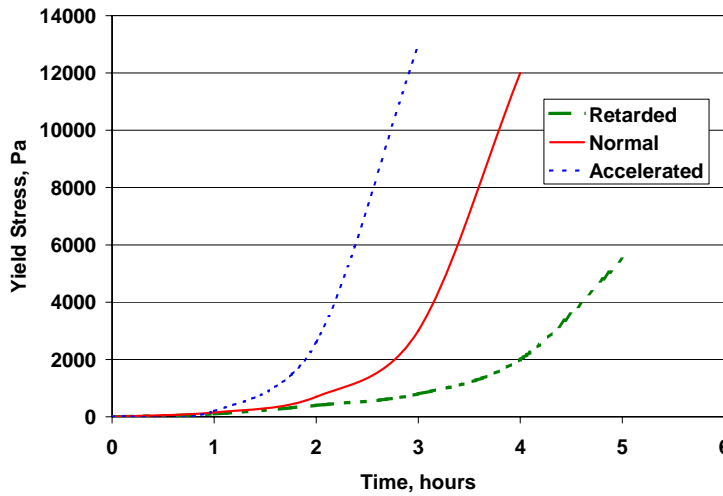
The rheology-based method to measure yield stress uses the stress-growth procedure. The cement paste is sheared at a very low shear rate (the lowest possible with the rheometer used) and the shear stress is measured. The shear stress increases linearly with time until the yield stress is reached (figure 13). At that point, the shear stress reaches a peak and then decreases. The linear portion is caused by the elastic response of the viscoelastic material. After the yield stress is reached, the material flows, and the reduction in shear stress is measured. The plot of the

yield stress versus the time (figure 14) will gradually increase until initial setting is reached. After initial setting is reached, the shear stress will increase very fast until the rheometer can no longer measure flow because the shear stress is too high.



Point A, the end of the linear (elastic) portion, is the yield stress point. Point B, the peak point, is taken as an approximation of the yield stress because it is more readily identified.

**Figure 13. Stress growth measurement.**



Note: These data are presented to illustrate the method, and they were not produced with the project materials.

Unit conversions:  
 $1 \text{ kPa} = 0.145 \text{ psi}$

**Figure 14. Typical plots of yield stress versus time for accelerated, untreated, and retarded cementitious systems.**

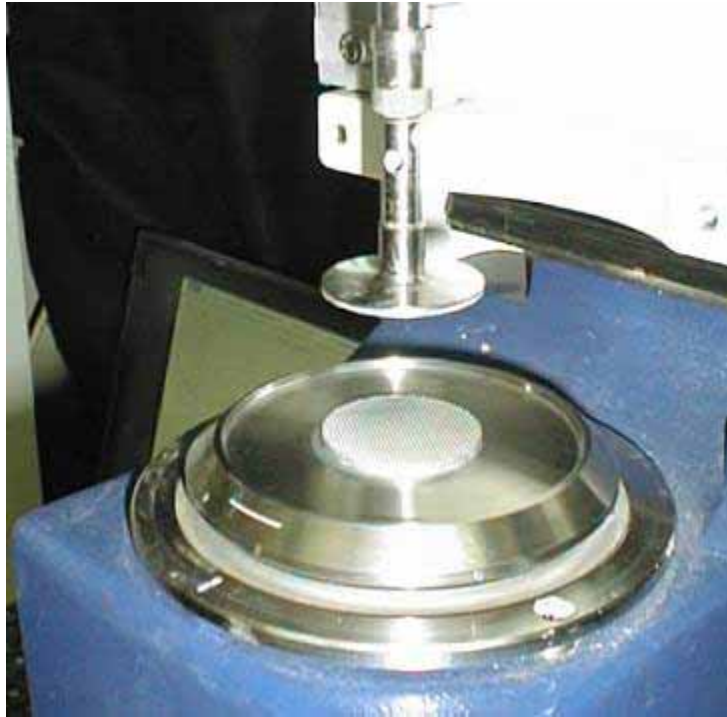


**Figure 15. A photograph of the rheometer used at NIST.**

The cement pastes were mixed with a blender for 10 s before being placed in the rheometer (figure 15). The rheometer is somewhat specialized, and it may require expert operation and interpretation. It does have the advantage of being relatively quick to run, and a number of cementitious systems can be compared in a single day. This makes it useful for materials prequalification work. Many State DOTs reportedly own the equipment for use in testing asphalt, and a small interchangeable modification is required to make it suitable for use with cementitious pastes. As shown in figure 3, the initial setting times determined using this test method were generally consistent with those found by other methods. Of more interest is that the slope of the yield stress/time plot determined for the cementitious systems could be used to predict the systems that were rapid setting or very reactive (table 9, final column). The systems that were indicated as rapid stiffening included many of those made with cements 2, 4, and 5, without supplementary cementing materials. This is consistent with the calorimetry data discussed in detail above. The method is useful for detecting problems related to the silicate reactions.

#### *Mortar Cube Strength*

Mortar cubes were prepared in accordance with ASTM C 109 except that mix proportions were at a fixed w/cm (0.5), and water-reducing admixture was included as required in the test matrix. Flow was recorded but not fixed or adjusted. The cubes were tested for compressive strength at 24 h (table 9).

A loose correlation was observed between the 24-h cube strength and the magnitude of the silicate peak in calorimetry tests. This is not surprising because both effects are governed by the early reactivity of the silicates. The strengths may be influenced by the following conditions:

- Setting time—retardation would suppress early strength.
- Air content—decreasing strength with increasing air.

It was considered that there were too many confounding effects and a lack of reliability to make this a useful approach for indicating incompatibility.

### *Air Content*

The amount of vinsol air entraining admixture required to achieve an air content of 18 percent was determined in accordance with ASTM C 185, except that the mix proportions were fixed as discussed above.

Little correlation was found between mortar air content and other test data except the 24-h cube strength as discussed in table 9.

### **Stiffening**

Stiffening was assessed by testing according to a modified version of ASTM C 359. Modifications were to use the same mix proportions as the rest of the paste work in this project, and room temperatures were controlled at 21, 32, or 10 °C ± 3 (70, 90, or 50 °F ± 5) and paste temperatures were not recorded (table 9).

It is notable that the systems that were indicated by this test to be false setting were not always the same as those indicated by the minislump test. In general, the systems that were indicated to be potentially problematic were those containing cements 2, 4, and 5, all of which have been similarly problematic in other test methods including time of setting, calorimetry, and minislump pat area.

A variation of this test method is being developed by the ASTM subcommittee (09-48) on incompatibility at ASTM for this application. Work is ongoing in this committee to refine the method and provide guidance on interpreting the data.

### **Pore Solution Chemistry**

Following is a summary of the introduction and conclusions of the pore solution chemistry analyses.

#### *Introduction*

Depending on initial time of setting for different mixes, extractions were done on either plastic-state or hardened-state paste. Mixing procedure for the paste was adapted from that described in the report, *Early Stiffening Test Development for Portland Cement*.<sup>(82)</sup> This method of mixing cement paste was also used for the minislump testing. Chemical analysis of the pore solution collected was conducted for sodium, potassium, calcium, and sulfate ion, as well as pH measurement.

Paste samples were mixed with water at w/cm of 0.5, and solutions extracted in either the plastic or hardened state at 5, 10, 30, 60, 360, and 1,440 min after mixing. Samples were taken from all four rounds of testing.

**Paste mixing:** Paste was mixed in a blender at 10,000 rpm for 90 s counting from the moment all cement and admixture were added to the water. Mixing proportions used were 500 g (17.6 oz) of cementitious material, 250 ml (8.5 oz) of water, and varied amounts of WRA admixture. Admixtures were measured and emptied into the mixer using 5-ml (0.17-oz) plastic syringes and dosed at single and double dosages recommended by the manufacturer. Lignin-based WRA A was dosed at 325 and 650 mL/100 kg (5 and 10 oz/cwt) of cementing material. Sugar-based WRA B was dosed at 163 mL/100 kg (2.5 oz/cwt) of cementing material. A w/cm of 0.5 was used in all paste mixes.

Because of the different effects on paste consistency experienced on initial time of setting and early stiffening by using different extraction conditions such as time after mixing, combination of materials, and mixing temperature, the solution extractions were performed either in plastic state where the sample was poured into disposable centrifuge tubes, or in hardened state where samples were cast in small cylinder molds.

**Extractions during plastic state.** An analytical centrifuge machine was used to extract solution before the cement paste reached initial set. The centrifuge machine was equipped with a 115-volt, 1.5-amp, 60-Hertz (Hz) motor, and it had a total capacity of six tubes. Plastic centrifuge tubes with a gradation scale and a total capacity of 15 ml (0.5 oz) were used.

Minimum extraction times were determined previously to obtain between 10 and 15 ml (0.3 and 0.5 oz) of solution. The extraction times were 1 min for very fluid paste and 3 min for less fluid paste. A funnel was used to put the paste in the six centrifuge tubes; and where the paste would not flow easily, a vibrating table was used. Twelve tubes were filled in with paste to obtain the desired amount of liquid from paste mixes that had not yet reached initial set but showed significant stiffening at 6 h after mixing.

**Extractions during hardened-state.** An extraction method for squeezing solution out of hardened cement paste was adopted from previous research studies at Purdue University.<sup>(83)</sup> A die and piston manufactured of steel and designed to carry loads of up to 1,330 newtons (N) (300,000 lb) of force, “squeezed” the pore liquid by applying pressure to the paste specimen. Liquid was collected through grooves in the base and carried out into test tubes tube using flexible tubing flushed with nitrogen gas. Specimens used for this extraction technique were discs cast in 50-mm (2-inch) diameter by 19-mm (.075-inch) height disc cylinders that provided a tight seal. An illustration of the press die set is shown in figures 16 and 17, showing in figure 16 the paste specimen and the cylindrical chamber before introducing the disc and applying the pressure. Normally four to five disc specimens were required to obtain the desired volume of liquid.

**Chemical analysis.** After the extraction, samples were sealed and kept in the refrigerator before analysis the next morning. After refrigeration, samples were allowed to reach room temperature, pH was measured, and solutions were acidified to minimize potential changes in chemical composition resulting from carbonation. Samples were analyzed within the next 24 h for sulfate,

calcium, sodium, and potassium concentration. Sulfate analyses were done according to ASTM C 114 wet method for chemical analysis, determined by the gravimetric method after precipitation with reagent-grade barium chloride. Calcium, sodium, and potassium analyses were done using Atomic Absorption Flame Emission Spectroscopy (AAS) using a spectrometer. Sample preparation in most cases did not require more than 10 times dilution of the original volume, and in no case exceeded 100 times. Concentrations were calculated in mg/L of solution and used in parts per million (ppm) for data reduction and analysis.



**Figure 16. Die set for squeezing pore solution from hardened cement paste specimens.**



**Figure 17. Pore fluid being collected from die set.**

## **SUMMARY**

The setting or stiffening behavior of hydrating portland cement or cements with SCMs during the first 10 min after mixing is generally attributed to the reactions involving  $C_3A$  and the sulfate from the added gypsum and from alkali sulfates in the clinker. In cases when the system is not in balance with respect to these reactions, changes in rheology of the mixture may result, and the mixture may exhibit early stiffening, false set, or flash set. False set is related to precipitation of gypsum because of a high concentration of sulfate in the pore solution. Flash set, the result of too little sulfate available in the pore solution, is caused by formation of  $C_3A$  hydrates instead of ettringite, which is the normal hydration product.

Early after mixing, the concentration of the constituent ions in the pore solution varies according to the specific cement. For example, in cements high in alkali sulfates, the concentration of sulfate ions as well as alkali ions will be high. At the same time the hydration of the  $C_3S$  will contribute calcium ions as well as hydroxyl ions to the pore solution. In special cases where the

concentrations of sulfate and calcium ions are high, the pore solution can be supersaturated with, for example, gypsum, and this may cause gypsum to precipitate. The criterion for this is whether the so-called solubility product for gypsum is higher than that corresponding to gypsum in equilibrium with the pore solution, which in this case is said to be saturated with respect to gypsum. The solubility product of gypsum is calculated according to the equation in figure 18.

$$K_{\text{gyp}} = [\text{Ca}^{2+}][\text{SO}_4^{2-}]$$

**Figure 18. Equation. Solubility product of gypsum.**

Where  $[\text{Ca}^{2+}]$  and  $[\text{SO}_4^{2-}]$  are the concentrations of calcium ions and sulfate ions respectively in the pore solution. Solubility products for other compounds can be calculated in similar ways, and for saturated solutions, the solubility products at a given temperature are constants specific for the considered compound. Strictly, another term, “activity,” should be used rather than the term “concentration.” “Activity” takes into consideration the presence of other ionic constituents of the pore solution; therefore, the term “ion activity product” (IAP) is used rather than the term “solubility product.” For gypsum, this term is expressed as the equation in figure 19.

$$\text{IAP}_{\text{gyp}} = (\text{Ca}^{2+})(\text{SO}_4^{2-})$$

**Figure 19. Equation. Ion activity product of gypsum.**

Where  $(\text{Ca}^{2+})$  and  $(\text{SO}_4^{2-})$  respectively are the activities of the calcium ions and sulfate ions of the pore solution, and these can be calculated from the total composition of the pore solution.

One way to characterize the pore solution regarding possible supersaturation with, for example, gypsum or other constituents, is to define the saturation factor, SF, as the ratio between the actual  $\text{IAP}_{\text{gyp}}$  of the pore solution and the corresponding value for the saturated condition.

SF values larger than 1 indicates supersaturation, SF = 1 corresponds to the saturated solution, and for SF smaller than 1 the solution is undersaturated. A crystal cannot exist in a solution with SF < 1; it is not stable, and it will dissolve. In a solution with SF > 1 it will grow; it cannot dissolve.

For the selected systems, the saturation factors for gypsum ( $\text{CaSO}_4 \cdot 2\text{H}_2\text{O}$ ),  $\text{SF}_{\text{gyp}}$ , syngenite ( $\text{K}_2\text{Ca}(\text{SO}_4)_2 \cdot \text{H}_2\text{O}$ ),  $\text{SF}_{\text{syn}}$ , and calcium hydroxide ( $\text{Ca}(\text{OH})_2$ ),  $\text{SF}_{\text{CH}}$ , were studied. Syngenite is a potassium-calcium-sulfate that can precipitate in systems with cements with high sulfate and potassium concentrations.

For cement pastes of grey and white portland cement, it is known from the literature that  $\text{SF}_{\text{gyp}}$  and  $\text{SF}_{\text{syn}}$  can be larger than 1 for up to about 10 h or later and  $\text{SF}_{\text{CH}}$  is larger than 1 for up to 28 days or more.<sup>(84,85)</sup> The supersaturation of gypsum is related to the dehydration of gypsum to hemihydrate (plaster of paris) in commercial cements during grinding. The plaster is much more soluble than gypsum, and it can deliver sulfate to the pore solution faster than it can be consumed by the reaction with  $\text{C}_3\text{A}$  phase. Extra sources of sulfate such as alkali sulfates also can contribute to supersaturation. The reason for the prolonged super saturation of calcium hydroxide is probably the continued hydration of  $\text{C}_3\text{S}$  and  $\text{C}_2\text{S}$ .



Water reducers are in many ways similar to retarders. Taylor makes references to work showing that calcium ion concentration and hydroxyl ion concentrations increase in pore solution when such chemical admixtures are used.<sup>(53)</sup> The mechanism is probably that they modify the reaction products by being adsorbed and allow the calcium ion concentration in solution to be higher than in pore solutions with the unmodified hydration product.

For the four systems 2P, 2C, 4P and 5P (no admixture) considered “early stiffening” at 21 °C (70 °F), the  $SF_{\text{gyp}}$  values for 2P, 2C, and 5P were similar  $\sim 6.5$ , and for 4P it was  $\sim 2.5$  without any significant change up to 360 min. After this time, all values decreased to below 1, signaling all gypsum has been consumed. During the period from mixing until 360 min, the  $SF_{\text{gyp}}$  values indicate supersaturation, and hence, a potential for precipitation of gypsum with possible effect on the workability. The supersaturation in 4P is lower than in the other systems, and it would be expected that this system would show less early stiffening compared to the others.

In the  $SF_{\text{syn}}$  system, 4P is again the lowest—around 1 up to 10 min and then for later times smaller than 1, indicating no presence of syngenite. This makes sense because cement 4P is low in potassium. The other systems all have  $SF_{\text{syn}}$  higher than 10, indicating potential for precipitation of syngenite, which can cause the same effects as precipitation of gypsum. Because syngenite is a sulfate-bearing phase, it might compete with the  $C_3A$  for the sulfate ion in the pore solution and cause flash set.<sup>(53)</sup>

Regarding calcium hydroxide the  $SF_{\text{CH}}$  values for 4P again is the lowest of the set, with values from 2.5 increasing to about 10 at 360 min, after which time it decreases but maintains values  $> 1$ . The other systems have values from around 9 increasing to 26 at 360 min. As mentioned above, the pore solution is expected to be supersaturated by calcium hydroxide for some time after mixing; but, the individual differences in supersaturation cannot be explained at this time. The reasons can be many—different reactivity of the clinker minerals of the cement contributing calcium ions and hydroxyl ions at different rates to the pore solution, effect of alkalis on the calcium ion concentration, or different ratios between calcium and silica in the calcium-silicate-hydrate formed during the early hydration process.

Addition of water reducers A and B (single (A) and double dosage (DA) of A and single dosage of B) generally resulted in an increase of the hydroxyl ion concentration of the pore solution for all systems and in calcium ion concentration except for 4PA and 4PDA. The  $SF_{\text{gyp}}$  for 4PA and 4PDA was not changed significantly, but for the other systems it increased with progressive addition of water reducer A. Addition of B had a similar effect as addition of a single dosage A. This indicates increasing tendency for early setting with increasing addition of water reducer. For  $SF_{\text{syn}}$  the addition of water reducers had similar effects.

For  $SF_{\text{CH}}$ , the addition of water reducer had an effect for all systems: The  $SF_{\text{CH}}$  increased with increasing addition. The increases in SF values are in line with the findings reported in literature referred to above; however, the effect of the supersaturation with respect to calcium hydroxide on the early stiffening behavior is not understood.

One set considered “Fast Stiffening”—(2PA, 5PA, 5PB, and 5P) and a set considered “Normal”—(1PA, 1CA, 1PB, and 6PA) at 21 °C (70 °F), were also tested at 32 °C (90 °F). Up to 60 min after mixing, the “Fast Stiffening” systems had higher  $SF_{\text{gyp}}$  and  $SF_{\text{syn}}$  values than the

“Normal.” The “Fast Stiffening” had  $SF_{\text{gyp}} > 5$  and the “Normal”  $< 3$ . Changing the temperature from 21 to 32 °C (70 to 90 °F) had only a small effect on the level of individual SF values until about 60 min after mixing. Then the  $SF_{\text{gyp}}$  and  $SF_{\text{syn}}$  values decreased to less than 1 for the 32 °C (90 °F) treated systems. This indicates the following:

- The “Fast Stiffening” systems have higher potential for precipitation of gypsum and syngenite with the possible effects on workability and early stiffening behavior.
- The higher temperature accelerates hydration of  $C_3A$ , and hence, the consumption of gypsum is at a much earlier time. For both the “Fast Stiffening” and “Normal” sets, this will lead to shorter setting time in general.

The  $SF_{\text{syn}}$  values for the “Normal” are around or below 1 in all cases, indicating the nonexistence of syngenite, and hence, no negative effect of this phase on the rheology. For the  $SF_{\text{CH}}$  no clear tendency was observed other than the “Fast Stiffening” systems increased at 32 °C (90 °F) relative to 21 °C (70 °F).

Four systems considered “Slow Stiffening” at 21 °C (70 °F)—2CA, 2FA, 2CDA, and 1B— together with “Normal” systems mentioned above were tested at 10 °C (50 °F). Regarding the gypsum the  $SF_{\text{gyp}}$  values for the “Slow” with the exception of 1B were around 10 to 14 and the “Normal” slightly lower. The effect of decreasing the temperature from 21 to 10 °C (70 to 50 °F) was a slight increase in SF values for the “Slow Stiffening” as well as the “Normal” set up to 360 min after mixing. With the exception of 6PA, after this time, the  $SF_{\text{gyp}}$  values for the “Normal” decreased to less than 1, indicating total consumption of gypsum; but the  $SF_{\text{gyp}}$  values for the “Slow Stiffening” treated at 10 °C (50 °F) remained almost unchanged at their levels larger than 1, indicating that gypsum was still present at 1,440 min after mixing. For the “Slow Stiffening” set, the  $SF_{\text{syn}}$  behavior was similar. The values for the system 1B indicated no existence of syngenite either at 21 or 10 °C (70 or 50 °F), which was also the case for the “Normal” systems. No clear trend could be observed regarding calcium hydroxide.

The following list of findings is based on the study of saturation factors for gypsum, syngenite, and calcium hydroxide:

- Addition of water reducers results in an increase in the saturation factors for gypsum, syngenite, and calcium hydroxide in the systems studied.
- For “Fast Stiffening” systems tested at 32 °C (90 °F), the saturation factors for gypsum and syngenite were not affected until after 60 min after mixing comparing to those of samples tested at 21 °C (70 °F). After 60 min the 32 °C (90 °F) saturation factors decreased to below 1, indicating total consumption of gypsum. When tested at 21 °C (70 °F), this change took place after 360 min after mixing.
- Testing “Slow Stiffening” systems at 10 °C (50 °F) had only minor effect on the saturation factors for gypsum and syngenite up to 360 min after mixing when compared to samples tested at 21 °C (70 °F). After 360 min the saturation factors decreased to below 1 for samples tested at 21 °C (70 °F), indicating the presence of gypsum at least up to 1,440 min after mixing.

- Comparing “Fast Stiffening” systems with “Normal” showed that the levels of gypsum saturation factors were highest for the “Fast Stiffening” systems. The difference in saturation factor values might be an indicator of whether a system could be considered fast or normal; however, when comparing “Normal” with “Slow Stiffening” systems, the gypsum saturation factors for the “Slow Stiffening” are slightly higher than for the “Normal.” Based on the present study, it is not possible to characterize early stiffening behavior based solely on pore-solution chemistry.

## Slump Loss

**Concrete Slump Loss.** Three slump cones were prepared after the concrete mixtures had been mixed. The samples were covered to prevent moisture loss, and they were kept in a room controlled to the temperature selected (10, 21, or 32 °C (50, 70, or 90 °F)). Slumps were measured 15, 30, and 60 min after initial mixing in accordance with ASTM C 143. The data reported are the percentage slump losses at each time (100 percent meaning that slump has reached 0 mm (0 inch)).

Some mixes had a slump of zero initially; therefore, valid slump loss data were not obtained. These included mixes containing cements 2 and 4 at 32 °C (90 °F). All mixes at 32 °C (90 °F) exhibited significant slump loss reaching zero slump within 30 min. At 21°C (70 °F), mixes made with cements 2, 4, and 6 had reached near zero slump in 30 min. Cements 1 and 5 were still showing some workability at this time. The rapid slump loss of cement 6, even from a high initial slump, is surprising because this is not consistent with the paste and mortar test results. The slump loss data are not consistent with other test methods and may be questionable for the following reasons:

- The slump test is only appropriate for values between 12 and 225 mm (0.5 and 9 inches), and therefore, values less than 12 mm (0.5 inch) are not reliable. Likewise, the precision of the test is approximately 25 mm (1 inch), therefore, a 100 percent slump loss from 25 to 0 mm (1 to 0 inch) is not necessarily meaningful. A number of mixes had a zero slump initially making the test meaningless. In paving, low slump mixes are required to prevent edge slump; therefore, the usefulness of this test may be limited in this application.
- The approach used here was to test specimens that were undisturbed from the time of initial mixing. This was done to reduce variability induced by breaking up early hydration bonds that would influence slump; however, this approach is not typical of normal field handling of concrete, which is significantly disturbed during transport (even in a flat bed truck), placing, and compaction.

**Mortar Flow Loss.** Samples of mortar were sieved from the same concrete mixtures used to determine concrete slump loss. Three mortar flow cones (ASTM C 1437) were filled and covered until tested at 15, 30, and 60 min after initial mixing. Similar to the concrete slump loss data, the results are presented as percentage reduction in flow at each time.

Cement 2 at 21.1 °C (70 °F) exhibited relatively low slump loss at either temperature or admixture dosage. This is consistent with the minislump observations that show high risk of false

setting that is balanced with the use of water reducing admixture. Cement 5 exhibited significant loss of flow at 21.1 °C (70 °F) that decreased at the higher temperature or with increasing water reducer dosage. Cement 4 had a moderate slump loss at 32 °C (90 °F), but otherwise reasonably low slump loss at the other temperatures. Cements 1 and 6 did not exhibit much loss of flow over the time measured. These observations are consistent with other test methods that detect stiffening because of silicate reactions, and they appear to be more reliable than the concrete slump loss tests.

## Ultrasonic P-Wave

**Theory of Wave Propagation.** Longitudinal (compression) waves, transversal (shear) waves, and surface (Rayleigh) waves are the three common types of stress waves that propagate through an elastic medium. The velocity of these waves depends on the elastic properties of the medium. The pulse velocity  $V$  of longitudinal stress waves in a concrete is related to its elastic properties and density according to the relationship expressed in the equation in figure 20.

$$V = \sqrt{\frac{E(1-\mu)}{\rho(1+\mu)(1-2\mu)}}$$

**Figure 20. Equation. Pulse velocity.**

Where

$V$  = Wave velocity.

$E$  = dynamic modulus of elasticity.

$\mu$  = dynamic Poisson's ratio.

$\rho$  = density.

The Ultrasonic Pulse Velocity (UPV) test is a stress wave propagation method that involves measurement of the travel time of compression waves pulse over a known path length. Pulses of longitudinal stress waves are generated by an electro-acoustical transducer that is held in contact with one surface of the concrete under test. After traversing through the concrete, the pulses are received and converted into electrical energy by a second transducer located a distance  $L$  from the transmitting transducer. The transit time  $T$  is measured electronically. The pulse velocity  $V$  is calculated by dividing  $L$  by  $T$ . ASTM C 597 is the standard test method for pulse velocity through concrete.

**Test Procedure and Instrumentation.** Concrete specimens were cast and compacted in a purpose-made 150- by- 150- by 300-mm (6- by 6- by 12-inch) acrylic mold. Transducers were then bolted on each side of the mold. An ultrasonic couplant was applied between the transducer and the acrylic to ensure good wave transmission. Both transducers were then connected to a commercial UPV device. Transit time was recorded automatically at desired intervals, and the wave velocity was calculated by dividing the length of the mold by the transit time.

**Test Results.** The test results show that initial and final set can be determined using this technique. The two points are marked by a sudden change in the rate of increase of the wave

velocity. As shown in figure 3, the results are reasonably consistent with other methods used to assess initial setting times.

## **Impedance**

Consolidation of the concrete was determined at initial mixing and after setting using the impedance-based apparatus described by Alexander et al.<sup>(86)</sup> There was little correlation between the initial impedance and the initial slump. This method does not appear to provide useful data regarding potential incompatibility. It is the loss of workability of a concrete as it makes its way to and through a paving machine that is the most common and problematic occurrence of “incompatibility” in pavements. A number of mechanisms can cause this phenomenon, meaning that a number of approaches may be required to detect them all.

In some cases it may be a slow occurrence of false set (gypsum deposition), such as Cement 2, influenced by the solubility rate of the sulfate compounds. Rapid false set often may go unnoticed because mixing continues for some time during transport if an agitating truck is used. On the other hand, this problem will be significant if a dump truck is used. Early stiffening caused by insufficient sulfate in the system is another cause of early stiffening (flash set). Both of these reactions will be accelerated by high temperatures and the presence of some WRAs.

In other cases, the rate of silicate reaction will be the issue, either accelerated by high temperatures, high alkali content, and high fineness; or retarded by some WRAs and earlier aluminate reactions reducing the amount of calcium in the pore solution. The formation of syngenite also appears to be a potentially significant factor.

The following test methods appear to be appropriate for detecting the various mechanisms of stiffening and setting related incompatibility discussed earlier:

- False set: minislump, stiffening.
- Flash set: minislump, calorimetry, stiffening, time of setting, rheometer.
- Accelerated or retarded silicate hydration: time of set, calorimetry, mortar slump loss, semi-adiabatic temperature monitoring.

Selection of which tests to use should be based on urgency, availability of test equipment, cost of testing, and cost of failure. This is discussed further in Volume II of this report.

## **TASK 2.1.2—CRACKING**

### **Introduction**

This task includes a suite of tests intended to evaluate the potential for early-age cracking. The work examined the tendency of concrete to crack under conditions of full restraint, the stresses that develop in the concrete under those conditions, the heat evolution, and the development of stiffness (as measured by modulus of elasticity). The test program also measured the development of the ability of the concrete to resist cracking in terms of the splitting tensile

strength and nondestructive tests suitable for field monitoring of pavement concrete. Initial and final setting times and compressive strengths were measured.

The test program involved a 24-h period of intensive monitoring of the properties of the concrete immediately after casting. The purpose of this monitoring was to examine the development of the properties of interest at early ages. It is not anticipated that such an intensive test program would be incorporated into an evaluation of the materials and mix designs for pavement projects; however, it should indicate which measurements are the most critical so that these could be adopted as necessary. It will also allow for the correlation of the various types of measurements.

## **Materials**

Materials were obtained from projects that reported incompatibility problems during construction. These reports were gathered during the information collection phase of this project. Chemical analyses of the cements are given in table 24 and the fly ashes in table 25.

The first scenario involves a particular portland cement that appeared to be incompatible with one brand of lignosulfonate water reducer, but not with a comparable admixture made by another manufacturer. The problem was seen during hot weather concreting. The test program used the same brand of cement and the two water reducers. The cement had been received from the field and stored for some time before laboratory testing was conducted. The tests were conducted at a nominal 32 °C (90 °F). The mixes in this scenario were labeled WRA1 and WRA2.

The second scenario simulates a combination of a cement with 20 percent of a Class C fly ash that was reported to be problematic in the field, along with a lignosulfonate admixture. An alternative fly ash reported to be satisfactory was used in the companion mixture. The chemical analyses of these materials were very similar, as shown in table 25. The C<sub>3</sub>A content of both fly ash samples was estimated by x-ray diffraction XRD to be similar in both materials. The mixes in this scenario were labeled FA1 and FA2.

The third scenario simulates a concrete containing fly ash along with two chemical admixtures that at elevated temperatures exhibited false set in the field. Four mixtures were conducted, two at 32 °C (90 °F) using 25 percent and 4 percent fly ash by mass of cement, and the same mixtures prepared at 21 °C (70 °F). These mix parameters were selected to mirror those used on the site where the problem was observed. These mixtures were labeled 25FA90, 4FA90, 25FA70, and 4FA70, respectively.

All mixtures were prepared using the same aggregates comprising siliceous gravel coarse aggregate and siliceous fine aggregate from the same source (table 26). Cement 2 was the same material used in Task 2.1.1. It was identified as Cement 5 in that series.

All WRAs were ASTM C 494 Type A, and both air entraining admixtures were nonvinsol-based materials.

**Table 24. Oxide analyses of cements.**

Analyte	Mass (percentage)		
	Cement 1	Cement 2	Cement 3
SiO <sub>2</sub>	19.99	20.83	26.91
Al <sub>2</sub> O <sub>3</sub>	5.10	4.20	6.46
Fe <sub>2</sub> O <sub>3</sub>	3.83	3.26	1.86
CaO	62.68	62.55	54.45
MgO	1.18	3.23	5.67
SO <sub>3</sub>	2.42	2.75	2.64
Na <sub>2</sub> O	0.10	0.13	0.24
K <sub>2</sub> O	0.52	0.65	0.49
TiO <sub>2</sub>	0.18	0.30	0.33
P <sub>2</sub> O <sub>5</sub>	0.19	0.09	0.23
Mn <sub>2</sub> O <sub>3</sub>	0.04	0.53	0.23
SrO	0.06	0.05	0.05
Cr <sub>2</sub> O <sub>3</sub>	0.01	<.01	<.01
ZnO	0.02	0.22	0.03
L.O.I. (950 °C)	3.74	1.45	-0.03
Total	100.08	100.24	99.56
Alkalies as Na <sub>2</sub> O	0.44	0.56	0.56
<b>Calculated Compounds per ASTM C 150-02a</b>			
C <sub>3</sub> S	57	56	*
C <sub>2</sub> S	15	18	*
C <sub>3</sub> A	7	6	*
C <sub>4</sub> AF	12	10	*

\* Cement 3 was a Type IS blended cement, making calculated Bogue values meaningless.

**Table 25. Oxide analyses of supplementary cementing materials.**

Analyte Material	Mass (percentage)		
	Fly Ash 1	Fly Ash 2	Fly Ash 3
SiO <sub>2</sub>	36.42	36.14	33.83
Al <sub>2</sub> O <sub>3</sub>	19.18	18.33	17.99
Fe <sub>2</sub> O <sub>3</sub>	6.01	5.20	6.08
CaO	24.27	26.04	26.11
MgO	4.57	4.84	6.12
SO <sub>3</sub>	2.13	2.41	2.17
Na <sub>2</sub> O	1.63	1.59	2.14
K <sub>2</sub> O	0.51	0.47	0.39
TiO <sub>2</sub>	1.55	1.61	1.46
P <sub>2</sub> O <sub>5</sub>	1.18	0.98	1.33
Mn <sub>2</sub> O <sub>3</sub>	0.04	0.03	0.03
SrO	0.40	0.44	0.36
Cr <sub>2</sub> O <sub>3</sub>	0.02	0.02	0.02
ZnO	0.02	0.02	0.02
L.O.I. (950 °C)	0.36	0.40	0.38
Total	98.28	98.52	98.39
Alkalies as Na <sub>2</sub> O	1.96	1.91	2.39
Moisture	0.22	0.21	0.09
SiO <sub>2</sub> +Al <sub>2</sub> O <sub>3</sub> +Fe <sub>2</sub> O <sub>3</sub>	61.61	59.67	57.90

**Table 26. Physical properties of aggregates.**

	19-mm Coarse Aggregate	9-mm Coarse Aggregate	Siliceous Fine Aggregate
<b>Sieve Analysis</b>			
<b>Sieve</b>	<b>Percentage Passing</b>		
25-mm	100.0		
19-mm	94.5		
12.5-mm	0.9		
9.5-mm	0.1	100.0	
4.75-mm		0.6	99.1
2.36-mm		0.1	89.7
1.16-mm		0.1	75.7
0.600-mm			48.9
0.300-mm			13.6
0.150-mm			1.3
0.075-mm			0.3
Pan	0.0	0.0	0.0
Fineness Modulus			2.72
<b>Density</b>			
Bulk Specific Gravity (SSD)	2.68	2.65	2.63
Absorption	1.20	1.51	1.15
Dry Rodded Unit Weight, kg/m <sup>3</sup>	1,665.00	1,680.00	1,780.00

Unit conversions:

1mm =0.0394 inch

1 kg/m<sup>3</sup> = 1.69 pcy



## MIX DESIGNS

A total of six sets of mix proportions were prepared for testing. All mixes were based on the information obtained from the field where material incompatibilities had been observed. Of the six mixes, three mixes are labeled as “incompatible,” and the remaining three as “compatible.” Two of the mixes were also conducted at 21 °C (70 °F) to investigate temperature sensitivity of the reported incompatibility. The matrix of concrete mixtures is summarized in table 27.

**Table 27. Concrete mixtures.**

Incompatible Mix	Compatible Mix	Temperature	Materials
WRA1	WRA2	32 °C	Cement 1 Water reducer 1 Water reducer 2 Air entrainer 1
FA1	FA2	32 °C	Cement 2 Fly ash 1 Fly ash 2 Water reducer 3 Air entrainer 1
25FA90	4FA90	32 °C	Cement 3 Fly ash 3 Water reducer 1 Water reducer 4 Air entrainer 2
25FA70	4FA70	21 °C	

Unit conversions:

$$1\text{ }^{\circ}\text{C} = (X - 32)/1.8\text{ }^{\circ}\text{F}$$

Because of the large volume of concrete required to cast all the specimens, two batches of each mix were made. The first batch was used to cast specimens for setting time, AASHTO ring test, P-wave, temperature monitoring, and compressive strength, modulus of elasticity, and splitting tensile strength for 1-, 3-, 7-, and 28-day testing. The second batch was used to cast specimens for setting time and compressive strength, modulus of elasticity, and splitting tensile strength for testing during the initial 24 h after the final set.

Both batches of each mix were made on the same day to keep the variability of materials to a minimum. Immediately after mixing, fresh concrete properties were measured and specimens were cast.

Proportioning and material selection of each mix are summarized in table 28.

**Table 28. Concrete mix proportions.**

Mix ID	WRA1	WRA2	FA1	FA2	25FA90	4FA90	25FA70	4FA70
Temperature, °C	32	32	32	32	32	32	21	21
Cement	1	1	2	2	3	3	3	3
Cement, kg/m <sup>3</sup>	356	356	281	281	267	341	267	341
Fly Ash	—	—	1	2	3	3	3	3
Fly Ash, kg/m <sup>3</sup>	0	0	70	70	89	15	89	15
Fine Aggregate, kg/m <sup>3</sup>	610	610	800	800	599	599	599	599
Coarse Aggregate— 19 mm, kg/m <sup>3</sup>	569	569	489	489	569	569	569	569
Coarse Aggregate— 9.5 mm, kg/m <sup>3</sup>	569	569	489	489	569	569	569	569
Water, kg/m <sup>3</sup>	959	959	824	824	959	959	959	959
Water Reducer	1	2	3	3	1, 4	1, 4	1, 4	1, 4
Water Reducer dosage (mL/100 kg)	534	980	331	331	55, 392	55, 392	55, 392	55, 392
Air Entraining Admixture	1	1	1	1	2	2	2	2
Air Entraining Admixture dosage (mL/100 kg)	36	56	33	33	260	260	260	260

Unit conversions:

$$1\text{ }^{\circ}\text{C} = (\text{X} - 32)/1.8\text{ }^{\circ}\text{F}$$

$$1\text{ kg/m}^3 = 1.69\text{ pcy}$$

$$1\text{ mm} = 0.0394\text{ inch}$$

$$1\text{ mL}/100\text{ kg} = 0.0154\text{ oz/cwt.}$$

## Tests and Results

### *Fresh Concrete Properties*

The following test methods were used to measure fresh concrete properties:

- Slump—ASTM C 143.
- Air content—ASTM C 231.
- Unit weight—ASTM C 138.

Mixes conducted at room temperature exhibited high slumps. As a result, slump flow, rather than slump, was measured.

The fresh concrete properties are presented in table 29.

**Table 29. Fresh concrete properties.**

Mix ID	Slump (mm) Slump Flow (mm)		Unit Weight (kg/m <sup>3</sup> )		Air Content (percentage)	
	Batch 1	Batch 2	Batch 1	Batch 2	Batch 1	Batch 2
WRA1	51	64	2278	2278	7.3	7.0
WRA2	95	95	2323	2323	5.3	5.3
FA1	95	89	2291	2284	6.8	6.8
FA2	114	114	2259	2278	7.2	7.0
25FA90	222	267	2278	2284	5.1	3.7
4FA90	248	248	2284	2281	5.1	4.5
25FA70	(559)	(610)	2259	2271	7.5	7.5
4FA70	(559)	(584)	2259	2262	7.5	7.8

Unit conversions:

1mm =0.0394 inch

1 kg/m<sup>3</sup> = 1.69 pcy

In general, there was little variation in fresh concrete properties between two batches of the same mix.

**Setting Time.** The time of set was measured in accordance with ASTM C 403. The results are presented in table 30.

**Table 30. Setting time data.**

Mix ID	Initial Set (min)		Final Set (min)	
	Batch 1	Batch 2	Batch 1	Batch 2
WRA1	340	349	422	396
WRA2	251	234	341	306
FA1	339	354	430	460
FA2	389	403	477	482
25FA90	No data	298	No data	1511
4FA90	452	464	530	539
25FA70	844	No data	1421	No data
4FA70	726	720	872	848

The 25FA90 mixture exhibited rapid stiffening in the mixer, followed by extremely slow and erratic setting behavior. Final set occurred eventually after 2.5 days. The same mixture prepared at 21 °C (70 °F) was also somewhat erratic. This mix was the only one that exhibited classic stiffening incompatibility behavior in this set of work. In these mixtures in which final set occurred after 1 day, initial measurements of hardened properties were not taken.

**Cracking Tendency.** Cracking tendency and stress development were investigated using the ASTM C 1581 ring test method on samples stored at the same temperature as the mixing temperature. A modification to the test was that the specimens were 125 mm (5 inches) high rather than 150 mm (6 inches) based on the equipment available. For each mix, five rings were cast and monitored until cracking occurred. A summary of the results is presented in table 31.

**Table 31. Results of ASTM ring tests.**

Mix	WRA1	WRA2	FA1	FA2	25FA90	4FA90	25FA70	4FA70
Average initial strain (millionths)	18.60	9.20	5.00	4.30	*	2.00	3.40	6.30
Average maximum strain (millionths)	34.70	34.40	26.00	27.70	*	20.70	13.90	18.90
Average strain rate factor (millionths per root day)	9.90	20.80	10.1	20.80	*	12.10	6.40	11.50
Average stress rate, (MPa/day)	0.14	0.24	0.15	0.17	*	0.20	0.11	0.20
Average time to crack, days	6.79	5.40	5.81	5.54	*	4.50	-	4.51

\* Sample 25FA90 did not crack.

Unit conversions:

1 MPa = 145.0 psi

The results show that mix WRA2 did crack slightly earlier than WRA1, but there was little apparent difference between the two FA mixtures. The mixtures in the third scenario that exhibited setting incompatibility did not crack, while the other two cracked very early.

### *Hardened Concrete Properties*

Hardened concrete properties were measured by testing concrete for compressive strength, modulus of elasticity, and splitting tensile strength. The measurements were conducted every 2 h from time of final set up to 24 h, then at 3, 7, and 28 days. Samples for longer term tests were stored at the mixing temperature for 24 h, then moved to standard storage.

The tests were conducted in accordance with the following methods:

- Compressive strength—ASTM C 39.
- Modulus of elasticity—ASTM C 469.
- Splitting tensile strength—ASTM C 496.

Individual test results are presented in tabular form in tables 32 through 39. Graphical compressive strength, modulus, and splitting tensile strength development are shown in figures 21, 22, and 23, respectively.

**Table 32. Hardened concrete properties for mix WRA1.**

Age	Compressive Strength	Modulus of Elasticity	Splitting Tensile Strength
Hours	MPa	Gigapascal (GPa)	MPa
2	5.7	18.4	0.7
4	8.9	16.4	1.1
6	12.1	18.3	1.3
8	14.1	17.9	1.7
10	16.1	22.8	1.8
12	16.5	23.7	2.1
14	18.6	24.0	2.2
16	19.9	24.1	2.4
18	22.1	25.6	2.2
20	21.2	25.0	2.3
22	21.5	26.8	2.2
24	23.6	27.2	2.4
72	28.1	29.6	2.9
168	33.0	31.0	3.5
672	41.0	34.0	4.0

Unit conversions:

1 MPa = 145.0 psi

**Table 33. Hardened concrete properties for mix WRA2.**

Age	Compressive Strength	Modulus of Elasticity	Splitting Tensile Strength
Hours	MPa	GPa	MPa
2	5.4	13.5	0.6
4	8.8	16.5	0.9
6	11.2	20.4	1.5
8	13.0	19.5	1.7
10	14.9	22.6	1.7
12	17.6	23.3	2.1
14	17.7	24.9	2.2
16	18.1	23.8	2.2
18	20.3	22.6	2.7
20	19.8	22.8	2.3
22	19.1	24.4	2.2
24	21.7	27.1	2.2
72	31.2	28.1	3.1
168	35.2	32.1	3.7
672	45.0	35.6	3.9

Unit conversions:

1 MPa = 145.0 psi

**Table 34. Hardened concrete properties for mix FA1.**

Age	Compressive Strength	Modulus of Elasticity	Splitting Tensile Strength
Hours	MPa	GPa	MPa
2	7.0	15.0	0.9
4	8.8	16.2	1.0
6	10.7	18.5	1.2
8	12.1	19.5	1.5
10	12.5	20.0	1.9
12	13.8	21.2	1.9
14	15.2	20.6	2.0
16	16.4	21.5	2.2
18	16.3	22.1	2.2
20	17.6	23.9	2.3
22	18.7	22.1	2.3
24	23.3	25.3	2.6
72	28.2	28.3	3.0
168	37.8	32.8	3.7
672	7.0	15.0	0.9

Unit conversions:

1 MPa = 145.0 psi

**Table 35. Hardened concrete properties for mix FA2.**

Age	Compressive Strength	Modulus of Elasticity	Splitting Tensile Strength
Hours	MPa	GPa	MPa
2	6.1	13.6	1.0
4	8.3	15.7	1.1
6	9.4	18.4	1.3
8	10.8	18.4	1.6
10	12.3	19.0	1.8
12	14.1	21.3	2.0
14	14.3	25.1	1.9
16	15.1	22.5	2.1
18	15.7	22.9	2.2
20	17.7	23.6	2.2
22	18.4	20.8	2.1
24	18.6	22.0	2.3
72	22.8	26.3	2.6
168	28.3	30.8	3.0
672	36.8	32.1	3.6

Unit conversions:

1 MPa = 145.0 psi

**Table 36. Hardened concrete properties for mix 25FA90.**

Age	Compressive Strength	Modulus of Elasticity	Splitting Tensile Strength
Hours	MPa	GPa	MPa
72	1.4	7.7	0.2
168	13.5	21.2	1.6
672	41.7	32.3	4.4

Unit conversions:

1 MPa = 145.0 psi

**Table 37. Hardened concrete properties for mix 4FA90.**

Age	Compressive Strength	Modulus of Elasticity	Splitting Tensile Strength
Hours	MPa	GPa	MPa
2	2.1	9.1	0.3
4	2.5	10.9	0.3
6	3.2	13.8	0.4
8	4.0	13.9	0.5
10	4.3	15.3	0.6
12	5.9	13.6	0.8
14	7.2	16.2	0.9
16	7.7	17.7	1.0
18	9.2	18.1	1.1
20	10.2	18.5	1.2
22	10.9	19.4	1.4
24	11.7	18.4	1.6
72	22.2	25.5	2.3
168	30.9	30.5	3.4
1176	44.8	35.7	4.1

Unit conversions:

1 MPa = 145.0 psi

**Table 38. Hardened concrete properties for mix 25FA70.**

Age	Compressive Strength	Modulus of Elasticity	Splitting Tensile Strength
Hours	MPa	GPa	MPa
48	1.0	6.1	0.2
72	2.6	12.1	0.4
168	7.1	15.8	0.9
672	16.9	21.5	2.2
1416	36.5	31.8	4.0

Unit conversions:

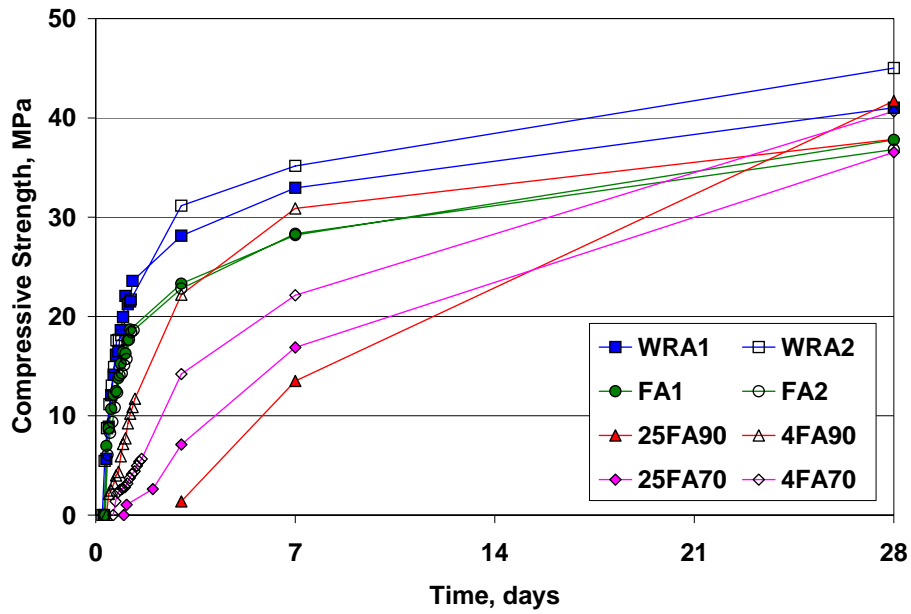
1 MPa = 145.0 psi

**Table 39. Hardened concrete properties for mix 4FA70.**

Age	Compressive Strength	Modulus of Elasticity	Splitting Tensile Strength
Hours	MPa	GPa	MPa
2	1.4	11.0	0.2
4	2.3	9.7	0.3
6	2.6	9.4	0.4
8	2.7	12.0	0.4
10	2.8	10.9	0.4
12	3.2	11.1	0.4
14	3.7	11.0	0.6
16	4.1	12.1	0.6
18	4.4	13.3	0.6
20	5.0	16.7	0.8
22	5.4	15.1	0.8
24	5.7	15.6	0.8
72	14.2	23.9	1.8
168	22.1	33.1	2.6
672	40.7	29.6	4.3

Unit conversions:

1 MPa = 145.0 psi

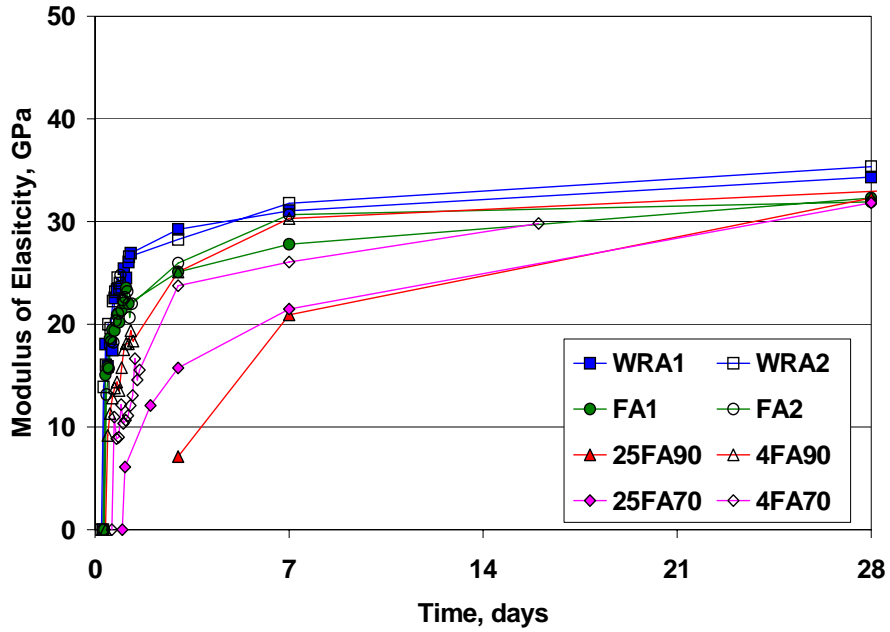


Unit conversions:

1 mm<sup>2</sup> = 0.00155 inch<sup>2</sup>

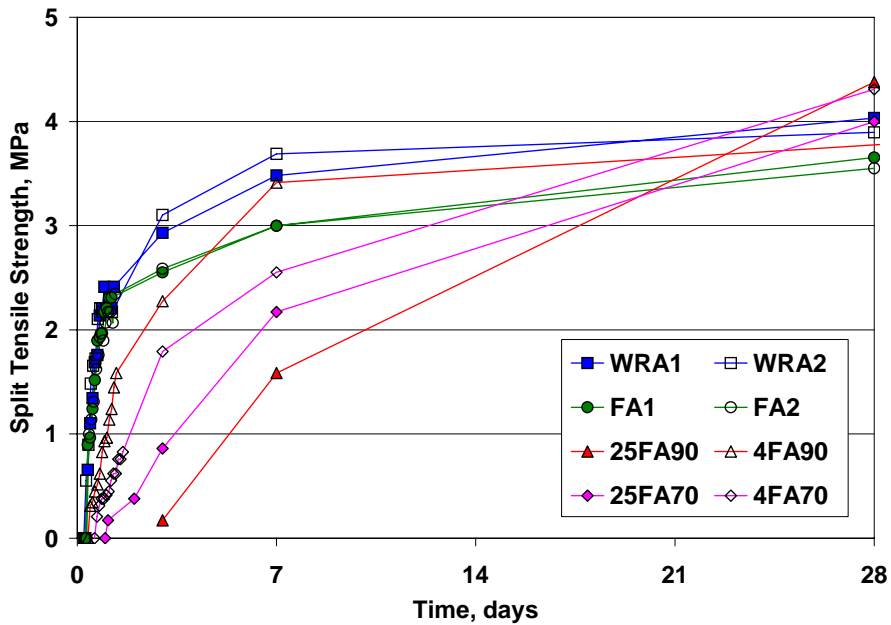
**Figure 21. Compressive strength development.**





Unit conversions:  
 1 MPa = 145.0 psi

**Figure 22. Modulus of elasticity development.**



Unit conversions:  
 1 mm<sup>2</sup> = 0.00155 inch<sup>2</sup>

**Figure 23. Splitting tensile strength development.**

The graphs in figures 21, 22, and 23 show that the 28-day properties of the incompatible mixtures and their respective compatible pairs are similar. Differences are observed in the 7-day data for the mixtures in scenario 3. Properties for the mixtures containing 25 percent fly ash are significantly lower than for the corresponding mixtures containing 4 percent fly ash. This is not unexpected based on trends reported in the literature.

**Heat Evolution.** Thermocouples were used to record the temperature rise of samples stored in semi-adiabatic conditions. This was achieved by casting the thermocouples into 100- by 200-mm (4- by 8-inch) cylinders that were stored inside a similarly sized Dewar flask. Temperatures were monitored for up to 36 h. The data are presented graphically in figures 24, 25, 28, 29, 32, 33, 37, and 38.

**Ultrasonic P-waves.** Ultrasonic P-wave testing was conducted on all of the mixtures. The test is discussed in detail under Task 2.1.1. The data are presented graphically in figures 25, 28, 29, 32, 33, 37, and 38.

## Results Comparison

The following discussion is based on comparing the results for each pair of mixtures.

### *Scenario 1—Influence of Chemical Admixtures, WRA1 and WRA2*

The properties measured for the two mixtures are presented in figures 24 to 27. In an attempt to correlate the development of strength with the time of cracking, a parameter was calculated by dividing the compressive strength by the modulus of elasticity at each age. The results of the calculation ( $f_c/E$ ) have no units and may be considered equivalent to a strain. They are plotted in figures 26 and 27. It is notable that both of the mixtures cracked when this factor ( $f_c/E$ ) had a value of approximately 1 MPa/GPa (pounds per square inch per thousand pounds per square inch (psi/ksi)).

The results of the tests indicate that the risk of cracking as reflected by the ring test data is somewhat higher for the WRA2 mix, based on the higher stress rates and shorter time to cracking. This is in contrast to the field reports that WRA1 was the more problematic. The initial strain in the WRA1 mix was double that of the WRA2 mix. This parameter is described by the test method as being caused by early-age autogenous shrinkage and heat of hydration. The maximum temperature for both mixtures was similar. This indicates similar heats of hydration. The same cement and w/cm was used in both mixtures, which are considered the controlling parameters for autogenous shrinkage. The differences result more from the timing of early hydration in that setting, which was somewhat earlier in the WRA1 mix than the WRA2 mix. The differences in hydration rates would be strongly associated with the chemistry of the different admixtures. A high initial strain would be expected to increase the risk of cracking, depending on the rate of subsequent strain development.

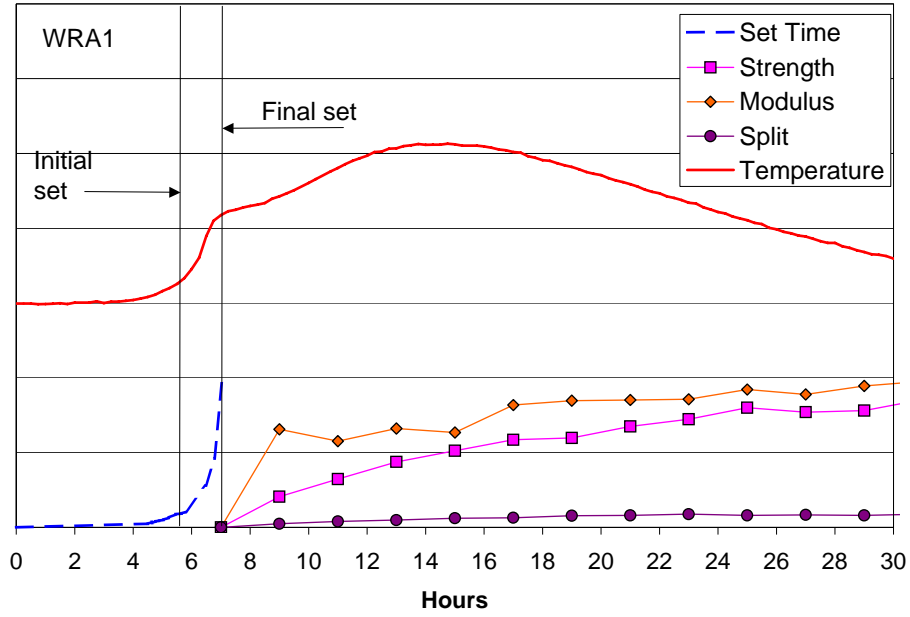


Figure 24. Early age properties for mix WRA1.

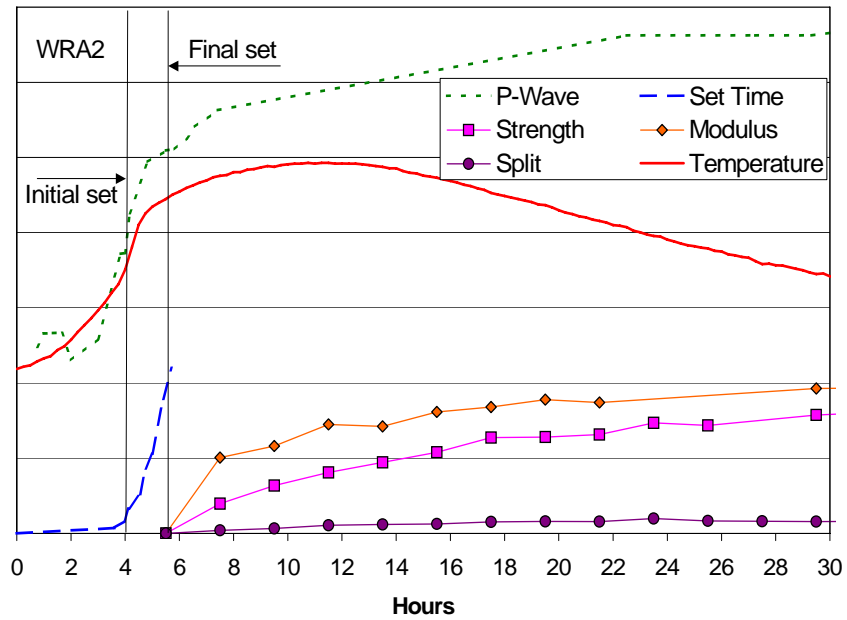
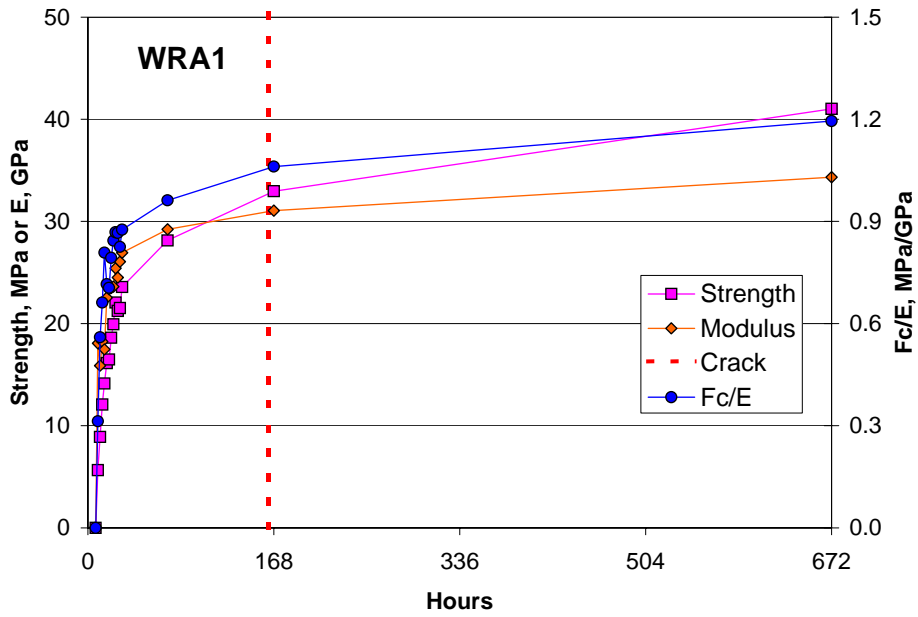
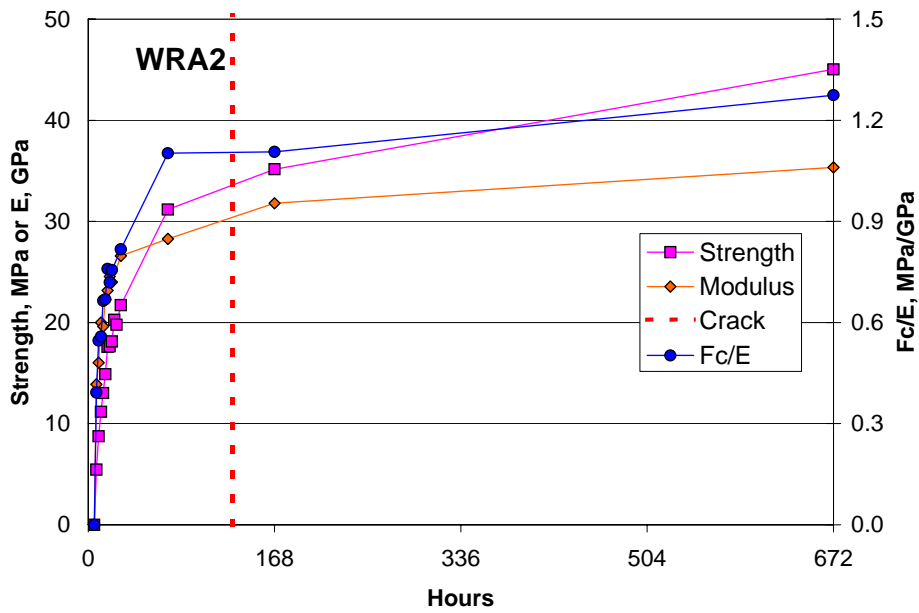


Figure 25. Early age properties for mix WRA2.



Unit conversions:  
1 MPa = 145.0 psi

**Figure 26. Long-term properties for mix WRA1.**



Unit conversions:  
1 MPa = 145.0 psi

**Figure 27. Long-term properties for mix WRA2.**

Long-term properties of the two mixes were similar, highlighting the issue that incompatibility is often related more to early properties that influence constructability than later properties that influence serviceability of the concrete.

*Scenario 2—Influence of Fly Ashes, FA1 and FA2*

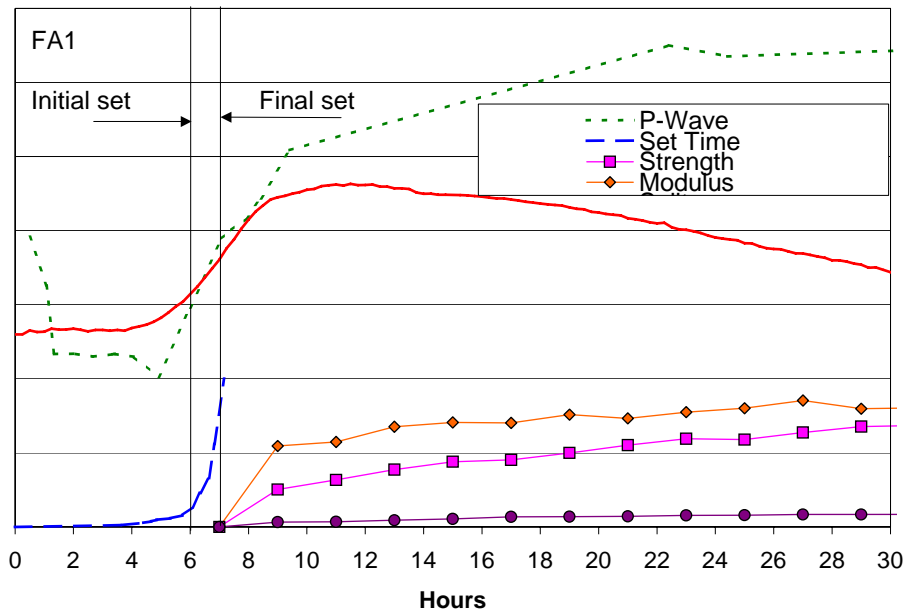


**Figure 28. Early age properties for mix FA1.**

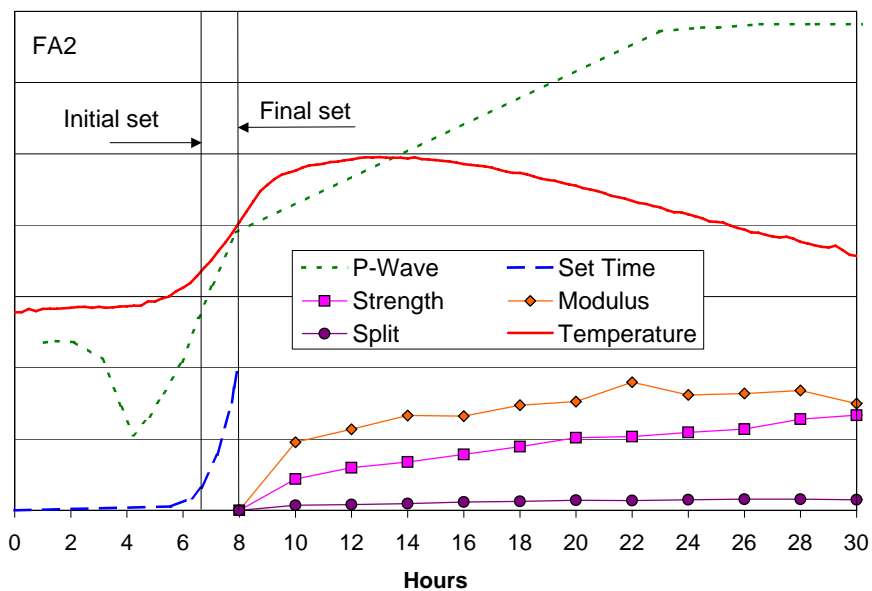
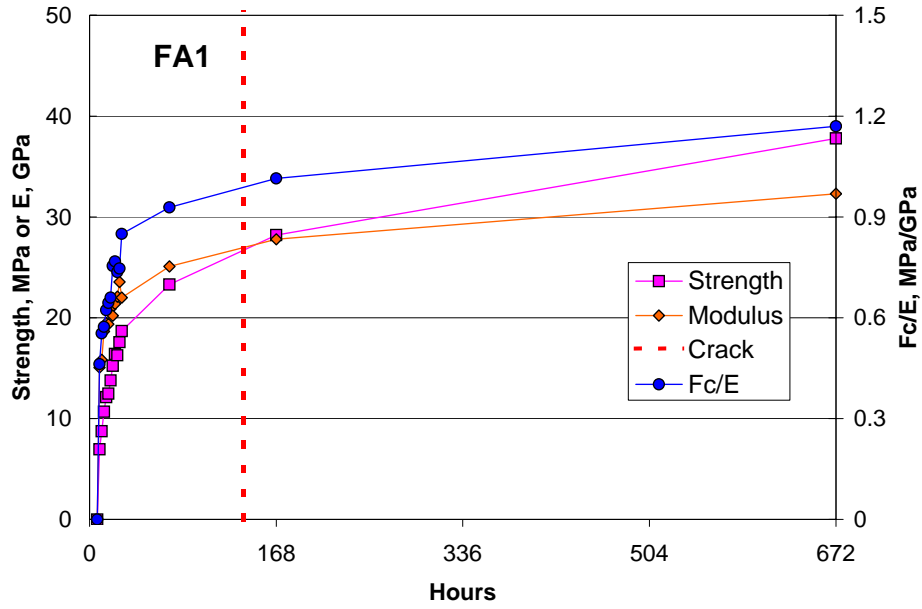
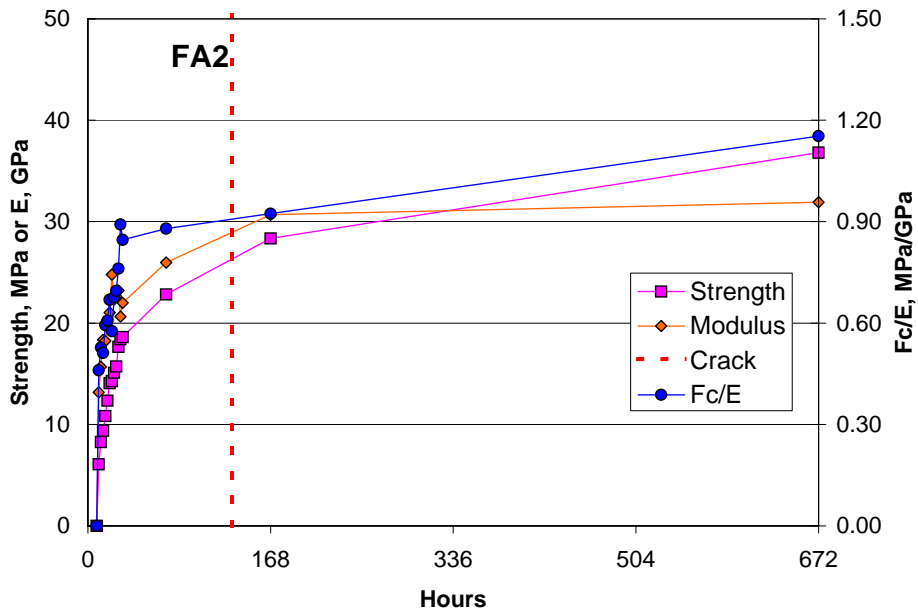


**Figure 29. Early age properties for mix FA2.**



Unit conversions:  
1 MPa = 145.0 psi

**Figure 30. Long-term properties for mix FA1.**



Unit conversions:  
1 MPa = 145.0 psi

**Figure 31. Long-term properties for mix FA2.**

Very little difference was observed in any of the properties measured using these two sets of materials (figures 28 to 31). This is not surprising because the chemistries of both fly ashes were very similar. This supports the contention that chemical analysis of the materials in a mixture may be a good first step in identifying potential incompatibility.

The  $f_c/E$  parameter again showed a reasonable correlation with cracking occurring when a value of approximately 1 psi/ksi was reached.

*Scenario 3a—Influence of Fly Ashes at High Temperature, 25FA90 and 4FA90.*

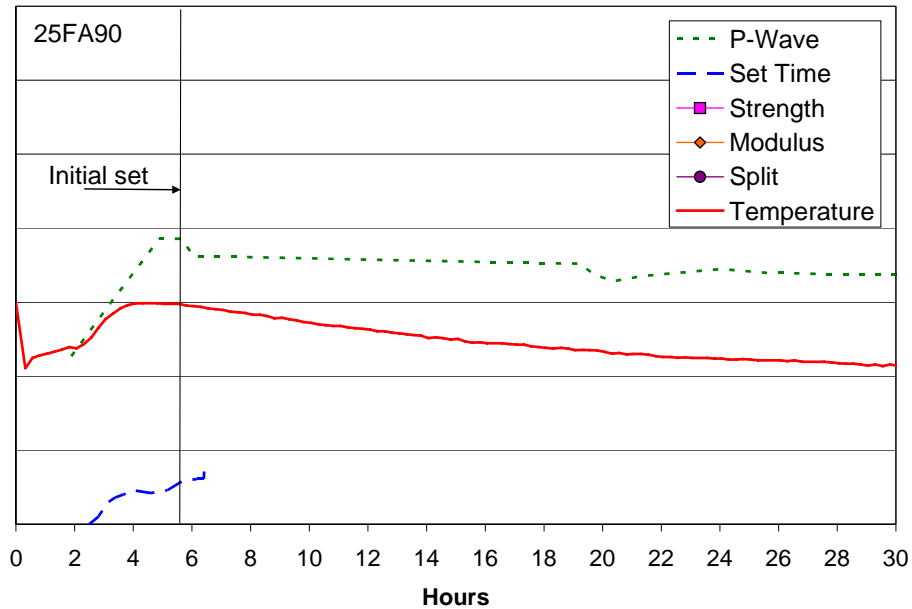


**Figure 32. Early age properties for mix 25FA90.**

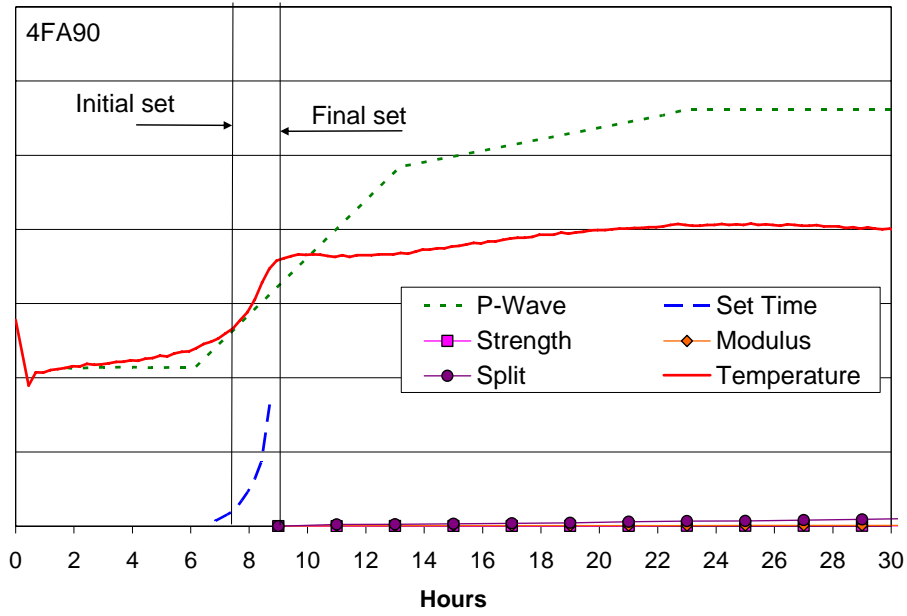
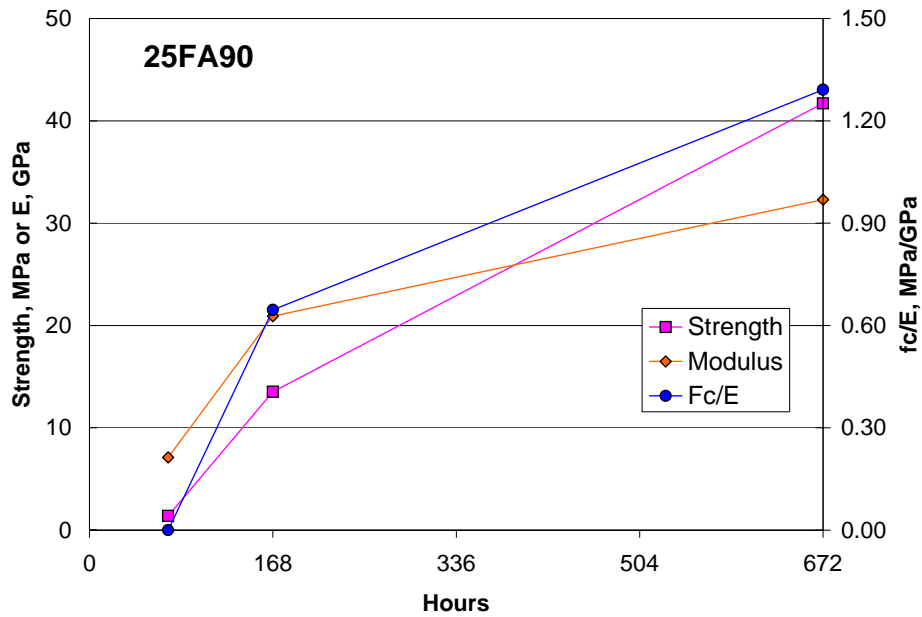


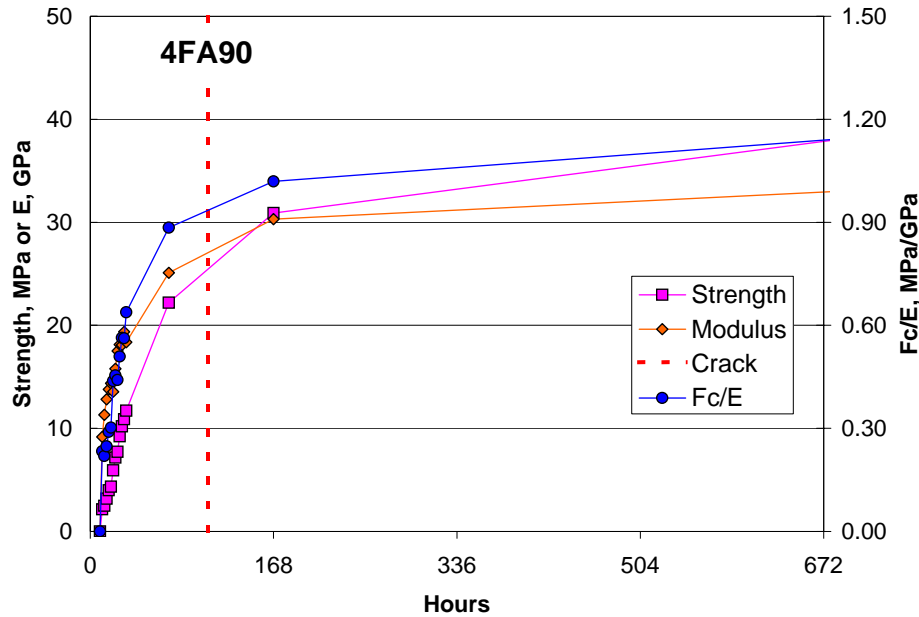
Figure 33. Early age properties for mix 4FA90.



Unit conversions:  
1 MPa = 145.0 psi

Figure 34. Long-term properties for mix 25FA90.





Unit conversions:  
 1 MPa = 145.0 psi

**Figure 35. Long-term properties for mix 4FA90.**

The 25FA90 mixture exhibited classic stiffening and setting incompatibility resulting from the chemistry of the cementitious materials. The mixture was observed to stiffen significantly in the mixer as is typical of flash set. This is caused by uncontrolled hydration of the  $C_3A$  in the cement causing early stiffening. The mixture then did not set for about 2½ days (figures 32 and 34). Again, this is typical of a system where the calcium in solution is at a lower concentration because it has been consumed in the early  $C_3A$  hydration. This retards  $C_3S$  hydration and slows or stops setting. It is also notable that the 28-day strength of this mixture was greater than the other mixtures in this series. It is not uncommon for mixtures to gain high early strengths if early hydration is slowed.

The same materials were submitted for calorimetry and minislump testing to observe whether these tests reported similar information, as would be expected from the Task 2.1.1 work. The minislump data (table 40) indicate that there was extreme loss of workability within a short period of time. Removing one of the admixtures mitigated the degree of stiffening. The calorimetry plot is consistent with the observations of the concrete because there is a large initial peak, followed by little heat generation for the remainder of the 72 h that the test was run (figure 36).

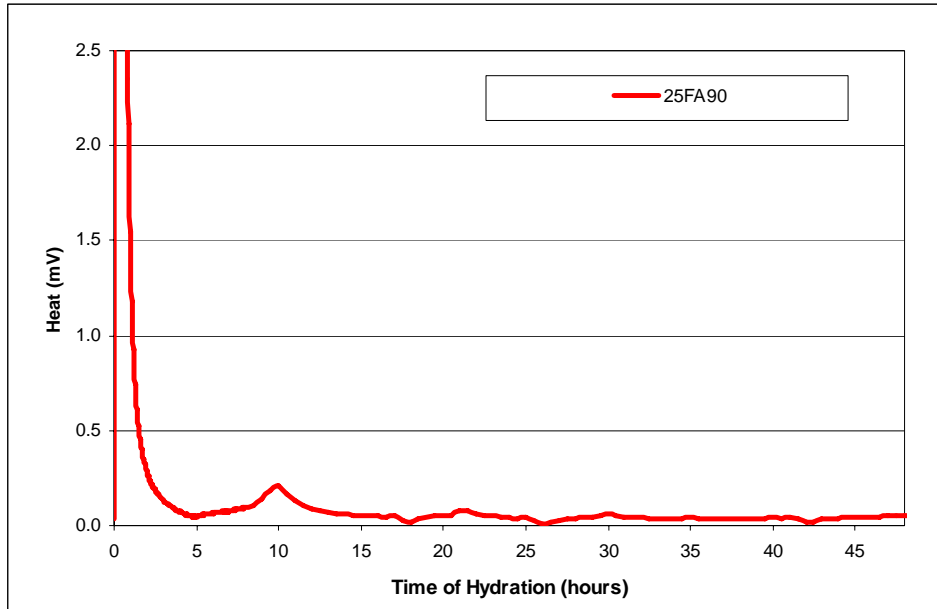


**Figure 36. Conduction calorimetry plot of paste system for mixture 25FA90 conducted at 32 °C (90 °F).**

**Table 40. Results of minislump tests conducted on 25FA90 pastes.**

	Area (mm <sup>2</sup> )				False set Index	Stiffening Index
	2 min	5 min	10 min	30 min		
25FA90 paste system without one admixture	9,480	7,870	6,190	3,870	0.8	0.4
25FA90 paste system	10,000	5,810	2,900	0	0.6	0.0

Unit conversions:  
1 mm<sup>2</sup> = 0.00155 inch<sup>2</sup>

This mixture did not crack, again supporting the contention that systems that set and stiffen quickly are at higher risk of cracking than slower reacting systems.

The mixture prepared using a lower fly ash dosage did not exhibit the stiffening incompatibility and performed in a manner similar to the mixtures tested in the other scenarios (figures 33 and 35).

Scenario 3b—Influence of Fly Ashes at Normal Temperature, 25FA70 and 4FA70

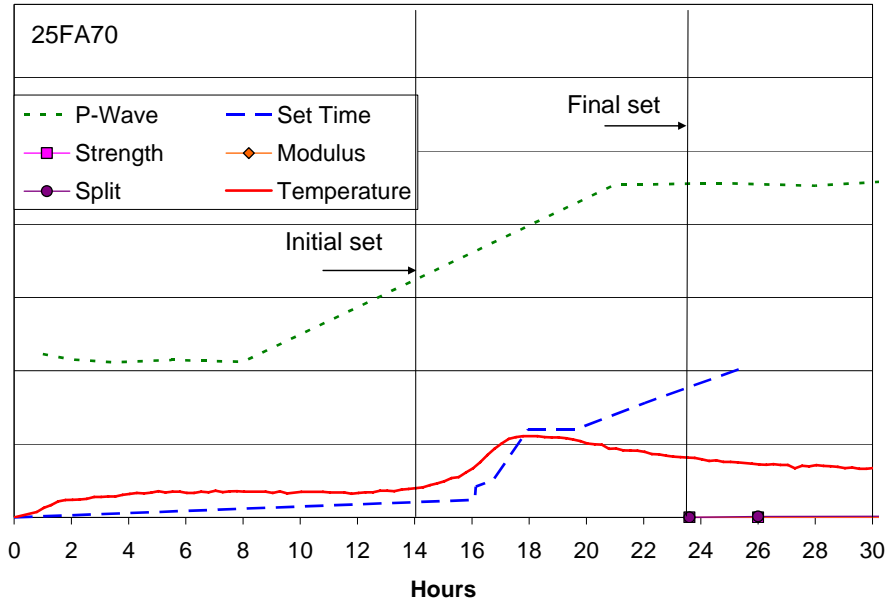


Figure 37. Early age properties for mix 25FA70.

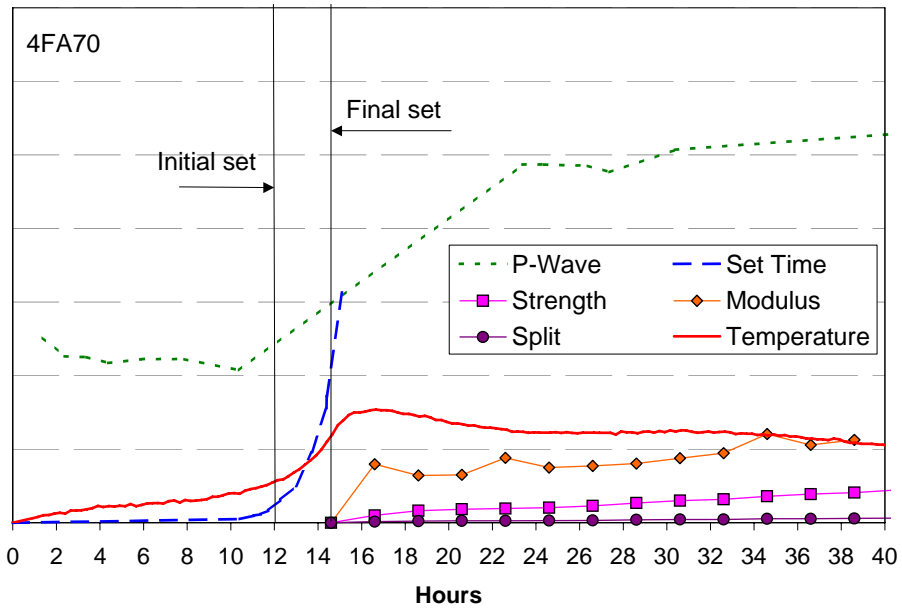
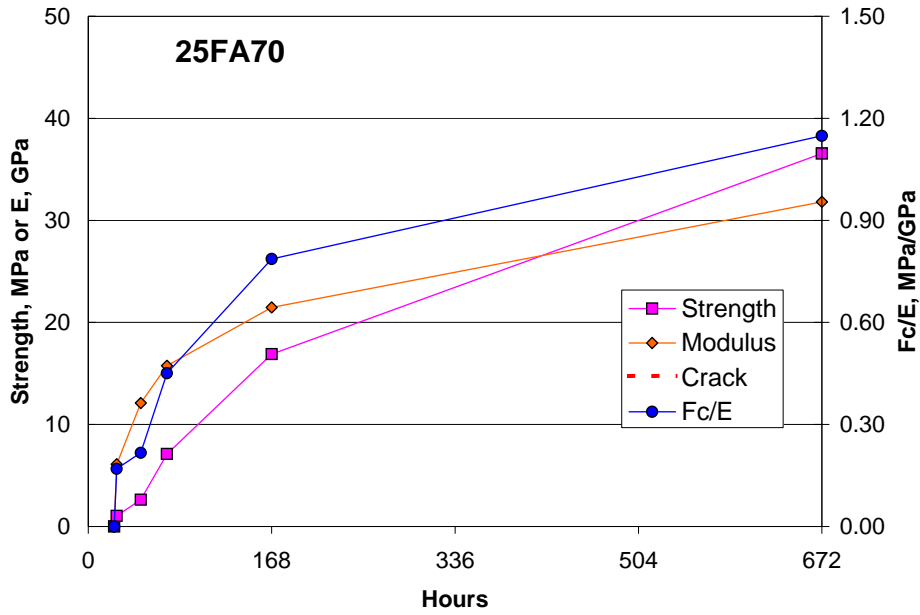
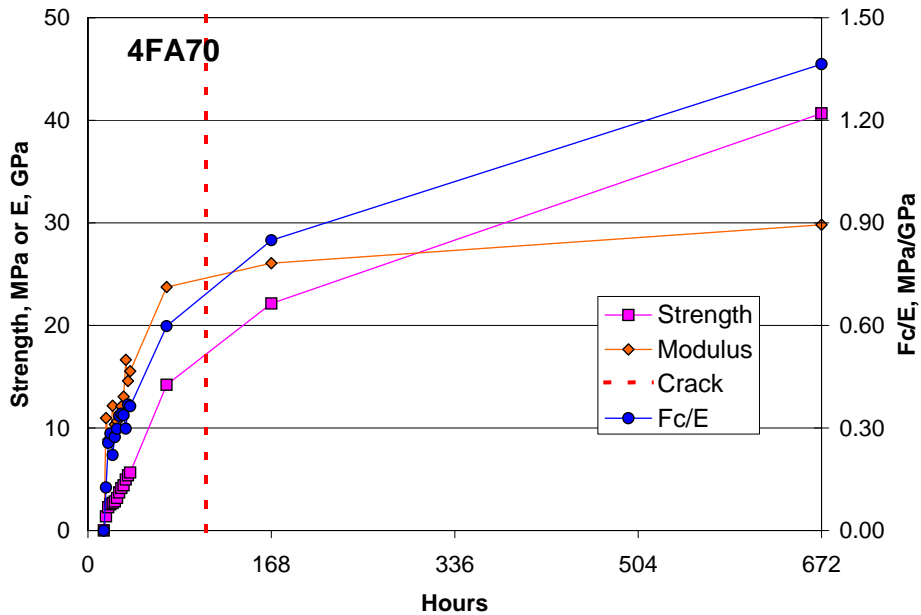


Figure 38. Early age properties for mix 4FA70.



Unit conversions:  
1 MPa = 145.0 psi

**Figure 39. Long-term properties for mix 25FA70.**



Unit conversions:  
1 MPa = 145.0 psi

**Figure 40. Long-term properties for mix 4FA70.**

The mixture containing the high fly ash dosage prepared at 21 °C (70 °F) was also significantly retarded and did not crack, although the effects were less marked than the same mix prepared at 32 °C (90 °F) (figures 37 and 39). The low fly ash mixture prepared at 21 °C (70 °F) was not affected by the change in temperature (figures 38 and 40). Both mixtures prepared at 21 °C (70 °F) exhibited considerably more workability than the same mixtures made at 32 °C (90 °F). This is likely related to the observed rapid stiffening in the high temperature mixtures.

## Summary

The following observations may be drawn from the work conducted in this task:

- The risk of cracking is associated with the chemistry of the reactive materials.
- Systems that are less reactive or more slowly reactive appear to be at lower risk of cracking. There is some value in monitoring setting times of mixtures.
- The ASTM ring exhibited poor correlation with reported field observations. The difference between field reports and laboratory data are probably because not all of the same materials were used in the laboratory tests as in the field.
- It would appear that monitoring the parameter  $f_c/E$  for the first 24 h may provide useful data on when cracking is likely to occur. More work is required to validate this approach.

## TASK 2.1.3—AIR VOID SYSTEM

### Introduction

Concrete strength and durability issues related to problematic air void systems can be costly. Unfortunately, air void problems are usually not identified until analyses are conducted on hardened concrete. To save time and money, these problems must be identified much earlier. Currently, the most widely accepted method being used to evaluate the air void system of fresh concrete is to obtain the total air content of a mixture, often using the pressure meter. Basing acceptance on total air content can be misleading. Total air measurements of fresh concrete may meet the limits outlined in job specifications, but that does not guarantee that those mixes will contain a satisfactory air void system and perform as intended. The total air content of fresh concrete provides no identification of the distribution, size, or spacing of the air bubbles, which are the parameters critical to performance. Clustering of air voids around aggregate particles and poor spacing factors are examples of problems that occur in otherwise ordinary concrete, but they cannot be identified in the fresh state using currently recognized methods. The purpose of this task was to evaluate tests that could be used to identify problematic air void systems in fresh concrete.

### *Materials*

Air entraining admixtures are reputed to have problematic interactions when combined with some types of water-reducing admixtures. The most common problems associated with these

interactions include requiring increased dosage of air-entraining admixtures (AEA), decreased total air contents, and increased spacing factors.

A total of 10 AEAs were procured and evaluated. The selection of AEAs was based primarily on the recent experience of the State highway departments in South Dakota, Michigan, Delaware, and New Jersey. Admixtures were obtained from the major chemical companies in the concrete industry. Vinsol resins as well as various synthetic admixtures were included in the program. Specific properties and classifications of these admixtures are presented in table 41. The chemical compositions of the materials are presented in table 42.

**Table 41. Air entraining admixtures and related properties.**

Admixture Identification	Admixture Classification	Physical Properties		
		pH	Specific Gravity	Solids by mass (%)
A	vinsol resin	12.49	1.045	13.78
B	vinsol resin	12.7	1.050	17.49
C	vinsol resin	12.34	1.030	13.51
D	resin/rosin	10.5	1.010	5.97
E	resin/rosin	11.75	1.018	6.99
F	resin/rosin	11.06	1.015	12.51
G	alpha sulfonate	10.8	1.01	6.66
H	tall oil	9.92	1.020	6.58
I	benzene sulfonate	10.18	1.011	6.04
J	fatty acid	9.92	1.020	11.38

**Table 42. Cementitious materials composition and fineness.**

Composition	High alkali cement (% mass)	Class C fly ash (A) (% mass)	Class C fly ash (B) (% mass)	Class F fly ash (% mass)
SiO <sub>2</sub>	19.24	36.14	38.45	52.56
Al <sub>2</sub> O <sub>3</sub>	5.61	18.33	19.59	20.26
Fe <sub>2</sub> O <sub>3</sub>	2.28	5.20	5.73	11.46
CaO	62.27	26.04	15.83	4.29
MgO	2.36	4.84	4.02	1.00
SO <sub>3</sub>	4.41	2.41	2.54	0.64
Na <sub>2</sub> O	0.28	1.59	7.41	1.32
K <sub>2</sub> O	0.97	0.47	0.83	1.92
TiO <sub>2</sub>	0.30	1.61	1.32	0.97
P <sub>2</sub> O <sub>5</sub>	0.17	0.98	0.54	0.28
Mn <sub>2</sub> O <sub>3</sub>	0.21	0.03	0.04	0.05
SrO	0.07	0.44	0.80	0.08
Cr <sub>2</sub> O <sub>3</sub>	*	0.02	0.02	0.02
ZnO	*	0.02	0.01	0.04
L.O.I. (950 °C)	1.54	0.40	0.31	4.22
Total	99.71	98.52	97.45	99.1

**Table 42. Cementitious materials composition and fineness (continued).**

Composition	High alkali cement (% mass)	Class C fly ash (A) (% mass)	Class C fly ash (B) (% mass)	Class F fly ash (% mass)
Total alkalis as Na <sub>2</sub> O <sub>equiv.</sub>	0.91	1.91	7.96	2.58
Blaine fineness, kg/m <sup>2</sup>	352	*	*	*
Phases:				
C <sub>3</sub> S	54	*	*	*
C <sub>2</sub> S	15	*	*	*
C <sub>3</sub> A	11	13.7	*	*
C <sub>4</sub> AF	7	*	*	*
SiO <sub>2</sub> +Al <sub>2</sub> O <sub>3</sub> +Fe <sub>2</sub> O <sub>3</sub>	*	59.67	63.8	84.3

\* = No data

Two types of WRAs (sugar-based and lignin-based) were procured for analysis in this study. Both admixtures met ASTM C 494 requirements for Type A water-reducing admixture. The cementitious materials used in this study included a high alkali Type I cement, two Class C fly ashes, and a Class F fly ash. Except for one of the Class C fly ashes, these were materials used in other tasks of this study. A rounded siliceous coarse aggregate and siliceous fine aggregate were used in the concrete analysis portion of this study. The gradations of the coarse and fine aggregates are shown in tables 43 and 44 respectively.

**Table 43. Coarse aggregate grading.**

Sieve size (mm)	Rounded siliceous (% passing)	Crushed dolomitic (% passing)
25.00	100.0	100
19.00	99.0	92
12.50	42.0	47
9.50	41.0	25
4.75	0.4	9

Unit conversions:

1mm =0.0394 inch

**Table 44. Fine Aggregate Grading**

Sieve size (mm)	Passing (%)
4.750	99.00
2.360	90.00
1.180	76.00
0.600	49.00
0.300	14.00
0.150	1.30
0.075	0.30
Fineness Modulus	2.72

Unit conversions:

1mm =0.0394 inch

## Work Plan

The testing program of this study consisted of three stages. In the first stage, a foam drainage analysis was conducted where AEAs were blended with various raw materials to generate foams. The stability of these foams was rated on the basis of how much and how fast water drained from the foam structures. The second and third stages comprised testing of concrete mixtures. The second stage focused on testing fresh concrete properties; the third stage dealt with the testing and analysis of hardened concrete at early ages. The three-stage testing program was used to determine if a correlation among the various air content determination methods could be discerned to identify air void problems at the earliest possible stage in construction.

### *Stage 1—Foam Drainage Analysis*

The foam drainage test was developed in the late 1980s to provide a preliminary means of evaluating the stability of entrained air void systems developed from commercially available AEAs.<sup>(81)</sup> The test was meant to identify poorly performing admixtures before their use in concrete. The method consists of rapidly blending an air entrainer with water to generate foam. Other concrete raw materials and admixtures have also been blended with air entrainers to evaluate how those materials influence the stability of the foam and the resulting air void system.<sup>(68)</sup> After it is mixed, the foam is poured into a graduated cylinder and the rate at which water drains from the foam is recorded for 60 min.

A stable air void system will usually have a lower drainage rate and retain more water than an unstable system.<sup>(68,81)</sup> The rate of drainage depends on the hydrodynamic characteristics of the foam, which include the size and shape of bubbles and the mobility of the liquid-air interface. Over the years, this test has been slightly modified by other researchers. The foam drainage test procedures used in this study were based on the work conducted by the South Dakota DOT.<sup>(68)</sup>

For this study, a total of 50 tests were conducted. Foam drainage characteristics for 10 admixtures were analyzed for the following amounts and combinations of raw materials:

- 300 ml (10 oz) water, 10 ml (0.33 oz) AEA.
- 250 ml (8.5 oz) water, 10 ml (0.33 oz) AEA, 50 ml (1.7 oz) WRA.
- 300 ml (10 oz) water, 10 ml (0.33 oz) AEA, 5 g (0.18 oz) cement.
- 250 ml (8.5 oz) water, 10 ml (0.33 oz) AEA, 50 ml (1.7 oz) WRA, 4 g (0.14 oz) cement, 1 g (0.04 oz) Class C fly ash.
- 250 ml (8.5 oz) water, 10 ml (0.33 oz) AEA, 50 ml (1.7 oz) WRA, 4 g (0.14 oz) cement, 1 g (0.04 oz) Class F fly ash.

The procedure for conducting this test is illustrated in figure 41. Water, admixtures, and cementitious materials are added to the blender. The mixture is blended for 10 s and the resulting foam is immediately poured into a 1,000 ml (34 oz) graduated cylinder. Then the level of the foam/water interface is recorded as a function of time. All tests are carried out for 1 h.





**Figure 41. Foam drainage procedure.**

A 50 ml (1.7 oz) dosage of water reducer compared to the 10 ml (0.33 oz) air entrainer dosage was chosen to reflect the relative difference in the standard concrete dosages of the two types of admixtures. For tests using water reducers, the total water was dropped to 250 ml (8.5 oz) to maintain the 300 ml (10 oz) liquid level before the addition of air entrainer.

The amount of water drained as a function of time is fitted to an equation shown in figure 42 and the values of  $V_0$  and  $-1/k$  are calculated.

$$V_d = V_0 - \frac{1}{kt}$$

**Figure 42. Equation. Foam drainage.**

Where

$V_d$  is the amount of liquid drained from the foam at time  $t$ .

$1/k$  is a parameter specific to the system being tested.

$V_0$  may be considered the amount of water drained from the foam at the end of the test (y-intercept on a plot of  $V$  versus  $1/t$ ).

$V_0$  and  $1/k$  are determined by plotting the amount of drained water versus  $1/t$ . The slope of the line is  $-1/k$  and  $V_0$  is the intercept. When comparing admixtures, the more useful parameter is  $-1/k$ , which indicates the rate of drainage of fluid from the foam. The higher the value of  $-1/k$ , the slower the drainage rate and the more stable the foam is considered to be. Such admixtures are expected to produce more stable foams than those producing foams that do not retain water as effectively. The percent of water drained is calculated using the equation in figure 43.

$$\% \text{ Drained} = 100 - \frac{(310 - V_0)}{310} \times 100$$

**Figure 43. Equation. Percent drained.**

Admixtures with significant differences in the  $-1/k$  values and in the percentage of water drained from the foam (percentage drained) are expected to have different air void systems and different performance.

Based on the results obtained from the foam drainage analysis, 3 of the 10 admixtures were selected for further analyses in the second and third stages. The selection of admixtures was also based on having at least one vinsol-based product, no two products from the same manufacturer, and three different chemical compositions. Admixtures B, D, and H were the 3 admixtures chosen—a vinsol resin (control), a resin/rosin, and a tall oil-based air entrainer, respectively.

### *Stage 2—Fresh Concrete Properties and Air Void Analyzer Investigation*

In the second stage, the focus of the investigation shifted to evaluating the effects of air entraining admixtures on the fresh properties of concrete. A correlation among test results for this stage would be essential because the goal of this study is to develop the ability to identify air void problems in concrete before placement.

The fresh properties of the concrete were evaluated in accordance with the following American Association of State Highway and Transportation Officials (AASHTO) standards:

- AASHTO T 119, “Slump of Hydraulic Cement Concrete.”
- AASHTO T 152, “Air Content of Freshly Mixed Concrete by the Pressure Method.”
- AASHTO T 121, “Mass per Cubic Meter (Cubic Foot), Yield and Air Content (Gravimetric) of Concrete.”

**Air void Analyzer Test.** A promising technique was developed in Europe in the early 1990s as an alternative method for measuring the air void parameters of concrete. The commercially available equipment for this test is known as the Air Void Analyzer (AVA). The main advantage of this technique is that the test is conducted on fresh concrete and takes less than 30 min to complete. The method is based on the fact that large bubbles rise through a column of liquid faster than small bubbles do, and therefore, bubble size can be accurately inferred from how long it takes the bubble to rise. A mortar is extracted from a concrete sample taken from the as-placed concrete and injected by means of a syringe into the base of the AVA. The mortar sample is stirred into a viscous liquid to release the air voids. The air bubbles rise through the viscous liquid and water in the glass cylinder, and then they are gathered on a glass bell (petri dish). The petri dish is suspended from a bracket attached to a sensitive balance. Knowing the viscosity of the system and using Stoke’s Law, it is possible to compute the size of the air bubbles with time and calculate the air void parameters.

This method is used to determine three parameters:

- Air content.
- Spacing factor.
- Specific surface.

Measurement of air void parameters of concrete at the fresh state is the optimum procedure for evaluating the air void system of concrete. The AVA is the only method available at this time for such measurements, although its reliability is still to be proven.

For this project, the mortar samples used in the AVA test were obtained from one of two 150- by 150- by 530-mm (6- by 6- by 21-inch) beams cast from each mix. In the case of mixes 12 and 13 (vibration effect), the sample was collected from the top 50 mm (2 inches). The information obtained from this test included total air content and spacing factor. These values were obtained for correlation with the same parameters obtained from the Stage 3 ASTM C 457 analysis on hardened concrete.

**Concrete Mix Regimen and Design.** The selected mix compositions used in the second stage are presented in table 45. As shown in the table, a variety of admixtures, materials, and mixing conditions were chosen to simulate the field conditions under which unstable air void systems or coalescence of air voids around aggregates have been observed. These selections were based on a literature review, field experience, and information from personal contacts. The goal of such selections was to provide realistic conditions to evaluate the ability of the proposed tests to identify air void problems in the fresh concrete system.

As shown in table 45, the concrete mixtures were as follows:

- Three mixes using the three selected AEAs. These mixes will be prepared at normal laboratory temperature and contain a single dose of WRA (mixes 1 to 3).
- One mix with no WRA (mix 4).
- One mix with a double dose of WRA (mix 5).
- One mix with a single dose of a different WRA (mix 6).
- Two mixes using coarse sand (mixes 7 to 8).
- Three mixes containing a single dose of three different supplementary cementing materials (mixes 9 to 11).
- Two mixes subjected to excessive vibration (mixes 12 and 13).

**Table 45. Concrete test matrix used in stages 2 and 3 of subtask 2.1.3.**

Mix No.	AEA Identification	Sand Gradation	Water-Reducer	Water-Reducer Dosage	Temperature	Pozzolans	Consolidation
1	B (vinsol)	Normal	A	Normal	Normal	None	Normal Vibration
2	H (tall oil)	Normal	A	Normal	Normal	None	Normal Vibration
3	D (resin/rosin)	Normal	A	Normal	Normal	None	Normal Vibration
4	H	Normal	None	Not applicable	High (32 °C)	None	Normal Vibration
5	H	Normal	A	High	High (32 °C)	None	Normal Vibration
6	H	Normal	B	Normal	Normal	None	Normal Vibration
7	H	Coarse	A	Normal	Normal	None	Normal Vibration
8	D	Coarse	A	Normal	Normal	None	Normal Vibration
9	H	Normal	A	Normal	Normal	20% (C) fly ash A	Normal Vibration
10	H	Normal	A	Normal	Normal	20% (C) fly ash B	Normal Vibration
11	H	Normal	A	Normal	High (32 °C)	20% (F) fly ash	Normal Vibration
12	D	Normal	A	Normal	Normal	None	Excessive Vibration
13	B	Normal	A	Normal	Normal	None	Excessive Vibration

The base concrete mixture used for the second stage is shown in table 46. The base mix contained 335 kg/m<sup>3</sup> (564 pcy) of ASTM Type I cement and had a water-cement ratio of 0.42. Changes in the base mix occurred in mixes 7–11. A coarse sand gradation was specified for mixes 7 and 8. The fine aggregate source for these mixes was not changed. Instead, the fine aggregate was sieved and manually reconstructed to obtain a fineness modulus of 2.55 to differentiate from its natural value of 2.97 (used in all other mixtures). Mixes 9–11 required the addition of various fly ashes to the base mix design. In these mixes the fly ashes were added as a percentage replacement by weight of cement.

Mixing procedures were altered from those specified in AASHTO T 126, “Making and Curing Concrete Test Specimens in the Laboratory,” to simulate field mixing technique typical of paving concrete. The modification was that a 2-min mixing cycle was used.

The dosage of air entrainer was varied for each mixture to obtain air contents in the range of 6 ± 1 percent. A fixed dosage of WRA was applied in all mixtures except for mixes 4 and 6. No water reducer was added in mix 4, and in mix 6 the dosage was doubled. Because of the

variability of mixture conditions, the dosage of water reducer that provided an approximate 100-mm (4-inch) slump for mix 1 was used as the fixed dosage for the rest of the program.

**Table 46. Base concrete mixture.**

Material	kg/m <sup>3</sup>	Pounds per cubic yard
Cement	335	564
Fine aggregate, SSD	715	1205
Coarse aggregate, SSD	1103	1860
Water	141	237
Approximate w/c	0.42	0.42

### *Stage 3—Hardened Concrete Analysis*

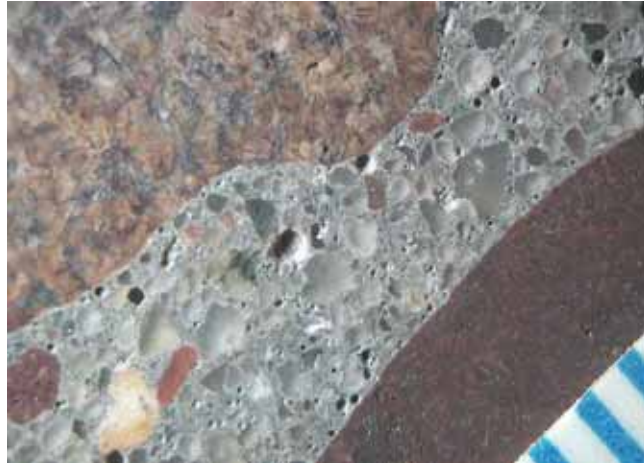
In this stage of the investigation, the properties of hardened concrete were determined to evaluate the validity of correlations to the fresh property tests established in the first and second stages. Stage 3 tests were conducted on the same concrete mixtures made during the Stage 2 study (see table 46). These tests were as follows:

- Compressive strength: Six 100- by 200-mm (4- by 8-inch) cylinders were tested for compressive strength in accordance with AASHTO T 22, “Compressive Strength of Cylindrical Concrete Specimens,” at the ages of 7 and 28 days.
- ASTM C 457, “Microscopical Determination of Parameters of the System in Hardened Concrete.” A specimen was cut from the 150- by 150- by 530-mm (6- by 6- by 21-inch) beam for this test. The cut was through the cross-section to show the variation in system between the top and bottom of the beam.
- Characterization of flocculation of air voids around coarse aggregates. The same specimens prepared for ASTM C 457 were used to assess clustering.

In cases where flocculation or clustering of air voids around coarse aggregates was witnessed, a technique developed in a past PCA study was used to rate the severity of the phenomenon.<sup>(68)</sup> According to the PCA study, a visual reference shown in figures 44 through 47 was developed to standardize the determination of clustering severity around individual aggregates. This reference standard is composed of four categories to differentiate between no clustering, minor, moderate, and severe air void clustering. Each category was assigned a numeric value of 0 to 3. A rating of 0 implies that no clustering exists. Minor clustering (Rating 1) involves the intermittent occurrence of clustering of entrained air voids around the periphery of coarse aggregate particles. For moderate clustering (Rating 2), most or all of an aggregate is surrounded by a layer of entrained air voids. Severe clustering (Rating 3) is defined as several layers of entrained air voids surrounding a single aggregate particle.

According to the method outlined in the PCA study, only coarse aggregate particles greater than 0.25 inch were given a rating.<sup>(69)</sup> Because lapped sections of concrete were being evaluated, the nominal size of an aggregate evaluated in the cut plane of those samples was unknown. An aggregate that appeared small on the lapped surface could have been the tip of a much larger

particle. It is not known if a relationship between the size of a clustered aggregate particle and the magnitude of the resultant compressive strength loss exists; therefore, all aggregate diameters 6 mm (0.25 inch) and larger were given consideration.



Note: Millimeter scale

**Figure 44. Rating 0—No clustering present. Visual rating guide for analysis of air void clustering severity (PCA R&D Serial No. 2789).**

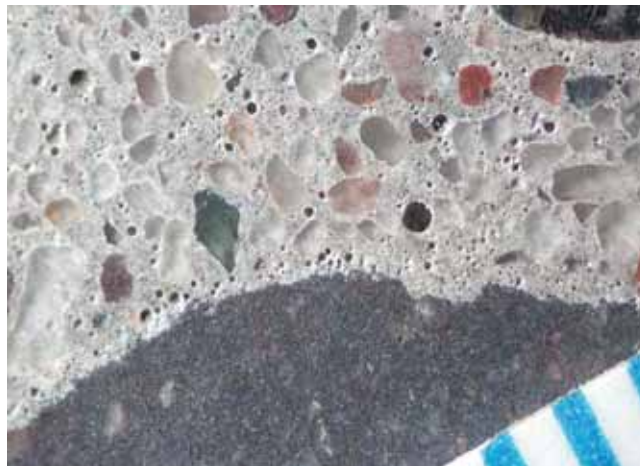


**Figure 45. Rating 1, Minor clustering. Visual rating guide for analysis of air void clustering severity (PCA R&D Serial No. 2789).**

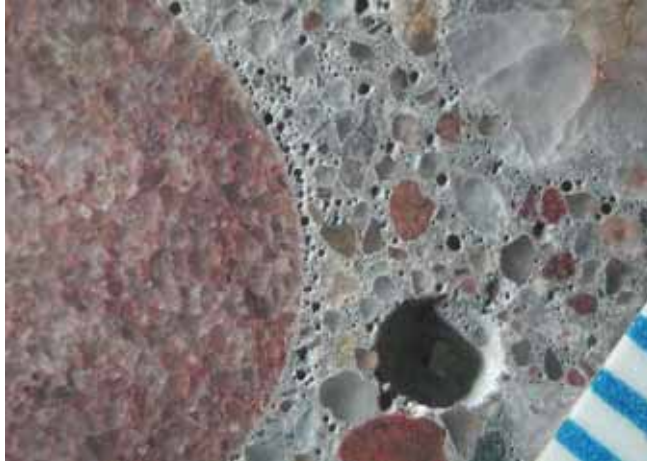
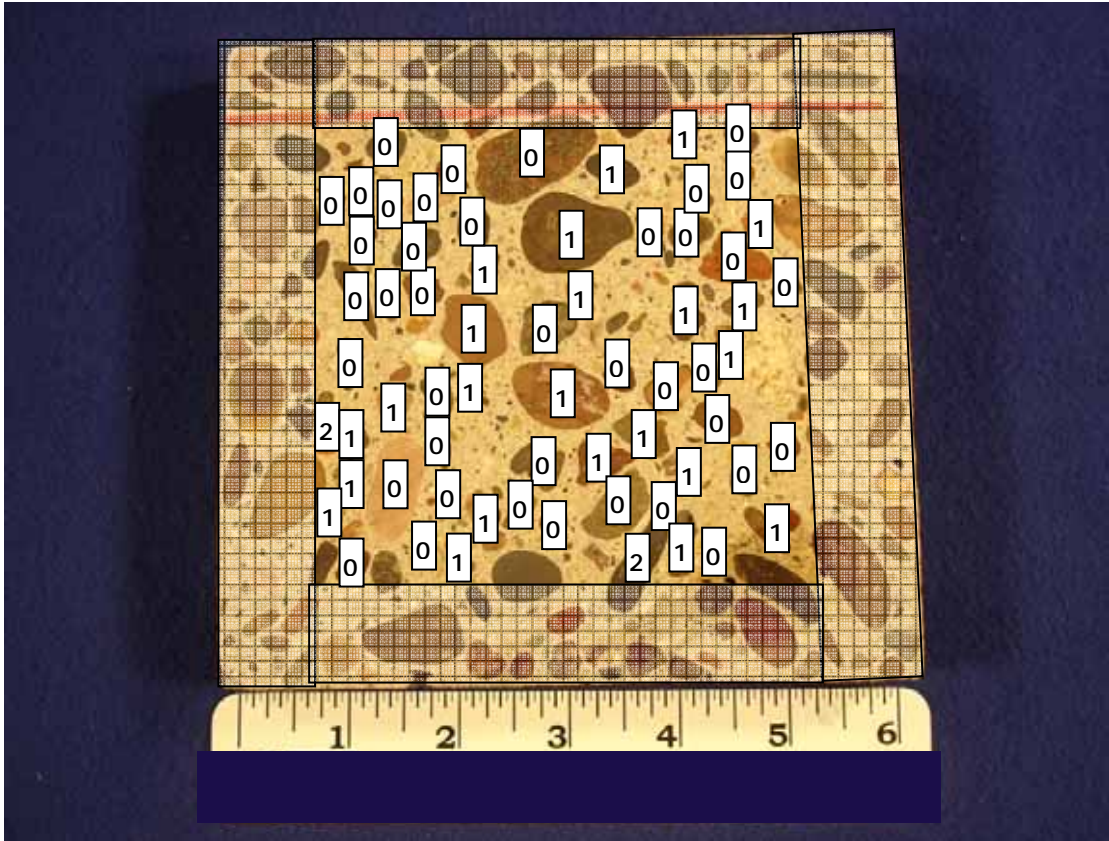


**Figure 46. Rating 2, Moderate clustering.**  
**Visual rating guide for analysis of air void**  
**clustering severity (PCA R&D**  
**Serial No. 2789).**



**Figure 47. Rating 3, severe clustering.**  
**Visual rating guide for analysis**  
**of air void clustering severity**  
**(PCA R&D Serial No. 2789).**

An example analysis and calculation of the average clustering rating for a lapped concrete sample is presented in figure 48. Table 47 shows the corresponding calculations. To improve the consistency of ratings, samples were marked off 2.54 cm (1 inch) from the top and bottom and the central 10.16-cm (4-inch) section was analyzed for clustering. As shown in figure 48, each coarse aggregate particle was assigned to one of the four clustering categories. Then the number of aggregates in each category was multiplied by the category or number (0 to 3). Finally, the totals from each category were averaged over the number of particles examined.



Unit conversions:  
1 inch = 2.54 cm

**Figure 48. Example of clustering rating for a cylinder.**

**Table 47. Corresponding calculations for average clustering rate.**

Clustering Rating	Aggregates Affected	Calculation
0–None	39	$0 \times 39 = 0$
1–Minor	24	$1 \times 24 = 24$
2–Moderate	2	$2 \times 2 = 4$
3–Severe	0	$3 \times 0 = 0$
Sum	65	28
Clustering rate = $28/65 = 0.43$		



## Results

### Stage I—Foam Drainage Analysis

The foam drainage results for the 10 admixtures included in this study are presented in table 48. Results for  $V_0$ ,  $-1/k$ , and percentage drained were ranked based on a scale of 1 to 10, with 10 being the best and 1 being the worst performer. Admixtures B, D, and H were selected for concrete analysis based on variations in their foam stability to determine if similar air void stability issues could be predicted in concrete mixtures. These three admixtures consisted of the top, middle, and worst performers among the group based on their overall ranking. The overall rankings shown in table 48 were determined by averaging all the individual performances ( $V_0$ ,  $-1/k$ , and percentage drained) for each admixture.

**Table 48. Foam drainage results.**

Admixture ID	Admixture Classification	Test Condition	Foam Drainage Statistics				Rank*			Overall
			$V_0$	$-1/k$	$r^2$	% drained	$V_0$	$-1/k$	% drained	
A	vinsol	AEA	301.0	6.5	0.445	97.1	2	1	1	4
		AEA+C	269.0	390.1	0.932	86.8	4	7	4	
		AEA+WR	303.0	330.2	0.986	97.7	1	3	1	
		AEA+C+WR+C-ASH	232.0	615.2	0.982	74.8	9	4	9	
		AEA+C+WR+F-ASH	235.0	714.7	0.978	75.8	10	8	10	
B	vinsol	AEA	285.0	285.2	0.993	91.9	8	6	8	10
		AEA+C	210.0	531.9	0.956	67.7	9	9	9	
		AEA+WR	228.0	905.4	0.944	73.5	8	5	8	
		AEA+C+WR+C-ASH	239.0	713.4	0.968	77.1	7	7	7	
		AEA+C+WR+F-ASH	245.0	794.4	0.985	79.0	8	10	8	
C	vinsol	AEA	301.0	348.7	0.974	97.1	1	8	2	7
		AEA+C	102.0	1191.0	0.793	32.9	10	10	10	
		AEA+WR	212.0	955.3	0.942	68.4	10	9	10	
		AEA+C+WR+C-ASH	252.0	623.9	0.983	81.3	5	5	5	
		AEA+C+WR+F-ASH	250.0	661.8	0.979	80.6	4	5	6	
D	resin/rosin	AEA	293.0	101.4	0.991	94.5	5	4	5	6
		AEA+C	253.0	182.9	0.986	81.6	8	5	8	
		AEA+WR	233.0	928.6	0.965	75.2	7	6	7	
		AEA+C+WR+C-ASH	249.0	697.1	0.984	80.3	6	6	6	
		AEA+C+WR+F-ASH	250.0	715.6	0.978	80.6	5	9	4	
E	resin/rosin	AEA	281.0	64.7	0.973	90.6	10	3	10	8
		AEA+C	264.0	81.6	0.973	85.2	5	3	5	
		AEA+WR	267.0	1030.0	0.959	86.1	5	10	5	
		AEA+C+WR+C-ASH	236.0	817.9	0.981	76.1	8	10	8	
		AEA+C+WR+F-ASH	240.0	712.7	0.982	77.4	9	7	9	
F	resin/rosin	AEA	291.0	120.4	0.969	93.9	7	5	7	5
		AEA+C	259.0	232.0	0.970	83.5	6	6	6	
		AEA+WR	239.0	938.4	0.946	77.1	6	7	6	
		AEA+C+WR+C-ASH	252.0	713.5	0.988	81.3	4	8	4	
		AEA+C+WR+F-ASH	247.0	639.1	0.971	79.7	7	4	7	
G	alpha sulfonate	AEA	298.0	734.8	0.920	96.1	4	10	4	2
		AEA+C	299.0	420.7	0.960	96.5	1	8	1	
		AEA+WR	291.0	467.0	0.904	93.9	3	4	3	
		AEA+C+WR+C-ASH	302.0	488.2	0.961	97.4	1	3	1	
		AEA+C+WR+F-ASH	299	334.1	0.928	96.5	2	3	2	
H	tall oil	AEA	300	297.5	0.945	96.8	3	7	3	1
		AEA+C	288	33.4	0.964	92.9	2	2	2	
		AEA+WR	294	76.8	0.875	94.8	2	2	2	
		AEA+C+WR+C-ASH	299	30	0.963	96.5	2	1	2	
		AEA+C+WR+F-ASH	304	29.47	0.947	98.1	1	1	1	
I	benzene sulfonate	AEA	282.0	51.2	0.897	91.0	9	2	9	9
		AEA+C	257.0	87.4	0.985	82.9	7	4	7	
		AEA+WR	227.0	938.7	0.932	73.2	9	8	9	
		AEA+C+WR+C-ASH	228.0	800.9	0.978	73.5	10	9	10	
		AEA+C+WR+F-ASH	250.0	696.0	0.983	80.6	6	6	5	
J	fatty acid	AEA	293.0	408.1	0.952	94.5	6	9	6	3
		AEA+C	281.0	21.7	0.976	90.6	3	1	3	
		AEA+WR	288.0	23.5	0.925	92.9	4	1	4	
		AEA+C+WR+C-ASH	289.0	89.2	0.976	93.2	3	2	3	
		AEA+C+WR+F-ASH	290.0	69.0	0.981	93.5	3	2	3	

Notes: \* Rankings based on a scale of 1 to 10, with 10 being the best and 1 being the worst performer.

*Stage 2—Fresh Concrete Properties and Air Void Analyzer Investigation*

The fresh properties including slump, air, and unit weight of the 13 concrete mixtures are presented in table 49. Table 49 also includes the air void system properties determined using the AVA.

The correlation between fresh air contents generated using the pressure meter (ASTM C 231) and AVA is shown in figure 49.

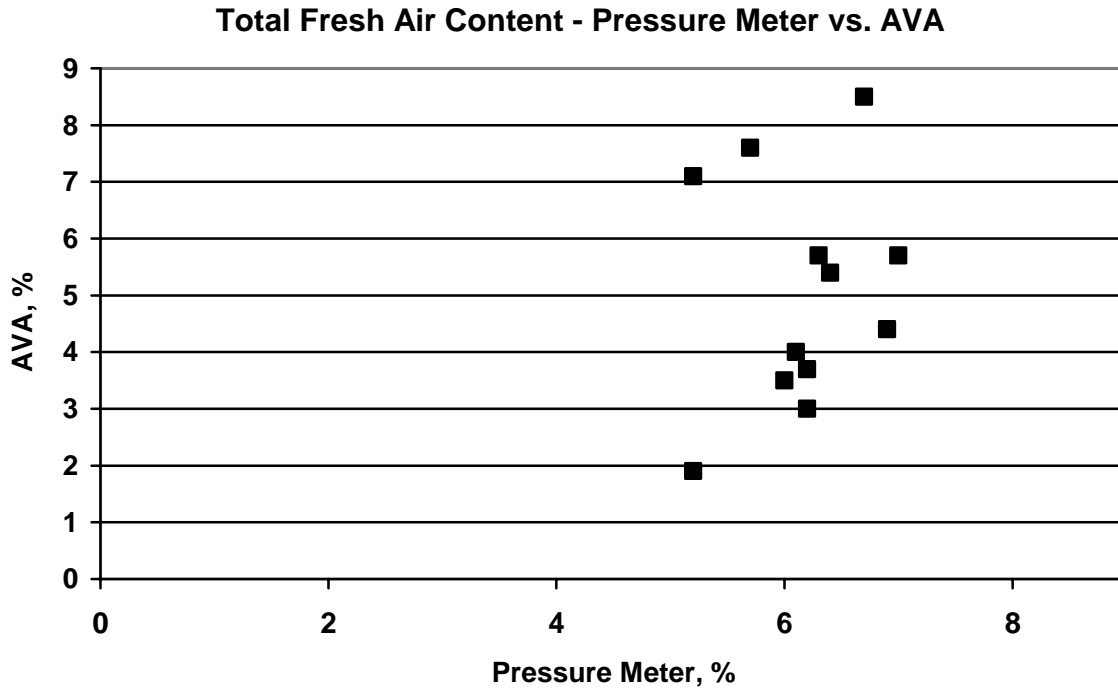


**Figure 49. Correlation between pressure meter and AVA-generated fresh air contents.**

*Stage 3—Hardened Concrete Analysis*

Hardened properties for the 13 concrete mixtures are presented in table 50. The data includes compressive strengths results and petrographic air void parameters. Compressive strengths of these mixes were evaluated at ages of 7 and 28 days. Petrographic analyses were performed on the hardened concrete samples to determine their total air void contents, spacing factors, and evidence of air void clustering.

**Table 49. Fresh concrete properties.**

Mix No.	Concrete Mix Variables							Fresh Properties				
	AEA Type	Sand Gradation	Water Reducer	Water-Reducer Dosage	Temperature	Pozzolans	Consolidation	Slump (mm)	Unit weight (kg/m <sup>3</sup> )	Air (%)	AVA Air (%)	AVA Spacing Factor (mm)
1	B	Normal	A	Normal	Normal	None	Normal Vibration	90	2,355	6.2	3.0	0.249
2	H	Normal	A	Normal	Normal	None	Normal Vibration	160	2,348	7.0	5.7	0.213
3	D	Normal	A	Normal	Normal	None	Normal Vibration	95	2,342	6.1	4.0	0.305
4	H	Normal	None	Not applicable	32 °C	None	Normal Vibration	50	2,347	6.0	3.5	0.099
5	H	Normal	A	Normal	32 °C	None	Normal Vibration	75	2,340	6.2	3.7	0.188
6	H	Normal	B	High	Normal	None	Normal Vibration	175	2,344	6.7	8.5	0.119
7	H	Coarse	A	Normal	Normal	None	Normal Vibration	20	2,372	5.2	7.1	0.104
8	D	Coarse	A	Normal	Normal	None	Normal Vibration	25	2,372	5.2	1.9	0.493
9	H	Normal	A	Normal	Normal	20% (C) fly ash A	Normal Vibration	120	2,327	6.9	n/a	n/a
10	H	Normal	A	Normal	Normal	20% (C) fly ash B	Normal Vibration	125	2,360	5.7	7.6	0.091
11	H	Normal	A	Normal	32 °C	20% (F) fly ash	Normal Vibration	65	2,327	6.3	5.7	0.086
12	D	Normal	A	Normal	Normal	None	Excessive Vibration	75	2,315	6.9	4.4	0.239
13	B	Normal	A	Normal	Normal	None	Excessive Vibration	120	2,363	6.4	5.4	0.163

Unit conversions:

$$1 \text{ kg/m}^3 = 1.69 \text{ pcy}$$

**Table 50. Hardened concrete properties.**

		Concrete Mix Variables						Hardened Properties					
Mix No.	AEA Type	Sand Gradation	Water Reducer	Water-Reducer Dosage	Temperature	Pozzolans	Consolidation	Strength 7 Day (MPa)	Strength 28 Day (MPa)	Air (%)	Spacing Factor (mm)	Specific Surface (mm <sup>2</sup> /mm <sup>3</sup> )	Air Void Clustering Rating
1	B	Normal	A	Normal	Normal	None	Normal Vibration	30.0	33.9	5.8	0.152	26.6	0
2	H	Normal	A	Normal	Normal	None	Normal Vibration	24.0	31.9	5.5	0.076	48.9	0
3	D	Normal	A	Normal	Normal	None	Normal Vibration	24.2	32.5	6.4	0.127	30.9	0
4	H	Normal	None	Not applicable	32 °C	None	Normal Vibration	25.6	29.7	5.5	0.102	50.0	0.85
5	H	Normal	A	Normal	32 °C	None	Normal Vibration	30.7	36.4	5.1	0.102	37.3	0
6	H	Normal	B	High	Normal	None	Normal Vibration	21.8	27.6	6.1	0.102	42.5	0.43
7	H	Coarse	A	Normal	Normal	None	Normal Vibration	32.5	36.7	4.5	0.152	32.5	0
8	D	Coarse	A	Normal	Normal	None	Normal Vibration	32.1	35.8	4.9	0.178	25.6	0
9	H	Normal	A	Normal	Normal	20% (C) fly ash A	Normal Vibration	25.6	38.7	3.3	0.178	29.4	0
10	H	Normal	A	Normal	Normal	20% (C) fly ash B	Normal Vibration	28.5	38.0	4.7	0.254	18.3	0
11	H	Normal	A	Normal	32 °C	20% (F) fly ash	Normal Vibration	26.0	33.9	4.7	0.127	35.2	0.3
12	D	Normal	A	Normal	Normal	None	Excessive Vibration	24.3	33.9	5.8	0.127	36.5	0
13	B	Normal	A	Normal	Normal	None	Excessive Vibration	26.4	34.9	5.1	0.178	25.2	0

Unit conversions:

1mm =0.0394 inch

1 MPa = 145.0 psi

Correlations between air void parameters generated from the pressure meter, petrographic, and AVA analyses are presented in the following figures. Figure 50 presents the correlation between total air void contents generated by ASTM C 457 and pressure meter analyses. Figure 51 presents the correlation between total air void contents generated by ASTM C 457 and the AVA analyses. The spacing factor correlation between the ASTM C 457 and AVA analyses is shown in figure 52. Finally, the air content versus spacing factor relationship for the ASTM C 457 and AVA analyses are shown in figure 53.

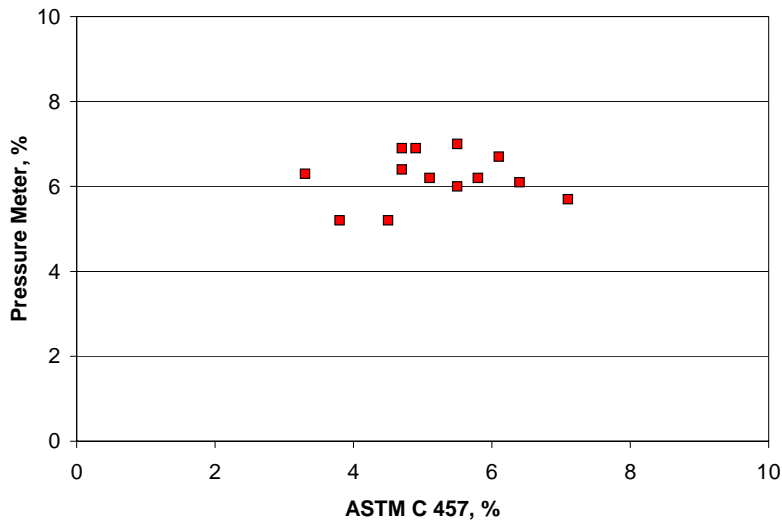


**Figure 50. Correlation of total air contents between pressure meter and ASTM C 457.**

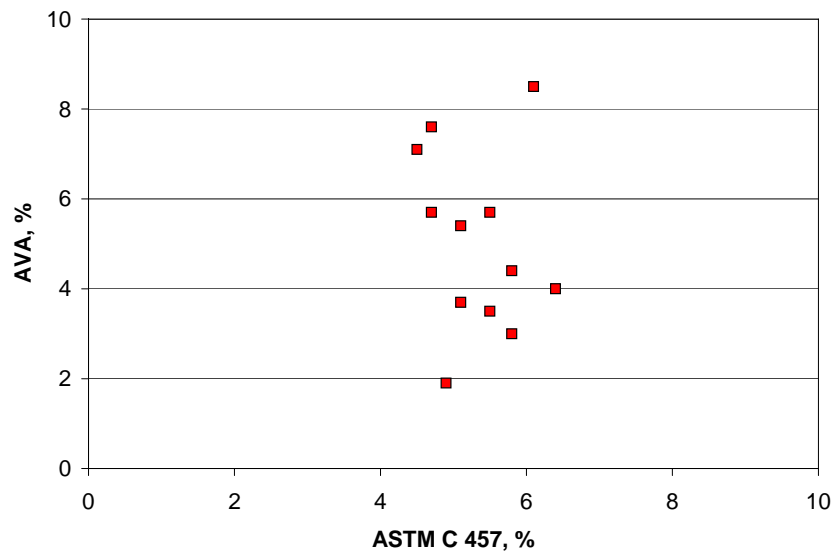
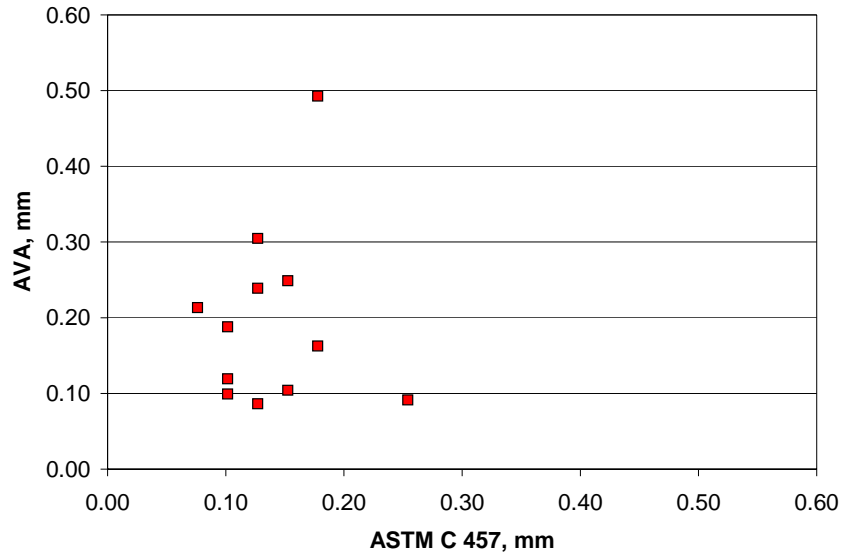


**Figure 51. Correlation of total air contents between AVA and ASTM C 457.**



Unit conversions:  
 1 mm = 0.0394 inch

**Figure 52. Correlation between AVA and ASTM C 457 generated spacing factors.**

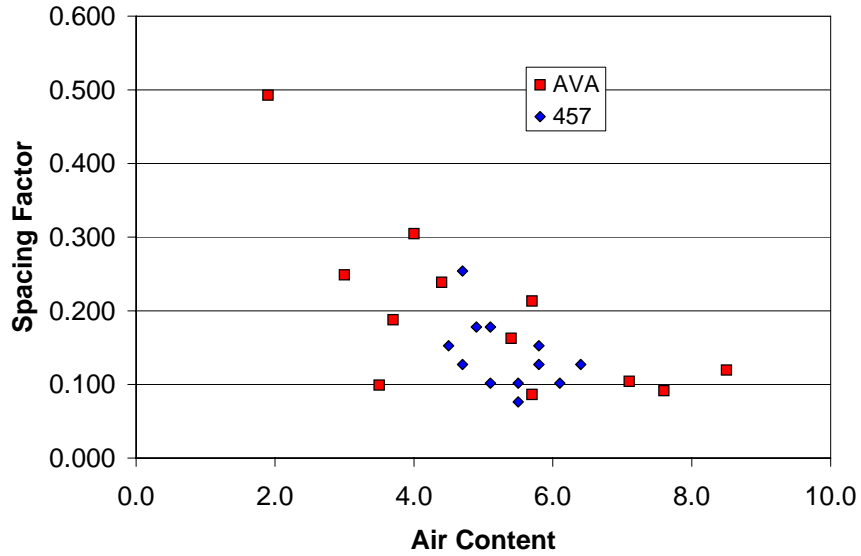


**Figure 53. Spacing factor versus air content relationship for ASTM C 457 and AVA.**

## Summary

The foam drainage test was used to screen admixtures in this study. The test method was used to evaluate the effects of various concrete raw materials on the stability of foams generated from different air entraining admixtures. Foam drainage parameters for the 10 admixtures evaluated in this study were ranked on a scale from 1 to 10, where 1 represented the worst performer and 10 represented the most stable admixture under all conditions. The overall rankings shown in table 48 were determined by averaging all the individual performances ( $V_o$ ,  $-1/k$ , and percentage drained) for each admixture. The best, middle, and worst performers or admixtures B, D, and H respectively were chosen for further evaluation in concrete mixtures to determine if a similar link to concrete air void quality existed. It was notable that some admixtures appeared to be sensitive to the presence of supplementary cementing materials and water reducing admixture (E), while others were not. Also of interest was that some air entraining admixtures appeared to perform well in this test when tested alone, but were less satisfactory when tested with cementitious systems (F), or vice versa (A, B). It is advisable that if this test is used in the field, the full system should be tested and not the AEA alone.

Concrete mixtures reported to have produced poor air void systems in the field were chosen to evaluate these admixtures. The 13 concrete mixtures chosen for evaluation are shown in table 45. The most unstable admixture was used in 8 of the 13 mixtures, while the top performer was used in two of the mixtures for comparison. Little correlation was observed in the effects of the variables changed in this test matrix.

According to most authorities, spacing factor and specific surface values calculated from an ASTM C 457 petrographic analysis can determine the potential freeze/thaw durability of a concrete mixture. Concrete mixtures with a spacing factor below 0.200 mm (0.008 in) and specific surface greater than  $24 \text{ mm}^2/\text{mm}^3$  ( $600 \text{ inch}^2/\text{inch}^3$ ) are thought to be freeze/thaw durable. Reviewing the ASTM C 457 results for the 13 concrete mixtures presented in table 50, only mix 10 failed the parameters discussed above.

Mix 10 was made using the most unstable admixture (H) as identified by the foam drainage test; however, this was the only mixture of the eight made with admixture H that was found to be outside the range of recognized air void parameters. It would appear that there is little correlation between the foam drainage test and the other parameters measured in this work. There is still potential value in the test as being an indicator of the stability of an air void system with time in the fresh concrete. These properties were not investigated as part of the concrete work here, but there are reports from the field of air content of a fresh mix changing with continued transporting and handling. This test would be a useful indicator in such an application. The test was also shown to be sensitive to changes in cementitious materials and may also have value as a monitor of system uniformity.

A review the correlations between air void parameters obtained using the pressure meter (ASTM C 231), AVA, and ASTM C 457 analyses show considerable scatter in the AVA data. The correlation of total air contents between the pressure meter and AVA shown in figure 49 is much more scattered when compared to the similar relationship between the ASTM C 457 and pressure meter presented in figure 50. The correlation between ASTM C 457 and AVA spacing factors shown in figure 52 shows significant scatter. There are reports that the instrument is being

successfully used as a quality management tool. It may be that the test is appropriate for use in a situation where the same, or similar, mixes are repeatedly tested from batch to batch. In that case it is more the repeatability of the results that is important than the absolute numbers obtained. These limited data indicate the test may not be immediately appropriate for testing a variety of mixtures without some form of calibration.

Of the 13 concrete mixtures made, only 3 showed signs of air void clustering when analyzed according to the clustering rating system. All three of these mixtures were made using the most unstable admixture (H). In addition, two of the three mixtures where clustering occurred were mixed at 32.2 °C (90 °F). This supports the belief that clustering is more prone to occur during the summer months when mixing temperatures are generally higher. The third mixture in which clustering occurred was made with a high dosage of water reducer.

Another test that was not conducted as part of this work has a history of being useful. The test is the foam index test. When used as a quick indicator of variability in cementitious materials (particularly fly ash), it has potential as a field materials acceptance test.



## CHAPTER 4. SUMMARY

### INTRODUCTION

As indicated in the preceding sections, a large number of mechanisms and effects contribute to so-called incompatibility. Many of these are complex and interrelated. This means that there is no simple means of providing a reliable measure of the risk of incompatibility. Some test methods are suitable for indicating risk of problems in the first 30 min because of aluminate/sulfate balance issues, while others are suitable for detecting later silicate hydration problems, and none is ideal for both.

There is a general trend that the lower-cost rugged tests are more prone to scatter and less sensitive than the more expensive delicate tests. Many of the tests take a long time to conduct, which is problematic for field application where an answer may be required in a few hours.

One of the interesting aspects of interpreting the data from the laboratory work conducted was that there was no clearly marked system identified as “incompatible” with a companion sample labeled “compatible.” Part of the work in assessing test methods to identify incompatibility was to use the same test methods to assess the apparent incompatibility of the test mixtures.

It was also observed that in many of the tests, there was no threshold that clearly indicated whether any given system was incompatible or not. A result that may be considered poor for one system may be considered acceptable for another. The greatest value of many of these tests is in monitoring the uniformity of a system over time. A marked change in a test result would indicate potential problems that would need to be investigated using other means. This tracking would need to be based knowing the acceptable ranges for that system, for the environment in which it is being used.

In seeking to develop a test protocol, there is some value in understanding and summarizing the multiple and complex mechanisms that are at play when considering the wide-ranging problem of incompatibility.

### EARLY SETTING AND EXCESSIVE RETARDATION

Hydraulic cement systems stiffen, set, and harden by a series of nonreversible chemical reactions with water, a process called hydration. This process is complex, and it still is the subject of extensive research. A discussion of the broad principles follows.

#### Cement Chemistry

Portland cement and cementitious materials comprise the same family of chemical elements. Chemical analyses of cementitious materials by X-ray fluorescence report the elements as oxides. This is for convenience only because these elements are not all likely to be present as pure oxides. The same convention is followed below.

**Calcium oxide.** Normally comprises 60 to 65 percent of cement by mass, while silica normally contributes about 20 percent. These combine to form the so-called “silicates,”  $C_2S$  and  $C_3S$ . The

hydration products (the compounds formed when they react with water) of  $C_2S$  and  $C_3S$  are similar to each other, albeit in different proportions. Hydration of silicates also produces some heat (figure 54). Calcium silicate hydrate (CSH) is the primary compound that gives hydrated cement paste the strength and impermeability that makes concrete useful in construction. Calcium hydroxide (CH) forms hexagonal crystals that do not contribute significantly to strength, but can be readily dissolved by acids and soft water.

$C_3S$ , also known as “alite,” is the compound that contributes to setting and early strength development of concrete. The contribution normally begins a few hours after mixing.  $C_2S$ , also known as “belite,” is the primary compound that contributes to later strength development of concrete. The contribution is considered to begin about a week after mixing. Portland cements currently contain approximately 60 percent  $C_3S$  and 20 percent  $C_2S$ .

**Alumina.** Included in the mixture introduced into a cement kiln because it helps to reduce the burning temperatures required to make cement. Iron oxide is also normally present in the raw materials. Alumina combines with calcium and iron oxide to form two aluminate compounds:  $C_3A$  and  $C_4AF$ . Typical portland cements contain approximately 5–8 percent  $C_3A$  and 8–12 percent  $C_4AF$ .  $C_4AF$  reactions do not contribute significantly to the properties of concrete except the gray color.  $C_3A$  reacts very rapidly when mixed with water and generates a large amount of heat (figure 54), unless it is controlled by the presence of calcium and sulfate.

**Calcium sulfate.** Added to clinker during grinding at about 5 percent dosage to control the initial reaction of  $C_3A$ . The dosage is carefully optimized because the strength of a cement is influenced by the amount of sulfate, and incompatibility (including uncontrolled stiffening and setting) can occur if the amounts of  $C_3A$  and sulfate are out of balance. Calcium sulfate is normally present in three forms, depending on the amount of water tied to the compounds. These are described in table 51.

**Table 51. Compounds of calcium sulfate in cement.**

Compound	Shorthand Notation
Anhydrous calcium sulfate (anhydrite)	$C\bar{S}$
Calcium sulfate dihydrate (gypsum)	$C\bar{S}H_2$
Calcium sulfate hemihydrate (plaster or bassanite)	$C\bar{S}H_{1/2}$

The reaction products of  $C_3A$  and sulfate are complex and change with time from mainly amorphous hydrates to form more crystalline hydrates over time, such as ettringite and monosulfoaluminate hydrate (figure 54). The formation of syngenite also appears to be a potentially significant factor.

### Hydration Reactions and Development of Microstructure

Hydration begins as soon as cementitious materials come in contact with water. The particles partially dissolve and the various components start to react at various rates.

There is no single mechanism behind the wide range of effects that are occurring. Many of the mechanisms are complex and interactive and may require expert evaluation if they occur in the field. Following are discussions of some of the chemical reactions that are occurring.

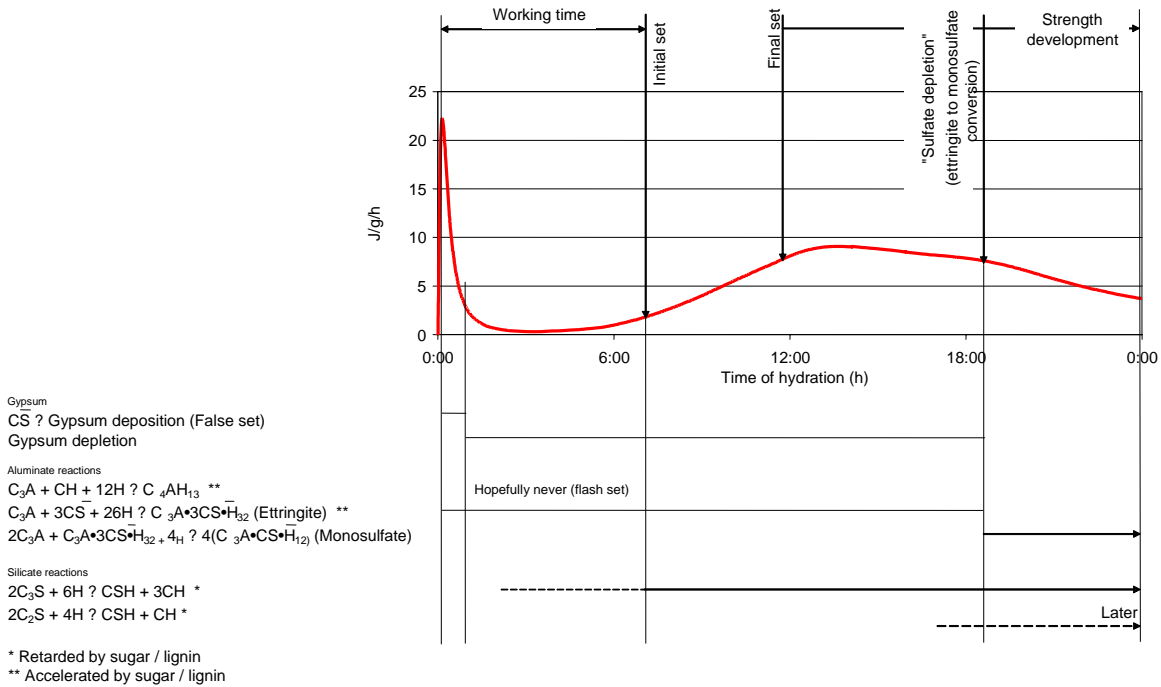
**Early Reactions.** Cement hydration in the first 15 min is a delicate balance between the  $C_3A$  in the cement, and sulfate in solution slowing the  $C_3A$  reaction (figure 54). If there is insufficient sulfate in solution, the  $C_3A$  begins to react immediately to form calcium aluminate hydrate, which can cause flash (immediate and permanent) set if it is not controlled.  $C_3A$  hydrates at a more controlled rate in the presence of sulfate to form ettringite while there is sulfate in solution. When the sulfates are consumed, ettringite continues to react to form monosulfate (figure 54). On the other hand, too much sulfate in solution may precipitate out as gypsum, causing false (temporary) set. These reactions are the basis of many incompatibility problems.

The amount of sulfate in solution is dependent not only on the amount of sulfate ion in the cement, but the form in which it occurs. Cement that has overheated in the mill may contain excess amounts of relatively fast dissolving plaster ( $CaSO_4 \cdot \frac{1}{2}H_2O$ ). Cement manufacturers will normally target a balance of plaster and gypsum ( $CaSO_4 \cdot 2H_2O$ ) suitable for the reactivity of a given clinker type and cement fineness, and they will optimize the sulfate content to balance the setting time of the concrete.

Addition of a supplementary cementitious material that contains additional calcium aluminates (typically high-calcium fly ash) can mean that the aluminate/sulfate balance can be compromised, causing the problems discussed above.

The fineness of the cement will also influence the reaction rates. The finer the cement is, the greater the risk of uncontrolled  $C_3A$  reactions with other ingredients in the concrete.

Some chemical admixtures will interfere with  $C_3A$  hydration and the solubility of calcium and sulfate in the pore solution; thus, they may significantly affect the workability of the concrete in the first few minutes. Type A water reducers tend to accelerate aluminate hydration and retard silicate hydration. Some chemical admixtures may reduce early slump when used with some cementitious combinations.



Unit conversions:

1 J/g/h (joule per gram per hour) = 0.008 calories per ounce per hour

**Figure 54. Reactions in hydrating cement.**

The solubility and reactivity of all of the compounds are also strongly influenced by temperature, with higher temperatures generally increasing solubility (except calcium) and accelerating reaction rates. These changes can affect the balance of the system and change stiffening rates and setting times.

**Later reactions.** After a dormant period of 1 to 3 h, the silicates ( $C_3S$  and later the  $C_2S$ ) start to hydrate. They form fibrous growths of calcium-silicate-hydrate (CSH) that gradually spread and merge with the growth from other cement particles or adhere to aggregate particles. This build up of new solid compounds results in progressive stiffening, hardening, and strength development. This reaction proceeds as long as the system contains water, explaining the need for curing.

Increasing alkali content and cement fineness, along with increasing temperature will increase reactivity of the silicate components and decrease setting times. Increasing reactivity will also tend to increase the rate of gain of stiffness, which may increase the risk of cracking.

The presence of some chemical admixtures will affect the reaction rates, often retarding setting. Type A water-reducing admixtures may retard silicate hydration.

The saturation of calcium may also affect the hydration of  $C_3S$ , which in turn is influenced by the reactions in early stages of hydration discussed above. Insufficient calcium in solution (that is, if

it has been consumed in early  $C_3A$  hydration) will slow or stop silicate hydration, leading to retardation of the concrete or failure to set.

### **Dimensional Stability and Cracking**

Concrete, and all of the components within it, tend to grow and shrink with changing temperatures, moisture conditions, and in some cases chemical reactions. By nature of its composition, concrete is mixed with water, some of which is consumed in hydration and some of which may leave the system by bleeding or evaporation as the concrete is allowed to dry. Hydrated cement paste is generally the phase that changes the most with changing moisture content, which is why it is recommended that the paste content of a mixture be minimized within constraints imposed by other requirements such as strength or impermeability.

The space occupied by the reagents of cement hydration is less than that of the hydrated system. This results in so called chemical shrinkage, and autogenous shrinkage (the amount of chemical shrinkage that can be measured). This phenomenon is greatest in systems with low w/cm.

Other chemical reactions including alkali aggregate reaction and sulfate attack may cause dimensional change in concrete, but these are outside the scope of this project.

All of the materials in concrete expand and shrink with changing temperature and moisture content. The consequences of these dimensional changes are a function of other properties of the concrete including restraint, stiffness, strength, and creep. A freestanding object that is not restrained internally or externally will shrink without damage; however, external restraint is almost always applied to concrete elements by their support systems and connections to adjacent elements. Internal restraint is also imposed by the different components (aggregates, paste) having different stiffness values and likely different amounts of dimensional movement. Such restraint will result in cracking.

The amount of stress set up in a shrinking, restrained material is a direct function of its stiffness (modulus of elasticity) with stiffer materials resulting in higher stresses. Creep helps to mitigate the amount of stress. The risk of cracking is governed by the balance of imposed stress and the material strength.

Adding to the complexity of this issue is that all of these properties are changing with time as the concrete hydrates, with the changes occurring rapidly at early ages and slowing with age, and with the changes occurring at different rates for the different properties. The rate of hydration will be influenced by the temperature and chemistry of the reactive materials. The rate of drying (and associated shrinkage) will also be influenced by the temperature and the environment to which the concrete is exposed. The rates and degree of temperature change are governed by the dimensions of the element, the environment, and the chemistry and degree of hydration.

Computer models are available to assess the risk of cracking in concrete pavements based on these parameters. Part of the work conducted in this project has been to determine the relative rates of change of strength and stiffness of the concrete mixtures tested.

The current standard test for concrete shrinkage (ASTM C 157) does not provide any information about the dimensional movement of concrete for the first 24 h, and limited

information before drying is allowed to start; however, such information is required if early age cracking is to be better understood and prevented. The ring shrinkage test provides a controlled method of tracking shrinkage-related stresses in a concrete under restraint from the time that the concrete is placed in the mold.

### **Air Void System**

It is important that a proper air void system be provided to concrete if it is to be protected from frost damage. Such a system may be considered as a uniform distribution of a large number of small air bubbles, the critical parameter being the maximum distance from any point in the paste to the nearest bubble.

The quality of an air void system is strongly influenced by the chemistry of the cementitious materials, particularly the carbon content of fly ash, if present. Different air-entraining admixtures will also produce different air void systems, with some materials being strongly influenced by the presence of other chemical admixtures and supplementary cementing materials. The grading of the fine aggregate will also influence development of the system along with the amount of mixing energy provided. It is easier to entrain air in a mixture with a higher slump than in one with a lower slump. The air void system of a concrete will also change with continued handling, placing, and compacting effort.

It is desirable that the spacing factor be determined in concrete, particularly in the fresh state to allow early decisions regarding its acceptability. It may also be preferred to measure it in the final position to allow for the effects of handling; however, there are no proven means of conducting this determination at present, making it important to be able to correlate final spacing factor with other, more easily measured parameters such as total air content measured using a pressure meter.

### **PROTOCOL**

The protocol has been developed on the premise of developing as much information as possible in a prequalification phase. This work would include calibrating the more sensitive central laboratory tests with the equivalent field tests using materials that are likely to be used in the field and under environments likely to be experienced in the field. The work may also include preparing alternative mix proportions and practices to accommodate changes in environment or changes in materials sources. Tests in the field would be based on the more portable tests being conducted regularly, primarily to monitor the uniformity of the materials and the final mixture as discussed above.

Most of the tests conducted in this work have some value, and the extent of prequalification and field testing will need to be based on the availability of equipment and the relative cost of testing compared to the cost and risk of failures. A typical example is the determination of setting time, which can be achieved by up to six different techniques, any of which is acceptable, and the selection of which should be based on the other requirements and conditions at the site.

It is likely that a relatively simple suite of field tests conducted regularly will provide much of the reassurance needed that a concrete mixture will perform satisfactorily:

- Foam index.
- Foam drainage.
- Slump loss.
- Unit weight.
- Semi-adiabatic temperature monitoring.
- Setting time.
- Chemistry of reactive materials.

Obtaining information of the materials' chemistry in the detail required for individual batches may be problematic. For a large project with significant costs associated with failure, negotiations may be made with the suppliers to conduct the reviews as part of the existing quality control and to provide certification that a set of critical parameters such as C<sub>3</sub>A content has not changed by more than X percent between loads.

The protocol is presented in volume II.

## **IMPLEMENTATION PLAN**

It is important the information generated in this project be implemented in the construction industry to reduce the occurrence of incompatibility and its attendant costs. Because many of the test methods are already standardized or in use, the primary need for guidelines and an implementation plan is to increase awareness about this work and the accompanying protocols among the makers and users of concrete. The intended audience of this report is State departments of transportation representatives, as well as contractors and ready-mix suppliers involved in pavement construction.

In addition, it is suggested that the recommended test methods that have not been standardized should be submitted to relevant authorities for adoption.

### **Publications**

The findings of this work will be disseminated in publications. In addition to the project report, a TechBrief publication summarizing the findings will be published by the Federal Highway Administration (FHWA) and a technical paper will be available for consideration in applicable journals.

### **Presentations**

The topic of this project has been the subject of at least six presentations already made at the Transportation Research Board (TRB) and several state and local ACPA symposia. A prepared presentation is provided in Microsoft® PowerPoint® format along with this report.

### **Standards**

The test methods that are not currently standardized have been prepared in AASHTO format and should be submitted to AASHTO or ASTM, or both, for adoption.





## ACKNOWLEDGEMENTS

The authors wish to acknowledge the work of the following people in completing the work described in this report:

From the CTLGroup:

Katie Amelio  
Pat Berry  
Barb Betke  
Javed Bhatti  
Fred Blaul  
Phil Brindisi  
Roberto Celestin  
Luis Duval  
Ken MacLeod  
Greg Miller  
Mohamad Nagi  
Agata Pyc  
Brian Szczerowski  
Shiraz Tayabji

From Braun Intertec:

Rachel Detwiler

From NIST:

Max Peltz  
John Winpigler

## DISCLAIMER

Commercial equipment, instruments, and materials mentioned in this paper are identified to foster understanding. Such identification does not imply recommendation or endorsement by the authors or NIST, nor does it imply that the materials or equipment identified are necessarily the best available for the purpose.

## MATCHING FUNDS

CTLGroup was required to provide a minimum of a 20 percent match of the Federal funding toward the project. The matching funds were obtained by reaching agreement with the Portland Cement Association. No specific task was solely funded by PCA, but rather, a proportion of every payment due through the duration of the project was invoiced to PCA. PCA's total contribution was \$110,000 of the total estimated project cost of \$451,245.



## REFERENCES

1. Gress, D., *Early Distress in Concrete Pavements*, Federal Highway Administration, FHWA-SA-97-045, Washington, DC, January 9, 1997, pp. 53.
2. Whiting, D., *Addendum to NCHRP Report 258, Control of Air Content in Concrete, Appendix F, State-of-the-Art Report*, Portland Cement Association, Skokie, IL, 1983, 263 pp.
3. Stark, D.C., *Effect of Vibration on the Air void System and Freeze-Thaw Durability of Concrete*, PCA Research & Development Bulletin RD092.01TT, Portland Cement Association, Skokie, IL, 1986.
4. Tymkowicz, S. and Steffes, R., *Vibration Study for Consolidation of Portland Cement Concrete*, Report No. MLR-95-4, Iowa Department of Transportation, January 1997, 94 pp.
5. Jennings, H., Johnson, D.L., Moss, G.M., and Saak, A.W. *Pooled Fund Study of Premature Rigid Deterioration*, Iowa Department of Transportation Research Project H-1063, Northwestern University Technological Institute, Evanston, IL, April 1997, 94 pp.
6. Powers, T.C., *The Properties of Fresh Concrete*, John Wiley & Sons, New York, 1968.
7. Whiting, D.A. and Nagi, M.A., *Manual on Control of Air Content in Concrete*, EB116, Portland Cement Association, Skokie, IL, 1998.
8. Stutzman, P.E. *Deterioration of Iowa Highway Concrete Pavements: A Petrographic Study*, NISTIR 6399, National Institute of Standards and Technology, December 1999, 72 pp.
9. Simon, M.J.; Jenkins, R.B.; and Hover, K.C. "The Influence of Immersion Vibration on the Void System of Air Entrained Concrete," *Durability of Concrete: G.M. Idorn International Symposium*, Toronto, ON, Canada, ACI SP-131, Jens Holm and Mette Geiker, Eds., American Concrete Institute, 1992, pp. 99–126.
10. Kosmatka, S.H., Kerkhoff, B. and Panarese, W.C., *Design and Control of Concrete Mixtures*, 14th Edition, EB001.14T, Portland Cement Association, Skokie, IL, 2002, 355 pp.
11. Senbetta, E. and Malchow, G. "Studies of Control of Durability of Concrete Through Proper Curing," *Concrete Durability, Katharine and Bryant Mather International Conference*, ACI SP-100, J.M. Scanlon, Ed., American Concrete Institute, 1987, pp. 73–87.
12. Hansen, W.C., "False Set in Portland Cement," *Proceedings of the 4th International Symposium on the Chemistry of Cement*, Washington DC, 1960, pp. 387–428.

13. Neville, A., "The Question of Concrete Durability: We Can Make Good Concrete Today," *Concrete International*, Vol. 22, No. 7, July 2000, pp. 21–26.
14. Sandberg, P.J. and Roberts, L.R., "Cement-Admixture Interaction Related to Aluminate Control," *Jr. ASTM International*, Vol. 2, No. 6, June 1, 2005, pp.1–14.
15. Wadso, L., "Unthermostated Multichannel Heat Conduction Calorimeter," *Cement, Concrete, and Aggregates*, Lund, Sweden, Vol. 26, No. 2, December 2004, pp.1–7.
16. Aitcin, P.C., Jolicoeur, C, and MacGregor, J.G., "Superplasticizers: How They Work and Why They Occasionally Don't," *Concrete International*, Vol. 16, No. 5, May 1994, pp. 45–52.
17. Helmuth, R.A., "Fly Ash in Cement and Concrete," Portland Cement Association, Skokie, IL, 1987.
18. Ferraris C., Obla K., Hill R., "The Influence of Mineral Admixtures on the Rheology of Cement Paste and Concrete," *Cement and Concrete Research*, Vol. 31, No. 2, 2001, pp. 245–255.
19. Bhattacharja, S. and Tang, F. J., "Rheology of Cement Paste in Concrete with Different Mix Designs and Interlaboratory Evaluation of the Mini-Slump Cone Test," PCA R&D Serial No. 2412, Portland Cement Association, Skokie, IL, 2000.
20. Hackley V.A., Ferraris C. F., "Guide to Rheological Nomenclature: Measurements in Ceramic Particulate Systems," NIST Special Publication 946, January 2001, pp. 35.
21. Kantro, D.L., Influence of Water-Reducing Admixtures on the Properties of Cement Paste—A Miniature Slump Test, *PCA R & D Bulletin, RD079.01T*, Portland Cement Association, Skokie, IL, 1980, pp. 95–102.
22. Helmuth, R.A., Hills, L.M., Whiting, D.A., and Bhattacharja, S., "Abnormal Concrete Performance in the Presence of Admixtures," PCA R & D Serial No. 2006, Portland Cement Association, Skokie, IL, 1995.
23. Ferraris C.F., "Measurement of the Rheological Properties of Cement Paste: A New Approach," *International RILEM Conference on the Role of Admixtures in High Performance Concrete*, J.G. Cabrera and R. Rivera-Villareal, Eds., Monterrey, Mexico March 21–26, 1999b, pp. 333–342.
24. Ferraris, C.F. and Gaidis, J.M., "Connection between Rheology of Concrete and Rheology of Cement paste," *ACI Materials Journal*, Vol. 88, No. 4, 1992, pp. 388–393.
25. Ferraris, C.F., "Measurements of Rheological Properties of High Performance Concrete: State of the Art Report," *Journal of Research of the National Institute of Standards and Technology*, Vol. 104, No. 5, 1996, pp. 461–478.

26. Wong, G.S., Alexander, A.M., Haskins, R., Poole, T.S., Malone, P.G., and Wakeley, L., *Portland-Cement Concrete Rheology and Workability: Final Report*, FHWA-RD-00-025, Federal Highway Administration, McLean, VA, April 2001.
27. Wang J.N., Kennedy T.W., McGennis R.B., “Volumetric and Mechanical Performance Properties of Superpave Mixtures,” *Journal of Materials In Civil Engineering*, Vol. 12, No. 3, August 2000, pp.238–244.
28. Struble, L.J. and Ji, X., “Rheology,” *Handbook of Analytical Techniques in Concrete Science and Technology, Principles, Techniques, and Applications*, Ed. Ramachandran, V.S. and J.J. Beaudoin, Noyes Publications, Park Ridge, NJ, William Andrew Publishing, Norwich, New York, 2001, pp. 333–367.
29. Tattersall, G.H. and Baker, P.H., “The Effect of Vibration on the Rheological Properties of Fresh Concrete,” *Magazine of Concrete Research*, Vol. 40, No, 143, 1988 pp. 79–89.
30. De Larrard, F., Hu C., Szitkar, J.C., Joly, M., Claux, F. and Sedran, T., “A New Rheometer for Soft-to-Fluid Fresh Concrete,” Laboratoire Central des Ponts et Chaussees (LCPC) internal report, 1995.
31. Popovics, S., *Fundamentals of Portland Cement Concrete: A Quantitative Approach*, John Wiley & Sons, 1982.
32. Aldea, C.M., Ghandehar, M., Shah, S.P., and Karr, A., “Estimation of Water Flow through Cracked Concrete under Load,” *ACI Materials Journal*, Vol. 97, No. 5, September–October 2000, pp. 567–575.
33. Chatterji, S., “Probable Mechanisms of Crack Formation at Early Ages of Concretes,” *International Conference on Concrete of Early Ages*, RILEM, 1982, pp. 35–38.
34. Springenschmid, R., Breitenbücher, R., and Mangold, M., “Practical Experience with Concrete Technological measures to Avoid Cracking,” *Thermal Cracking in Concrete at Early Ages*, RILEM Proceedings 25, R. Springenschmid, Ed. E&FN Spon, 1995, pp. 377–384.
35. Springenschmid, R. and Breitenbücher, R. “Influence of Constituents, Mix Proportions and Temperature on Cracking Sensitivity of Concrete,” *Prevention of Thermal Cracking in Concrete at Early Ages*, RILEM Report 15, R. Springenschmid, Ed. E&FN Spon, 1998, pp. 40–50.
36. Powers, T.C., “Void Spacing as a Basis for Producing Air-Entrained Concrete,” *ACI Journal*, RX049, Portland Cement Association, Skokie, IL, Vol. 50, May 1954, pp. 741–760.
37. Krauss, P.D. and Rogalla, E.A., *Transverse Cracking in Newly Constructed Bridge Decks*, National Cooperative Highway Research Board Report 380, National Academy Press, Washington, DC, 1996, p. 126.

38. Holt, E.E., "Where Did These Cracks Come From?" *Concrete International*, Vol. 22, No. 9, September 2000, pp. 57–60.
39. Bernander, S., "Practical Measures to Avoiding Early Age Thermal Cracking in Concrete Structures," Chapter 9, *Prevention of Thermal Cracking in Concrete at Early Ages*, RILEM Report 15, R. Springenschmid, Ed. E&FN Spon, 1998, pp. 255–314.
40. Van Breugel, K., "Prediction of Temperature Development in Hardening Concrete," *Prevention of Thermal Cracking in Concrete at Early Ages*, RILEM Report 15, R. Springenschmid, Ed. E&FN Spon, 1998, pp. 51–75.
41. Roper, H. and Anderson, T., "Laboratory and Site Studies of Early Dimensional Changes and Crack Development," *International Conference on Concrete of Early Ages*, RILEM, 1982, pp. 63–69.
42. Thomas, M.D.A. and Mukherjee, P.K., "The Effect of Slag on Thermal Cracking in Concrete," *Thermal Cracking in Concrete at Early Ages*, RILEM Proceedings 25, R. Springenschmid, Ed. E&FN Spon, 1995, pp. 197–204.
43. Chan, Y.W.; Liu, C.Y.; and Lu, Y.S., "Effects of Slag and Fly Ash on the Autogenous Shrinkage of High Performance Concrete," *Autogenous Shrinkage of Concrete*, Ei-ichi Tazawa, Ed., E & FN Spon, London, UK and New York, 1999, pp. 221–228.
44. Ziegeldorf, S., Müller, H.S., Plöehn, J., and Hilsdorf, H.K., "Autogenous Shrinkage and Crack Formation in Young Concrete," *International Conference on Concrete of Early Ages*, RILEM, Vol. I, 1982, pp. 83–88.
45. Sellevold, E., Bjøntegaard, Ø., Justnes, H., and Dahl, P.A. "High Performance Concrete: Early Volume Change and Cracking Tendency," *Thermal Cracking in Concrete at Early Ages*, RILEM Proceedings 25, R. Springenschmid, Ed. E&FN Spon, 1995, pp. 229–236.
46. Whiting, D.A. and Detwiler, R.J. "Silica Fume Concrete for Bridge Decks," *National Cooperative Highway Research Program Report 410*, Transportation Research Board, National Academy Press, Washington, DC, 1998, pp.47.
47. Breitenbücher, R. and Mangold, M., "Minimization of Thermal Cracking in Concrete Members at Early Ages," *Thermal Cracking in Concrete at Early Ages*, RILEM Proceedings 25, R. Springenschmid, Ed. E&FN Spon, 1995, pp. 205–212.
48. Japan Concrete Institute Technical Committee on Autogenous Shrinkage of Concrete, Committee Report, *Autogenous Shrinkage of Concrete*, Ei-ichi Tazawa, Ed., London and New York: E & FN Spon, 1999, pp. 1–62.
49. Holt, E.E. and Leivo, M.T. "Autogenous Shrinkage at Very Early Ages," *Autogenous Shrinkage of Concrete*, Ei-ichi Tazawa, Ed., E & FN Spon, London, UK and New York, 1999, pp. 135–142.

50. Rapoport, J.R., J.S. Popovics, S.V. Kolluru, and Shah, S.P., "Using Ultrasound to Monitor Stiffening Process of Concrete with Admixtures," *ACI Materials Journal*, Vol. 97, No. 6 (November–December 2000) pp. 675–683.
51. See, H.T., Attiogbe, E.K., and Miltenberger, M.A., "Shrinkage Cracking Characteristics of Concrete Using Ring Specimens," *ACI Materials Journal*, Vol. 100, No. 3, May-June 2003. pp. 239–245.
52. Hossain, A.; Pease, B.; and Weiss, J., "Quantitative Early-Age Stress Development and Cracking in Low W/C Concrete Using the Restraining Ring Test with Acoustic Emission," *Transportation Research Board*, 82<sup>nd</sup> Annual Meeting, Compendium of Papers CD ROM, January 12–16, 2003.
53. Taylor, H.F.W., *Cement Chemistry*, Academic Press, New York, 1990 pp. 233–234.
54. Plante, P., Pigeon, M. and Foy, C. "The Influence of Water-Reducers on the Production and Stability of the Air void System in Concrete," *Cement and Concrete Research*, Vol. 19, No. 4, 1989, pp. 621–633.
55. Stott, D., Rezansoff, T. and Sparling, B.F., "Loss of Freeze-Thaw Durability of Concrete Containing Accelerating Admixtures," *Canadian Journal of Civil Engineering*, Vol. 21, No. 4, 1994, pp. 605–613.
56. Attiogbe, E.K., Nmai, C.K., and Gay, F.T., "Air-Void System Parameters and Freeze-Thaw Durability of Concrete Containing Superplasticizers," *Concrete International*, American Concrete Institute, Vol. 14, No. 7, July 1992, pp. 57–61.
57. "Manufacturing Air-Entrained Concrete," *Betonwerk Fertigteile Technik (BFT)*, Vol. 1, 2002, pp. 46–52.
58. Pigeon, M., Plante, P., Pleau, R. and Banthia, N., "The Influence of Soluble Alkalies on the Production and Stability of the Air void System in Superplasticized and Nonsuperplasticized Concrete," *ACI Materials Journal*, Vol. 89, No.1, 1992, pp. 24–31.
59. Personal communication from David Stark, Construction Technology Laboratories, to Peter Taylor (2002).
60. Gebler, S.H. and Klieger, P., "Effect of Fly Ash on the Air void Stability of Concrete," Portland Cement Association, Skokie, IL, 1986, 40 pp.
61. Langan, B.W., Joshi, R.C. and Ward, M.A., "Strength and Durability of Concrete Containing 50% Portland Cement Replacement by Flyash and Other Materials," *Canadian Journal of Civil Engineering*, Vol. 17, No. 1, 1990, pp. 19–27.
62. Saucier, F., Pigeon, M. and Cameron, G., "Air Void Stability, Part V: Temperature, General Analysis and Performance Index," *ACI Materials Journal*, Vol. 88, No. 1, January-February, 1991, pp. 25–37.

63. Gardner, T.J.; Beushausen, H-D., and Alexender, M.G., “The Effect of Elevated Temperatures on the Properties of Concrete,” *BFT*, Vol. 70, No. 5, 2004 pp. 6–13.
64. Pang, Y.; Lou, H., Qiu, X., and Yang, D., “Influences of Modified Lignosulfonate Superplasticizer on Cement Hydration and the Durability of Concrete,” *Journal of Sichuan University (Engineering Science Edition)*, Chengdu, China, Vol. 37, No. 1, January 2005, pp. 74–77.
65. Khayat, K. H. and Assaad, J., “Air Void Stability in Self-Consolidating Concrete,” *ACI Materials Journal*, Vol. 99, No. 4, July/August 2002, pp. 408–416.
66. Nagi, M. and Whiting, D., “Achieving and Verifying Air Content in Concrete,” *Research and Development Bulletin RP324*, Portland Cement Association, Skokie, IL, 1994, 40 pp.
67. Hover, K.C., “Some Recent Problems with Air-Entrained Concrete,” *Cement, Concrete, and Aggregates*, Vol.11, No. 1, 1989, pp. 73–80.
68. Cross, W., Duke, E., Kellar, J. and Johnston, D., *Investigation of Low Compressive Strengths of Concrete Paving, Precast and Structural Concrete*, South Dakota Department of Transportation Report SD98-03-F, 2000, 78 pp.
69. Kozikowski, Jr. R.L., Vollmer, D.B.; Taylor, P.C., and Gebler, S.H., “Factors Affecting the Origin of Air Void Clustering,” *PCA R&D Serial No. 2789*, Portland Cement Association, Skokie, IL, 22 pp, 2005.
70. Higginson, E.C., “Some Effects of Vibration and Handling on Concrete Containing Entrained Air,” *Journal of the American Concrete Institute*, Vol. 24, No. 1, 1952, pp. 1–12.
71. Mehta, P.K., *Concrete: Structure, Properties, and Materials*, Prentice-Hall, Inc., Englewood Cliff, NJ, 1986, 449 pp.
72. Torrans, P.H. and Ivey, D.L., *The Void Spacing Indicator*, Texas Transportation Institute, Research Report No. 103–3, 1969, 42 pp.
73. Johansen, P.E., “Characterization of the Air void System in Concrete by a Vibration Test,” *RILEM-ABEM International Symposium on Concrete Admixtures*, Topic V, 1967, pp. 7–29.
74. Henrichsen, J.V., “Quality Assurance of Air void Structures in Concrete,” *International Symposium on Non-Destructive Testing in Civil Engineering*, (NDT-CE) 26.28.09, German Society for Non-Destructive Testing (DGZfP), Berlin, Germany, September,1995, 8 pp.
75. Germann Instruments, Evanston, IL, Personal Communication.
76. Magura, D.D., *Air void Analyzer Evaluation*, Report No. FHWA-SA-96-062, Federal Highway Administration, Washington, DC, 1996.



77. Redmond, Michael "Air void Analyzer," Priority Technology Program, Final Report, State of Maine, Department of Transportation, 1999, 7 pp.
78. Zhang, Z., Ansari, F., and Vitillo, N., "Automated Determination of Entrained Air Void Parameters in Hardened Concrete," *ACI Materials Journal*, Vol. 102, No. 1, January/February 2005, pp. 42–48.
79. Bruere, G.M., "Air Entrainment in Cement and Silica Paste," *Journal of the American Concrete Institute*, Vol. 26, No. 9, 1955, pp. 905–920.
80. Dodson, V., "Air-Entraining Admixtures," *Concrete Admixtures*, Chapter 6, Van Nostrand Reinhold, London, UK, 1990, pp. 129–158.
81. Gutmann, P.F., "Bubble Characteristics as They Pertain to Compressive Strength and Freeze-Thaw Durability," *Bonding in Cementitious Composites*, Materials Research Society Symposium Proceedings, Materials Research Society, Pittsburgh, PA. Vol. 114, 1988, pp. 271–277.
82. Tang, F. J. and Bhattacharja, S., *Early Stiffening Test Development for Portland Cement*, Portland Cement Association R&D Serial No. 1999, 1996, 31 pp., 1996.
83. Barneyback, R.S. Jr.; "Alkali-Silica Reaction in Portland Cement Concrete," Ph.D. Thesis, Purdue University, Lafayette, IN, 1987.
84. Gartner, Ellis M., Tang, Fulvio J., and Weiss, Stuart J., "Saturation Factors for Calcium Hydroxide and Calcium Sulfates in Fresh Portland Cement Pastes," *Journal of the American Ceramic Society*, Vol. 68, No. 12, 1985, pp. 667–673.
85. Rothstein, D., Thomas J., Christensen, B.J., Jennings, H.M., "Solubility Behavior of Ca-, S-, Al-, and Si-bearing Solid Phases in Portland Cement Pore Solutions as a Function of Hydration Time," *Cement and Concrete Research*, Vol. 32, No. 10, 2002, pp. 1663–1671.
86. Alexander, A.M., Haskins, R.W, Sari, A., Soroushian, P., and Hsu, J-W., "New Technologies for Improving the Consolidation of Concrete," U.S. Army Corps of Engineers, Waterways Experiment Station, CPAR-SL-97-2, September 1997.

